Metabolites of bacteria isolated from marine environments: chemistry and bioactivities

Dissertation

zur

Erlangung des Doktorgrades (Dr. rer. nat.)

der

Mathematisch-Naturwissenschaftlichen Fakultät

der

Rheinischen Friedrich-Wilhelms-Universität Bonn

vorgelegt von

Antonio Dávila Céspedes

aus

San Luis Potosí, México

Bonn, 2017

Angefertig mit Genehmigung der Matematisch-Naturwissenschaftlichen Fakultät

der Rheinischen Friedrich-Wilhelms-Universität Bonn

In Advance Publications of the Dissertation

Parts of this study have been published in advance under permission of the Faculty of Mathematics and Natural Sciences, represented by the supervisor of this study:

Research paper:

Davila-Cespedes, A., Hufendiek, P., Crusemann, M., Schäberle, T. F., & Konig, G. M. (2016). Marine-derived myxobacteria of the suborder Nannocystineae: An underexplored source of structurally intriguing and biologically active metabolites. *Beilstein journal of organic chemistry*, *12*, 969–984. https://doi.org/10.3762/bjoc.12.96

Acknowledgements

Table of contents

List of tables

List of figures

Abreviations

Abs	Absorbance
AC	Acetone
ACN	Acetonitrile
AN	Accession number
antiSMASH	Antibiotics & Secondary Metabolite Analysis Shell
ASW	Artificial sea water
B.megaterium	*Bacillus megaterium*
BLAST	Basic Local Alignment Search Tool
bp	Base pair
cAMP	Cyclic adenosine monophosphate
CDCl$_3$	Deuterated chloroform
CECT	Colección Española de Cultivos Tipo
DCM	Dichloromethane
DDT	Disc diffusion test
DSMZ	Deutsche Sammlung von Mikroorganismen und Zellkulturen
E. coli	*Escherichia coli*
ELSD	Evaporative Light Scattering Detector
EtoAc	Ethyl acetate
g	Gram
GPCR	G-protein coupled receptor
HPLC	High-pressure liquid chromatography
HR-MS	High resolution mass spectrometry
kb	Kilobase
KS	Keto synthase
L	Liter

LC	Liquid chromatography
M	Molar
MB	Mega base
MDOD	Deuterated methanol
MeOH	Methanol
mg	milligrams
MHz	Megahertz
MiBi	Institute for Pharmaceutical Microbiology
min	minute
mL	milliliter
mM	milimolar
MRSA	Methicillin-resistant *Staphylococcus aureus*
MRSE	Methicillin-resistant *Staphylococcus epidermidis*
MSSA	Methicillin-susceptible *Staphylococcus aureus*
MSSE	Methicillin-susceptible *Staphylococcus epidermidis*
NCBI	National Center for Biotechnology Information
nm	Nanometers
NMR	Nuclear magnetic resonance spectroscopy
NP	Normal phase
OD	Optical density
PCR	Polymerase chain reaction
PE	Petrol ether
PKS	Polyketide synthase
RP	Reversed phase
S. cerevisiae	*Saccharomyces cerevisiae*
UV	Ultraviolet
λ	Wavelength [nm]

μg	Micrograms
μL	Microliters
μm	Micrometers

1. INTRODUCTION

Microorganisms are among the most ancient forms of life. Their diverse characteristics have allowed a phylogenetic classification into different groups based on genome sequence comparison. Each group displays distinctive biochemical and structural features as well as a great capacity of adaptation to the most diverse and changing environmental conditions, *e.g.* pH fluctuations, temperature variations, salinity, dryness, etc. (*1*). A general classification based on salt tolerance capacity has been proposed (*2*). According to this classification, some bacterial genera comprise species that hold the capacity to live in both marine and terrestrial environments. These organisms are deemed halotolerant. Meanwhile, those unable to survive under ocean conditions have been classified as terrestrial. The ones requiring salinity in order to survive are considered halophilic. The present work focuses on bacteria able to live in the marine habitat; some of them, halophilic. The distinctive feature of this kind of bacteria is their strict need for salt in order to grow and thrive in nature. The main objectives of this work are two: 1) to understand the ecological implications of marine bacteria especially in regard to the production of secondary metabolites, 2) to investigate the profit that can be made out of these chemical tools within the context of research on behalf of public health improvement. Subjects of our research are marine-derived myxobacteria, members of the $\delta-$proteobacterial group and *Labrenzia* sp. strain 011 (Ostsee6), member of the α-proteobacteria group; lastly, other bacteria retrieved from marine environments.

1.1. Classification of bacteria

In order to illustrate bacterial taxonomy and timescale localization, Figure 1-1 shows different bacterial groups and the approximate time of appearance as well as the estimated evolutionary point in time whereby the capacity to adapt from marine to terrestrial environments was acquired (*3*).
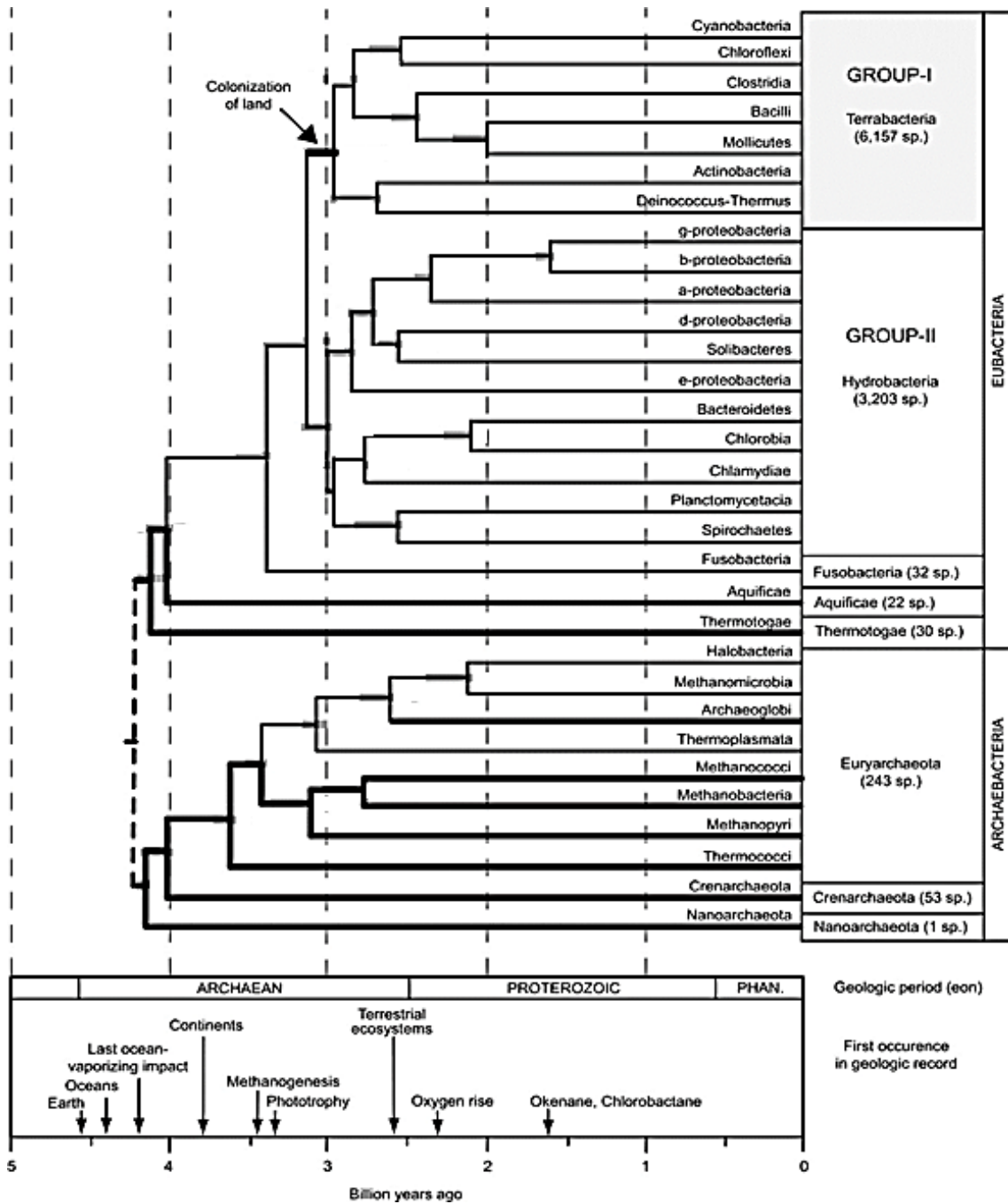
Figure 1-1 The illustration taken from (*3*) shows the approximate points of appearance of the different bacterial groups in the course of evolution. The black lines represent bacterial classes. Thicker lines are lineages that include hyperthermophilic species. The group with the number of species comprised is shown in the panel on the right side, and the time scale in billions of years ago is presented below. The arrows represent geological relevant phenomena.

Special emphasis will be put on group II of Figure 1-1, where the more relevant bacterial classes for the purposes of this work, namely α−proteobacteria, and δ−proteobacteria are clustered. According to the Figure 1-1, these groups of bacteria shared a common

ancestor about 3 million year ago (*3*). However, many members of these groups display either autotrophic or heterotrophic behavior (*4, 1*). In order to fulfill their nutritional demands, heterotrophic bacteria often require products of secondary metabolism to weaken or kill their preys and also to secure their habitats (*5*). These products play important roles in the way these organisms interact in their habitats.

Concerning classification based on salt-tolerance, it remains unclear whether some bacteria lost their capacity to live in marine ecosystems or developed salt-tolerance in the course of evolution, this way becoming apt for dwelling in sea-like conditions.

1.2. Microbial interactions in the marine environment

1.2.1. Ecological implications of secondary metabolites from marine microorganisms

The marine environment comprises a series of biotic and abiotic entities, whose coexistence is governed and balanced by different interactions. Mostly, interactions of macroscopic organisms are illustrated by predation and mutualism (*6*); small-scale interactions often involve microscopic organisms displaying, among others, parasitic or symbiotic relations with other microorganisms, algae and marine fauna (*7–10*). On this level of existence, it is often observed that chemical substances derived from secondary metabolism mediate these interactions. Examples of these are the bacteriocins, antibacterial proteinaceous compounds produced by bacteria, which probably act as anti-competitor agents in terrestrial and marine habitats (*11*). Interestingly, many of these substances may also be capable to exert biological effects in the clinical context (*12*). One example of this is the broad spectrum lantibiotic subtilomycin, produced by the marine sponge-associated bacterium *Bacillus subtilis* strain MMA7 (Figure 1-2) (*13*). This compound has shown growth inhibition of various Gram-positive and Gram-negative bacteria (*13*).
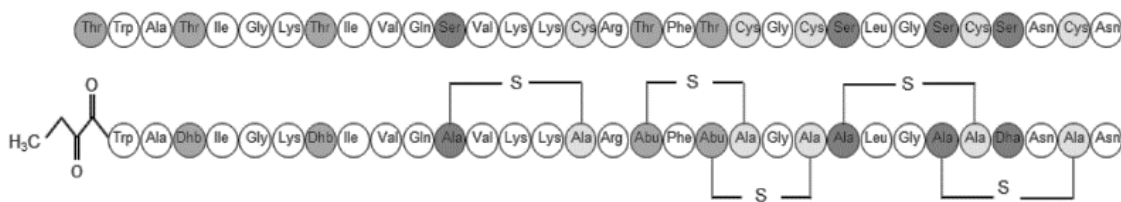
Figure 1-2 Subilomycin as presented by (*13*) is a marine derived lantipeptide that presents a broad range of antibacterial activity against Gram-positive and Gram-negative organisms (*13*). It also shows antifungal activity on strains of *Candida albicans* pathogenic to humans (*13*). This compound was isolated from the bacterium *Bacillus subtillis* MMA7 associated with marine sponges (*13*).

1.2.2. Marine microorganisms as potential producers of novel bioactive substances of clinical interest

Surely, the following question arises: why is it worthwhile to invest time and efforts in marine organisms? The answer is that compared to terrestrial environments, scientists have only marginally explored marine habitats in search for novel drugs or improvement of the current arsenal of available drugs. From this fact, an inference can be made considering the large number of terrestrial-derived compounds active *per se* or acting as scaffolds for synthetic modifications: the odds of finding structural novelty, and thus novel activities are much higher in marine organisms than in terrestrial ones (*14–17*).

This notion is supported by numerous works appointing substances of marine origin as potential candidates to become lead compounds and enter the drug market (*18–20*). Especially, efforts have been directed to anticancer drug testing (*20*). Examples of marine-derived compounds in medical use are scarce, but those undergoing clinical trials are numerous and promising (*21, 20, 22*). Table 1-1 shows the clinical status of some compounds isolated from marine environments and their putative producer or the organism from which the compounds were isolated. However, the true producer of the compounds remains in many cases unknown.

Table 1-1 This pipeline published by (*21*) presents the current perspective of relevant marine-derived substances and their clinical status. The information shown in the table corresponds to the status of the compounds in 2017. The reference provides a supplement, which is constantly updated and is available online.

Clinical status	Compound name	Marine organism	Chemical class	Disease area
FDA-Approved	Cytarabine	Sponge	Nucleoside	Cancer
	Vidarabine	Sponge	Nucleoside	Antiviral
	Ziconotide	Cone snail	Peptide	Pain
	Trabectedin	Tunicate	Alkaloid	Cancer
	Eribulin Mesylate	Sponge	Macrolide	Cancer
	Brentuximab	Mollusk/ Cyanobacterium	Antibody conjugate	Cancer
Phase III	Plinabulin	Fungus	Diketopyperazine	Cancer
	Plitidepsin	Tunicate	Depsipeptide	Cancer
	Glembatumumab	Mollusk/ Cyanobacterium	Antibody conjugate	Cancer
Phase II	DMXBA Polatuzumab Pinatuzumab Lifastuzumab AGS-16C3F Denintuzumab Depatuxizumab	All structures were isolated from Mollusk/ cyanobacterium associations	All structures are antibody conjugates	All structures have been investigated as anticancer drugs
	Lurbinectedin	Tunicate	Alkaloid	Cancer

	GTS 21	Worm	Alkaloid	Neurologic disorders
Phase I	Tisotumab Enfortumab MLN-0264 SGN-LIV1A ASG-15ME ASG-67E ABBV-838 ABBV-221 ABBV-399 ABBV-085 GSK2857916	All structures were isolated from Mollusk/ cyanobacterium associations	All structures are antibody conjugates	All structures have been investigated as anticancer drugs
	Bryostatin Marizomib PM060184	Bryozoan Bacterium Sponge	Macrolide Lactone Polyketide	All structures have been investigated as anticancer drugs

It is often thought that bacteria associated with macroscopic organisms produce the bioactive compounds (*23*). In some cases, it was indeed shown that microorganisms are responsible for the biosynthesis of active compounds (*18, 24*). This idea was recently illustrated by findings involving a strain of the marine bacterium *Labrenzia* sp. PHM005 (*25*). This marine sponge-associated microorganism was found to be the producer of a pederin-like substance with cytotoxic and antiviral capacities (Figure 1-3). These observations find further support in the insights gained through genomic mining experiments, which constantly reveal the biosynthetic potential encoded in bacterial genomes (*26–28*). Additionally, experiments involving sponge metagenomic sequencing revealed the bacterial origin of pederin-like molecules in sponges (*29*).

A) Pederin   **B)** Pederin-like compound
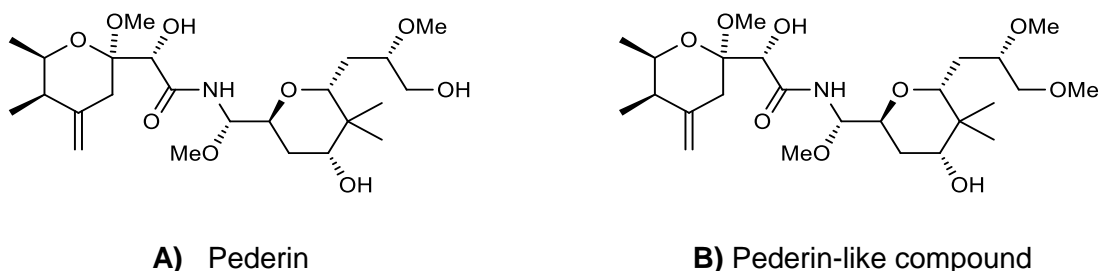
Figure 1-3 A) The structure of the antiviral and cytotoxic compound pederin is presented according to (*30*). Pederin was initially thought to be produced by the beetle *Paederus sabaeus*, but nowadays it is accepted that its endosymbiotic bacteria produce this compound and also bioactive derivatives thereof (*31*). **B)** The pederin-like compound modified from (*25*) is produced by the halophilic bacterium *Labrenzia* sp PHM005 and has shown cytotoxic activity against four different human cell lines: A549 (ATCC CCL-185) (lung carcinoma); HT-29 (ATCC HTB-38) (colon adenocarcinoma); MDA-MB-231 (ATCC HTB-26) (breast adenocarcinoma); and PSN-1 (ATCC CRL-3211) (pancreas adenocarcinoma).

This example proves that *in silico* explorations are a helpful tool for the isolation of compounds, and prediction of potential production of molecules, and their chemical nature. Further advantages of this approach were demonstrated through the isolation of the antimicrobial compound foxicin A (see Figure 1-4), which is produced by the terrestrial bacterium *Streptomyces diastatochromogenes* strain Tü6028 (*32*).
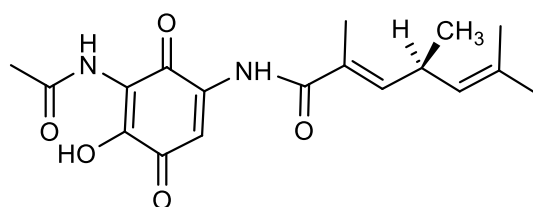
A) Foxicin A
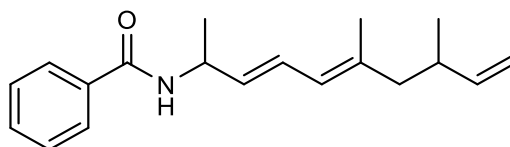
B) Haliamide

Figure 1-4 The terrestrial-derived antimicrobial compound foxicin A **A)** as presented by (*32*) and the marine-derived antitumor haliamide **B)** as presented by (*33*). These molecules represent results of successful *in silico* screening for biosynthetic genes with subsequent isolation of bioactive compounds.

Additional examples of these strategies are provided elsewhere (*34, 35*). Concerning marine-derived bacteria, *in silico* and chemical screening of the metabolome of the myxobacterium *Haliangium ochraceum* SP1 lead to the structural elucidation of haliamide (see Figure 1-4), a promising antitumor compound (*33*). Within this context, marine-derived myxobacteria represent a fruitful research topic concerning natural products. Recent works provide information yielded by experiments conducted *in silico* on genomes of marine myxobacteria, whereby gene clusters of putative secondary metabolites of diverse chemical nature, *e.g.* terpenes, polyketides, non-ribosomal peptides and hybrids thereof were detected (*36*).

1.3. Clinical applications of secondary metabolites: tackling antibiotic resistance.

Antibiotic resistance is one of the adaptation skills developed by pathogenic microorganisms. This phenomenon emerged almost simultaneously with the first prescription of antibiotics to treat infections about 80 years ago (*37*). Figure 1-5 illustrates the breakthrough of new drugs over time and the emergence of their first resistant bacterial pathogen (*38*).
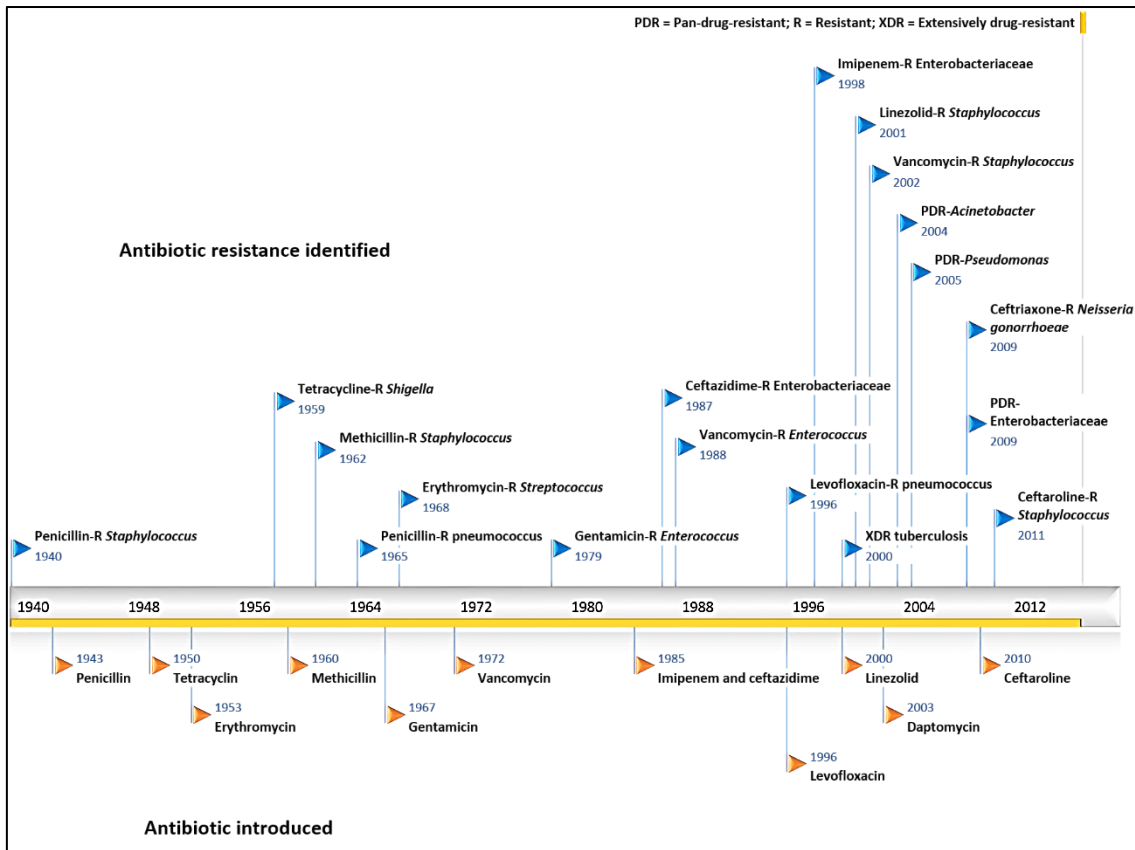
Figure 1-5 This timeline modified from Ventola *et al* (*38*) depicts clearly the constant appearance of antibiotic resistance along with the discovery and application of novel drugs. According to the author (*38*), penicillin was in limited use prior to widespread population usage in 1943.

Interestingly, Figure 1-5 shows that bacterial pathogens often require less than 10 years to undermine the efficacy of treatments, posing serious threats to human life and consequently to the public healthcare providers worldwide. Even the latest defensive lines, i.e damptomycin and ceftaroline have been overthrown. This is a heavy burden considering that multidrug-resistant pathogens develop infections usually in hospitalized patients with preexisting conditions, adding up to the severity of their ailments and thus to the cost of the medical care. Barriere and McGowan's publications provide deeper details regarding the economic implications of antibiotic resistance (*39, 40*).

In light of the global growing concern about antibiotic resistance, the potential and applications of marine-derived compounds in antimicrobial therapy are one of the main

goals in the field of modern natural product research. Thus, it is urgent to find novel structures to overcome, at least for some time, the resistance of pathogens.

The aforementioned premise, highlighting the structural novelty of marine-derived compounds, allows us to think that the ocean could provide efficient antimicrobials with novel mechanisms of action against pathogenic targets, which have successfully developed resistance to the drugs in use hitherto.

2. SCOPE OF THE PROJECT

The marine environment is a source of chemical compounds with unprecedented structures and probably, novel or improved biological effects within the context of clinical applications.

This work consists of investigations on marine-derived bacteria. The research conducted comprehends *in silico* genomic explorations of myxobacteria in order to evaluate their potential as producers of bioactive molecules.

Furthermore, bacterial isolates available in our group were investigated in their capacity to produce chemical substances of biological interest. From these investigations, two structurally unusual lipidic structures were obtained and were assessed as antimicrobial agents. Additionally, their possible role in inflammatory phenomena was investigated.

As a parallel objective, through the assessment of biological activities of the compounds isolated, it was intended to understand the ecological function of their microbial producers in the marine environment.

---

3. MATERIALS AND METHODS

3.1. Materials

3.1.1. Chemicals and solvents

Table 3-1 List of chemicals utilized for general procedures.

Chemicals	Manufacturer
Acetone	-----
Acetone – d	Deutero GmbH (Kastellaum, Germany)
Acetonitrile	VWR International GmbH (Darmstadt, Germany)
Agar	-----
Boric acid	Roth Chemie (Karlsruhe, Germany)
$CaCl_2$ x $2H_2O$	Merck KgaA (Darmstadt, Germany)
Chloroform – d	Deutero GmbH (Kastellaum, Germany)
DCM	Dichloromethane
DMSO	Roth Chemie (Darmstadt, Germany)
dNTPs	Promega GmbH (Mannheim, Germany)
Ethanol 99.8 p.a.	Roth Chemie (Karlsruhe, Germany)
Ethidium bromide	Roth Chemie (Karslruhe, Germany)
Ethyl acetate	---
Gel loading dye (6x)	Fermentas GmbH (St. Leon Rot, Germany)
Isopropanol	Roth Chemie GmbH (Karlsruhe, Germany)
Methanol	---
Methanol – d	Deutero GmbH (Kastellaum, Germany)
$MgCl_2$ x $6H_2O$	Merck KGaA (Darmstadt, Germany)
NaOH	Merck KGaA (Darmstadt, Germany)

peqGOLD Agarose	PEQLAB Biotecnologie GmbH (Erlangen, Germany)
Phosphoric acid	Roth Chemie (Karlsruhe, Germany)
Sepabeads 207	Supelco (USA)
Silica gel 60	Merck KgaA (Darmstadt, Germany)

Organic solvents such as chloroform, dichloromethane, ethyl acetate, acetone, and methanol were distilled prior to use. Water for HPLC and molecular biology assays was obtained from a Milli-Q Water Purify.

3.1.2. Antimicrobials

Table 3-2 List of antimicrobials employed for different purposes in this work.

Substance	Manufacturer
Ampicillin	Roth Chemie GmbH (Karlsruhe, Germany)
Streptomycin	Sigma Aldrich Co. LLC (St. Louis, MO, USA)
Miconazole	Sigma Aldrich Co. LLC (St. Louis, MO, USA)
Cycloheximide ≥96 %	Roth Chemie GmbH (Karlsruhe, Germany)

Ampicillin was necessary for the transformation of *E. coli* competent cells in LB-ampi medium. Additionally, was used as positive control in disc diffusion tests, as well as streptomycin and miconazole. Cycloheximide was needed to suppress fungal growth in WCX agar plates for isolation of bacteria.

3.1.3. Enzymes

Table 3-3 Enzymes used in molecular biology for cloning purposes.

Enzyme	Manufacturer
GoTaq Flexi DNA polymerase	Promega (Mannheim, Germany)
Proteinase K	Roth (Karlsruhe, Germany)
Restriction enzymes	Fermentas GmbH (St. Leon-Rot, Germany)
RNase (DNase free)	Promega (Mannheim, Germany)
T4DNA ligase	Fermentas GmbH (St. Leon-Rot, Germany)

3.1.4. Kits, standards and buffers

Table 3-4 Kits used in molecular biology for cloning purposes.

Article	Manufacturer
Gene rulerTM DNA ladder mix	Fermentas GmbH (St. Leon-Rot, Germany)
PureYieldTM Plasmid Miniprep System	Promega (Mannheim, Germany)
QIAprep Spin Miniprep Kit	Quiagen GmbH (Hilden, Germany)
QIAquick Gel Extraction Kit	Quiagen GmbH (Hilden, Germany)
QIAquick PCR purification Kit	Quiagen GmbH (Hilden, Germany)
TBE (10x)	0.89 M Tris base, 0.02 M EDTA, 0.87 M boric acid, pH 8.3
Wizard SV Gel and PCR Clean-Up System	Promega (Mannheim, Germany)

3.1.5. Culture media and related dissolutions

Table 3-5 Media for cultivation and isolation of bacteria and complementary substances utilized are listed.

Name	Constituents and proportions
Artificial sea water 100%	0.1 g KBr, 23.48 g NaCl, 10.61g $MgCl_2$ $6H_2O$, 1.47 g $CaCl_2$ $2H_2O$, 0.66 KCl, 0.04 g $SrCl_2$ $6H_2O$, 3.92 g Na_2SO_4, 0.19 g $NaHCO_3$, 0.03 g H_3BO_3, 1 L distilled water
ASW-WCX	15 g agar in 1 L ASW (75%); after autoclaving 1 mL vitamin B12, 1 mL trace element solution, 2 mL cycloheximide
Casitone broth	Casitone pancreatic digest of casein 1.0 g BD Bacto™ 225930, 100 mL distilled water, pH 7.5
CY/ASW	3.0 g casiton, 1.0 g yeast extract in 1 L artificial sea water, pH 7.2; after autoclaving add 1 ml filter sterilized trace element solution and 1 ml vitamin B12 solution (0.5 mg/ml)
CY/ASW agar	3.0 g casiton, 1.0 g yeast extract in 1 L artificial sea water, 15 g agar, pH 7.2; after autoclaving add 1 ml filter sterilized trace element solution and 1 ml vitamin B12 solution (0.5 mg/ml)
Halophilic	Bacteria that require sea-like salinity conditions to grow
Halotolerant	Bacteria able to grow in presence of sea-like salinity conditions as well as in the absence of salt
LB - ampicillin medium	10 g tryptone, 5 g yeast extract, 10 g NaCl in 1 L of water, pH 7.5; after autoclaving 1 mL of ampicillin 100

	mg/mL are added. 15 g/L were added to produce solid medium.
LB agar	10 g tryptone, 5 g yeast extract, 5 g NaCl, 15 g Agar, in 1 L of water, pH 7.5
LB medium	10 g tryptone, 5 g yeast extract, 10 g NaCl in 1 L of water, pH 7.5
Marine agar	Bacto peptone 5.00 g, Yeast extract 1.00 g, Fe(III) citrate 0.10 g, NaCl 19.45 g, Na_2CO_3 0.16 g, Na_2SO_4 3.24 g, $CaCl_2$ 1.80 g, $MgCl_2$ 8.80 g, KCl 0.55 g, KBr 0.08 g, $SrCl_2$ 34.00 mg H_3BO_3 22.00 mg, Na-silicate 4.00 mg NaF 2.40 mg, $(NH_4)NO_3$ 1.60 mg, Na_2HPO_4 8.00 mg, 1 L distilled water, 15 g agar, pH 7.5
Marine broth Difco 2216	Bacto peptone 5.00 g, Yeast extract 1.00 g, Fe(III) citrate 0.10 g, NaCl 19.45 g, Na_2CO_3 0.16 g, $NaSO_4$ 3.24 g, $CaCl_2$ 1.80 g, $MgCl_2$ 8.80 g, KCl 0.55 g, KBr 0.08 g, $SrCl_2$ 34.00 mg H_3BO_3 22.00 mg, Na-silicate 4.00 mg NaF 2.40 mg, $(NH_4)NO_3$ 1.60 mg, Na_2HPO_4 8.00 mg, 1 L distilled water, pH 7.5
SOC broth	20 g trypton, 5 g yeast extract, 0.5 g NaCl, 2.5 mL 1 M KCl, 1 L distilled water; after autoclaving 20 mL glucose 1 M
Trace element solution	20 mg $ZnCl_2$, 100 mg $MnCl_2$ x $4H_2O$, 10 mg boric acid, 10 mg $CuSO_4$, 20 mg $CoCl_2$, 5 mg $SnCl_2$ x $2H_2O$, 5 mg LiCl, 20 mg KBr, 20 mg KI, 10 mg Na_2MoO_4 x $2H_2O$ and

	5.2 g Na$_2$-EDTA x 2H$_2$Oin 1 L of water. The solution was sterilized by filtration.
VY/2	50 ml sterilized baker's yeast suspension (10%), 1.36 g CaCl$_2$ x 2 H$_2$O, in 1 L of water, pH 7.2; after autoclaving add 1 ml filter sterilized vitamin B12 solution (0.5 mg/ml)
VY/4-ASW	25 mL sterilized baker's yeast suspension, 375 mL artificial sea water 200%, in 600 mL distilled water (75%), pH 7.5; after autoclaving 1 ml filter sterilized trace element solution and 1 ml vitamin B12 solution (0.5 mg/ml)

3.1.6. Microorganisms

Table 3-6 Fungi and bacteria used as test strains for DDT are shown. The table includes microorganisms used for genomic mining and bacteria isolated during the present work, as well as the competent E. coli cells used for cloning.

Organism	Source
Arthrobacter crystallopoietes DSM 20117	Deutsche Sammlung von Mikroorganismen und Zellkulturen
Bacillus megaterium DSM32	Deutsche Sammlung von Mikroorganismen und Zellkulturen
Bacillus subtilis 168	MiBi collection
Candida albicans I-11134	MiBi collection
Candida albicans I-11301	MiBi collection
Citrobacter freundii I-11090	MiBi collection
Corynebacterium xerosis Va167198	MiBi collection
Echerichia coli I-11276b	MiBi collection

Echerichia coli O-19592	MiBi collection
Enhygromyxa salina DSM 15201	NCBI GenBank
Enterococcus faecium I-11054	MiBi collection
Enterococcus faecium I-11305b	MiBi collection
Escherichia coli DSM498	Deutsche Sammlung von Mikroorganismen und Zellkulturen
Eurotium rubrum DSM 62631	Deutsche Sammlung von Mikroorganismen und Zellkulturen
Haliangium ochraceum DSM 14365	NCBI GenBank
Klebsiella pneumoniae subsp. *ozeanae* I-10910	MiBi collection
KNS I-10925	MiBi collection
Labrenzia alba CECT5094	Colección Española de Cultivos Tipo
Labrenzia alba CECT5095[T]	Colección Española de Cultivos Tipo
Labrenzia alba CECT5096	Colección Española de Cultivos Tipo
Labrenzia alba CECT7551	Colección Española de Cultivos Tipo
Labrenzia sp. strain 011 (Ostsee6)	This study
Listeria welchimeri DSM 20650	Deutsche Sammlung von Mikroorganismen und Zellkulturen
Lysobacter sp	This study
Microbotryum violaceum MB#110229	MiBi collection
Micrococcus luteus ATCC 4698	MiBi collection
MRSA LT-1334	MiBi collection
MRSA LT-1338	MiBi collection
MRSE LT-1324	MiBi collection
MSSA 5185	MiBi collection
MSSA I-11574	MiBi collection

Mycobacterium smegmatis ATCC 70084	MiBi collection
Mycotypha microspora MB#271115	MiBi collection
Nannocystis exedens ATCC 25963	NCBI GenBank
Plesiocystis pacifica SIR 1	NCBI GenBank
Pseudomonas aeruginosa I-10968	MiBi collection
Pseudoroseovarius crassostreae DSM 16950	Deutsche Sammlung von Mikroorganismen und Zellkulturen
Saccharomyces cerevisiae	MiBi collection
Staphylococcus aureus 133	MiBi collection
Staphylococcus aureus SG 511	MiBi collection
Staphylococcus simulans 22	MiBi collection
Stenotrophomonas maltophilia I-10717	MiBi collection
Stenotrophomonas maltophilia O-16451	MiBi collection
Unknown bacterium called Siel 3	This study
Unknown bacterium called Siel 4	This study
XL1-Blue *E. coli* cells	Stratagene (La Jolla, CA, USA)

3.1.7. Vectors

Table 3-7 Here are shown the cloning vector used for 16S rDNA fragments during bacterial identification

Vector	Resistance	Manufacturer
pGEM-T easy	Ampicillin	Promega (Mannheim, Germany)

3.1.8. Cell cultures

Table 3-8 Embryonic kidney cells were used for cytotoxic assays

Cell type	Source
HEK293 ACC 305 embryonic kidney cell line	Deutsche Sammlung von Mikroorganismen und Zellkulturen

3.1.9. Primers

Primers used in this study were purchased from Eurofins MWG Operon (Ebersberg, Germany). After the reception, the oligonucleotides were dissolved in nuclease-free water to a concentration of 100 pmol/µl and stored at -20°C.

Table 3-9 Classic pair of primers pA/pH employed for identification of bacterial isolates

Primer	Sequence (5' to 3')	Purpose
pA	AGAGTTTGATCCTGGCTCAG	Identification of bacteria based on 16S rDNA
pH	AAGGAGGTGATCCAGCCGCA	

3.1.10. Software and databases

The bioinformatic analyses in this work were carried out mainly on NCBI platforms for genomic comparisons and identification of bacteria (mostly BLAST (*41*)); the prediction of secondary metabolite production from putative secondary metabolite gene clusters was implemented on antiSMASH (antibiotics and Secondary Metabolite Analysis SHell) software version 4.0.0 (*42*). For phylogenetic analyses, Clustal Omega was employed (*43*).

Table 3-10 Most frequently used software for bioinformatics

Software	Hyperlink	Reference
antiSMASH	http://antismash.secondarymetabolites.org/	(*42*)
Clustal omega	http://www.ebi.ac.uk/Tools/msa/clustalo/	(*43*)
NCBI/BLAST	https://blast.ncbi.nlm.nih.gov/Blast.cgi	(*41*)
PRINSEQ	http://edwards.sdsu.edu/cgi-bin/prinseq/prinseq.cgi?home=1	(*44*)

3.2. Microbiology methods

3.2.1. Isolation of bacteria from environmental samples

Environmental samples, *i.e.* sea sediment, algae, and marine mussels are put to dry for 24 hours. Once humidity decreases, small portions of them are placed on WCX-ASW agar plates on top of *E.coli* suspension spots. The Petri plates are then incubated and bacterial growth is monitored daily. Bacteria displaying one or all of the following traits: gliding motility, pigment production, lysis of *E. coli* spots, are transferred to VY/4 – ASW and VY/2 agar plates. Bacteria able to grow in both media are considered halotolerant; bacteria able to grow only on VY/4 – ASW (marine medium) are considered halophilic; bacteria able to grow only on VY/2 medium are considered terrestrial.

3.2.2. Gram staining modified from (*45*)

The Gram staining was performed using a modified and thereby simplified version of the standard procedure. First, a smear of bacteria was produced on a glass slide and heat-fixed using a Bunsen burner. 5 drops of crystal violet solution (2 g of crystal violet, dissolved in 10 ml ethanol, mixed with 50 ml water) were added and allowed to stand for 1 minute.

The stain was then gently rinsed off with water. Next, 5 drops of a 0.05 M iodine solution were added. After 30 seconds, the iodine solution was washed off with water. Decolorising solution (equal volumes of 95 % ethanol and acetone) was added until the decoloriser running down the slide was colorless. The remaining solution was then washed off with water. As a counterstain, 5 drops of a 0.2 % safranin solution were added. The safranin solution was washed off after 20 seconds and after the slide had dried, it was analysed under a light microscope using 1,000-fold magnification.

3.2.3. Preserving stock cultures

Bacteria isolated from environmental samples and certified bacterial strains purchased were grown according to standard protocols for five days in broth and stored in cryovials with 1% casitone broth 1:1 (v/v) at - 80°C (long-term storage). Bacteria described in chapter 3 were stored with glycerol instead of casitone broth 1%.

3.2.4. Cultivation of *Labrenzia alba*

Strains of *L. alba* CECT were reactivated from freeze-dried cultures according to provider's instructions and cultivated on marine agar plates; subsequently grown in marine broth in different scales, either for large-scale cultivation or small cultures for cryopreservation and storage purposes.

3.2.5. Cultivation of bacteria isolated in our group

Bacteria from chapter 2 and 3 were isolated accordingly as shown in section 3.2.1 and stored as described in section 3.2.3.

3.2.6. Bacterial pre-cultures in marine broth

Cryo cultures of the organism were thawed and placed in Petri dishes containing marine agar. The plates were incubated for three days. Thereafter, agar blocks of 1 cm were placed in 100 mL of marine broth previously adjusted to pH=7.6 with NaOH and incubated with shaking (120 rpm) at 30°C. These cultures were inoculated in

3.2.7. Large scale cultivation in marine broth

3.2.8. Sterilization

Every process intended to sterilize heat-resistant dissolutions, culture media, suspensions, and solid or liquid waste were carried out in steam sterilizers at 120°C for 20 min.

3.2.9. Disc diffusion test

This is a qualitative assay to determine the antimicrobial capacity of extracts and pure substances isolated from our bacteria. It was conducted according to Schulz (*46*). The following Bacteria and fungi were used as test organisms: Bacteria: *Escherichia coli* DSM 498, *Bacillus megaterium* DSM 32, *Pseudoroseovarius crassostreae* DSM 16950; fungi: *Eurotium rubrum* DSM 62631, *Mycotypha microspora* (this study), *Microbotrium violaceum* (this study)

50 μg of extract or pure compounds evaluated were taken from a solution of 1 mg/mL of extract or pure compound and applied on sterile paper discs on agar plates of the corresponding medium for each test organism. Thereafter, suspensions of the organisms were sprayed on the agar and incubated. Miconazole (50 μg), streptomycin (50 μg) and ampicillin (50 μg) were used as positive controls. Inhibition zones were measured from the edge of the disc to the end of the area free of growth. Only total inhibition (>1mm) was considered as a positive result.

3.2.10. Cytotoxicity test

Dr. Nicole Merten kindly conducted cell viability assays in the group of Prof. Dr. Evi Kostenis. Cell viability was assessed using a fluorimetric detection of resorufin (CellTiter-Blue Cell Viability Assay, Promega). HEK293 cells were seeded at a density of 27,000 cells per well into black 96-well poly-D-lysine–coated plates with clear bottom. Three hours after seeding cells were treated with 0.3% DMSO or compound dissolved in medium for 24 h. To detect cell viability, CellTiter-Blue reagent was added and cells were

incubated for 1 h at 37°C according to the manufacturer's instructions. Fluorescence (excitation 560 nm, emission 590 nm) was measured using a FlexStation 3 Benchtop Multimode Plate Reader and data were expressed as percentage of cell viability relative to DMSO control. (The cytotoxic anticancer drug etoposide was used as a positive control).

3.3. Physical – chemical methods

3.3.1. Liquid-liquid extraction

This protocol is employed to separate substances between two immiscible solvents (aqueous-organic). Substances of interest were found in the organic phase of the system. This process was rutinarily done in glass-made separation funnels of different capacities.

3.3.2. Standard method for recovery of secondary metabolites

Culture media with the organism of interest were added with 20 g of sepabeads 207 (brominated styrene-divinylbenzene adsorbent media, Supelco, USA) per liter of culture after corresponding cultivation time for each microorganism and left in contact for 24 hours in shaking condition at cultivation temperature (30°C). The resin was recovered and transferred into a suction strainer and washed with distilled water to remove adhered cells and hydrophilic compounds, *e.g.* sugars. Afterwards, the resin beads were exhaustively extracted with acetone to recover adsorbed substances (secondary metabolites mixed with unwanted compounds such as fat and similar). The acetone fraction containing the solids was evaporated yielding a crude extract, which was re-dissolved in 60 mL DCM. This Solution was extracted three times with 50 mL aqueous methanol (60:40) according to section 3.3.1. The Organic phase was evaporated and the residue analysed with various instrumental techniques.

3.3.3. Vacuum liquid chromatography

Normally, silica gel was used as stationary phase in the glass column capable to couple with vacuum pumps. The crude extracts were places atop the surface of the silica gel in the column and eluted with a gradient of increasing polarity, starting with petroluem ether as fist solvent, ethyl acetate as second solvent, acetone as third solvent, and methanol as fourth solvent. Amounts of solvents were used according to the needs of each experiment. The fractions collected were evaporated under vacuum and used for different biological testing.

3.4. Molecular biology methods

3.4.1. Genomic DNA isolation

Axenic cultures of bacteria were retrieved from 100 mL of corresponding broth for each bacterium after 5 days of growth with constant shaking at 30°C. The bacterial genome was extracted for gene isolation and amplification purposes. The extraction protocol was conducted using the Wizard Genomic DNA Purification Kit (Promega, Mannheim, Germany).

3.4.2. Polymerase Chain Reaction (PCR)

PCR is an *in vitro* technique used for the amplification of genes of interest. Specific primers (pA/pH) complementary to the regions flanking the 16S rDNA gene were employed for identification of bacterial isolates. Standard conditions of PCR protocol are described in the following tables:

Table 3-11 Description of the amounts of each reagent necessary to carry out the PCR protocol for amplification of genomic sequences of interest.

Reaction system	
Substance	**Volume**
5X *Taq*-buffer (green)	10.0 μL
DMSO	2.5 μL
dNTP mix (10mM)	1.0 μL
Forward primer (100 pmol)	1.0 μL
MgCl$_2$	2.5 μL
Reverse primer (100 pmol)	1.0 μL
Taq DNA Polymerase (5 units/μl)	0.5 mL
Template	2.0 μL
Water	29.5 μL

Table 3-12 Standard settings of the PCR thermal cycler devices.

Step	**Temperature**	**Time**	
Initial denaturation	94°C	2 min	
Denaturation	94°C	45 sec	
Annealing	55°C	1 min	30 cycles
Elongation	72°C	1 min	
Final elongation	72°C	4 min	

3.4.3. Agarose gel electrophoresis

Agarose gel electrophoresis is a common method used to separate DNA based on its molecular weight. Standard gels containing 1% electrophoresis grade agarose was used

to separate the DNA fragments. The electrophoresis was carried out with the running buffer (1X TBE) covering the gel. A volume range from 5-10 µl of 10 Kb DNA ladder was used as a standard size indicator. Electrophoresis was done in Horizon-58 and Horizon-11.14 gel chamber (Life Technologies, Karlsruhe, Germany) at a voltage of 100V during 40 min running time. To visualize the DNA, the gel was stained with ethidium bromide solution (10µg/ml) for 2 minutes. Subsequently, non-intercalated ethidium bromide was washed out for 2 minutes in demineralized water. DNA bands were visible under UV (254nm) and documented using intasiX imager (Intas Science Imaging Instruments GmbH, Göttingen, Germany).

3.4.4. DNA extraction from agarose gels

DNA fragments separated in the agarose gel were extracted and purified using Wizard SV Gel and PCR Clean-Up system (Promega, Mannheim, Germany) as per the manufacturer's instructions. The purified DNA was eluted with 30-50 µl water and stored at -20°C.

3.4.5. Ligation of PCR- amplified fragments

The PCR products were ligated into the plasmid using T4 DNA ligase. The reaction was performed in accordance to manufacturer's protocol using the pGEM-T and pGEM-T Easy Vector Systems (Promega, Mannheim, Germany). The product was used for transformation of *E. coli* XL1 blue competent cells.

3.4.6. Transformation of *E. coli* XL1 blue competent cells

In order to maximize the amplification of the PCR products, the pGEMT easy vector and the inserts were cloned in competent cells available in the S1 laboratory of the Institute for Pharmaceutical Biology of the University of Bonn. In order to achieve this goal, the frozen competent cells were thawed on ice for 5 min. 5µl of the plasmid DNA were added to the bacterial suspension and incubated on ice for 30 min. Then the cells were heat-shocked at 42°C for 50 sec. The cells were then incubated again on ice for 2 min. To the

cold shocked cells 900µl of LB medium was added and incubated at 37°C with shaking at 160 rpm for 1 hr. The cells were then centrifuged at 13,000 rpm for 5 min. The cell pellet was then resuspended in 300 µl of fresh LB medium. 100 µl of the cell suspension was then plated on LB agar plate containing ampicillin (100 µg/ml) as the selection marker. The plate was then incubated overnight at 37°C. The first-appearing colonies were selected and incubated overnight in 2 mL Eppendorf vials containing 1 mL LB-Ampicillin medium. Aliquots from each vial were then treated with the PureYield Plasmid Miniprep System in order to recover the plasmid. The final products were analysed by gel electrophoresis (section 3.4.3). The positive transformants were identified according to the expected size of the pGEM-T easy vector + PCR product (vector: 3 Kb + insert: 0.8 Kb ≈ 4 Kb). The vials containing the matching-size recombinant plasmids were sent for sequencing.

3.5. GPCR84 testing

The tests involved in this section were kindly conducted in the group of Prof. Dr. Christa Müller.

3.5.1. Biological assays

The recombinant CHO cell line expressing the human GPR84 (CHO-hGPR84 cells) with a β-galactosidase fragment and arrestin containing the complementary fragment of the enzyme for performing β-arrestin recruitment assays based on enzyme complementation technology with a luminiscent readout (Pathhunter®) was purchased from DiscoverX (Fremont, CA). This cell line was used for the β-arrestin recruitment assays as well as for cAMP accumulation and radioligand binding assays. The CHO-hGPR84 cells were cultured in F12 medium supplemented with 10% FCS, 100 units/mL penicillin G, 100 µg/mL streptomycin, 800 µg/mL G 418, 300 µg/mL hygromycin B, and 1% ultraglutamin (Invitrogen, Carlsbad, CA or Sigma-Aldrich, St. Louis, MO). Stock solutions of compounds including forskolin were prepared in DMSO (final DMSO concentration: 1 %). Data were analysed using Graph Pad Prism version 6.0 (San Diego, CA, USA).

Concentration-response data were fitted by nonlinear regression to estimate EC_{50} values. For the calculation of Ki values, the Cheng-Prusoff equation and a K_D value of 20.1 nM was used.

3.5.2. Radioligand binding assays

Radioligand binding assays were performed in 96-well plates as previously described (A). In brief, CHO cell membranes expressing GPR84 receptors (10 µg protein per vial) were incubated for 150 min at 25°C in 0.4 mL of a 50 mM Tris-HCl buffer (pH 7.4) containing 10 mM MgCl2, 0.05 % fatty acid free bovine serum albumin (BSA), 2 nM [³H]PSB-1584 (60 Ci/mmol) and increasing concentrations of test compound. Nonspecific binding was determined in the presence of 10 µM of unlabeled PSB-17365. Membrane-bound and free radioligand were separated by rapid filtration (GF/B-glass fiber filter) using a Brandel 96-channel cell harvester (Brandel, Gaithersburg, MD, USA) through Packard 96-well GF/B glass fiber filter plates. Filters were rinsed three times, 2 ml each, with ice-cold 50 mM Tris-HCl buffer, pH 7.4. Radioactivity of the wet 96-well filter plates was counted after 6 h of preincubation with 50 µL of Microscint-20 scintillation cocktail (Perkin Elmer, Rodgau, Germany). Three independent experiments, each in duplicates were performed.

3.5.3. cAMP accumulation assays

cAMP assays were performed as previously described [B, C]. In short, CHO cells overexpressing the human GPR84 were stimulated by addition of forskolin (10 µM) in the absence (control) or presence of test compound for 15 min. The reaction was stopped by the addition of hot (90°C) lysis solution containing 4 mM EDTA and 0.01 % Triton X-100 in water. cAMP levels were quantified by a radioactive assay using [³H]cAMP (Perkin-Elmer, Rodgau, Germany) and a cAMP binding protein prepared from bovine adrenal medulla. The forskolin-induced increase in cAMP concentration in the presence of test compound was expressed as percentage of the response to forskolin in

the absence of agonist (% of control). Three independent experiments, each in duplicates were performed.

3.5.4. β-Arrestin recruitment assays

β-Arrestin assays were performed as previously described [B, C]. Briefly, CHO cells expressing the human GPR84 with a β-galactosidase fragment and β -arrestin containing the complementary fragment of the enzyme (20,000 per well) were incubated with compound dilutions (in DMSO, final concentration: 1 %) for 90 min before adding the detection reagent (DiscoverX®). After 60 min of incubation at rt, the luminescence was measured using an NXT plate reader (Perkin-Elmer, Rodgau, Germany). Three to five independent experiments were performed, each in duplicates.

3.6. Instrumental analyses

3.6.1. Flash chromatography

For the first fractionation step of the crude extracts from the adsorption resin, a Reveleris® X2 chromatography system with evaporative light scattering detector (ELSD), UV detector, equipped with dry air supply was used. The column chosen was using a Reveleris silica column of 12 g (12 mg – 2.4 g sample load capacity, 12 μm). The mobile phase consisted of gradients of PE/Acetone. Equilibration time was 7.1 min. UV and ELSD detection thresholds were 0.05 AU and 20 mV, respectively. High ELSD sensitivity was chosen, slope detection high and dry flash mode. The flow rate typically used was 30 mL/min.

3.6.2. High Performance Liquid Chromatography

High performance liquid chromatography was executed on a Merck-Hitachi L-6200A Intelligent Pump device coupled to a diode array detector L-4500A. Mobile phases consisted of Water/MeOH and Water/ACN, each component added with H_3PO_4 at a concentration of 0.1 M). The column YMC-triart C18 / S-5μm /12 nm (250 x 4.6 mm I.D) was employed for this purpose. The typical flow rate was 1 mL/min.

3.6.3. Mass Spectrometry

Mass spectra were recorded on a micrOTOF-Q mass spectrometer (Bruker) with ESI-source coupled with an HPLC Dionex Ultimate 3000 (Thermo Scientific) using an Agilent Zorbax Eclipse Plus C18 column (2.1 x 50 mm, 1.8 μm). The column temperature was 45 degree Celsius. HPLC begins with 90% H2O containing 0.1% acetic acid. The gradient starts after 1 min to 95% Acetonitrile (0.1% acetic acid) in 4 min. 2 μL of a 1mg/mL sample solution was injected to a flow rate of 0.8 mL/min.

3.6.4. Nuclear Magnetic Resonance Spectroscopy

All NMR spectra were recorded on a Bruker UltraShield operating at 300 MHz (1H) and 75 MHz (13C) with CDCl3 as the solvent. Spectra were referenced to residual solvent signals with resonances at δH/C-7.26/77.16 for CDCl3. The multiplicity of the carbons was deduced by DEPT135 experiments. Structural assignmnts were based on spectra resulting from the following NMR experiments: 1H, 13C, DEPT135, 1H-homonucelar decoupling, 1H-1H-COSY, 1H-13C-HSQC (direct correlation), 1H-13C- HMBC (long-range correlation), 1H-1H- NOESY.

3.6.5. UV-Visible spectrometry

UV spectra were recorded on a Perkin-Elmer Lambda 40 with UV WinLab Version 2.80.03 software. Quartz cells of 1 cm length were selected.

3.6.6. Polarimetry

Optical activity measurements were carried out on a Jasco J-810 spectropolarimeter with sodium lamp.

4. CHAPTER 1: Genome mining of myxobacteria grouped in the suborder Nannocystineae

4.1. Prefatory matters

Myxobacteria are famous for their ability to produce most intriguing secondary metabolites. Till recently, only terrestrial myxobacteria were in the focus of research. In this chapter, however, we discuss marine-derived myxobacteria, which are particularly interesting due to their relatively recent discovery and due to the fact that their very existence was called into question. The to-date-explored members of these halophilic or halotolerant myxobacteria are all grouped into the suborder Nannocystineae. Few of them were chemically investigated revealing around 11 structural types belonging to the polyketide, non-ribosomal peptide, hybrids thereof or terpenoid class of secondary metabolites. A most unusual structural type is represented by salimabromide from Enhygromyxa salina. *In silico* analyses were carried out on the available genome sequences of four bacterial members of the Nannocystineae, revealing the biosynthetic potential of these bacteria**.**

4.2. Taxonomy and ecology of myxobacteria

Bacteria from the order Myxococcales, commonly known as myxobacteria, are Gram-negative, rod-shaped δ-proteobacteria, comprising compared to many other bacteria large genomes. The 14,782,125 bp large genome of *Sorangium cellulosum* So0157-2 is the largest bacterial genome reported to date (*47*). Myxobacteria are able to glide over surfaces in swarms in order to facilitate heterotrophic nutrition on macromolecules as well as on whole microorganisms, a distinctive trait of these bacteria (*48*). Additionally, under adverse environmental conditions, *e.g.* nutrient shortages, high temperature and dryness, individuals cooperate to create intercommunicated multicellular myxospore-containing fruiting bodies in order to ensure the distribution of nutrients they can still

harness, allowing germination as soon as conditions are favorable for the vegetative phase again (*49*). Based on our experience in the laboratory, fruiting bodies can occur on solid surfaces like agar plates, as well as in liquid cultures. These adaptive strategies play a fundamental role on how these organisms are able to endure under unfavorable conditions (*50, 48*). In terms of oxygen demand for growth, myxobacteria were thought to be strictly aerobic until the only anaerobic genus known to date, Anaeromyxobacter, was reported in 2001 (*51*). Also, for many years myxobacteria were considered to typically occur only in terrestrial habitats and much has been published in terms of their morphology, physiology and ecology (*50, 48, 52, 53*).

Recently, ever more myxobacteria from intertidal and marine environments were reported. According to salt requirements for growth, a straightforward classification of these bacteria has been provided (*2*): (I) halotolerant strains are capable to grow with or without NaCl; and (II) halophilic bacteria are unable to grow without sea salt. Bacteria of group (I) may be derived from terrestrial organisms, which have adapted to saline conditions, whereas those of group (II) may be of truly marine origin.

A typical halotolerant myxobacterium, originally obtained from coastal samples, is the *Myxococcus fulvus* strain HW-1 (suborder Cystobacterineae). In this case, it was demonstrated that salt concentration not only affects growth, but also myxobacterial motility systems as well as fruiting body formation (*54*). In the absence of salt, both capabilities were diminished. Mutational studies imply that the single, probably horizontally transferred gene hdsp, which was found in five halotolerant Myxococcus strains, but not in soil-derived Myxococcus strains, leads among other changes to sea water tolerance (*55*).

Only few myxobacteria dwelling in sea habitats are considered as halophilic, that is, of true marine origin. Indeed, early isolates from marine environments were thought to be halotolerant terrestrial myxobacteria whose myxospores had been washed into the ocean (*56*).

This opinion prevailed until Fudou and Iizuka (*57–60*) discovered the first strictly halophilic myxobacteria within the suborder Nannocystineae, namely Enhygromyxa, Haliangium, and Plesiocystis, which strictly require sea-like salinity conditions in order to grow. Whether the adaptation to the marine environment was acquired independently several times, or if these entire marine clades share one common ancestor, is not clarified yet due to the relatively low number of species known to date.

Regarding the strategies employed by these bacteria to cope with salt and desiccation stress, the accumulation of organic osmolytes instead of the salt-in strategy can be expected. This hypothesis is supported by the fact that all strains investigated so far can grow within a relatively wide range of salinity. Also, the terrestrial strain M. xanthus, which is slightly halotolerant, uses organic osmolytes, *i.e.* glycine betaine to combat osmotic stress (*61*). Analyses on the osmoprotective strategies of *Enhygromyxa salina* SWB007 and *Plesiocystis pacifica* SIR-1 revealed that both closely related strains rely on organic osmolytes. For instance, *E. salina* SWB007 biosynthesizes the osmolytes betaine, ectoine, and especially hydroxyectoine under high salt concentrations. In contrast, *P. pacifica* SIR-1 does not synthesize specialized compatible solutes; this strain rather accumulates amino acids as osmoprotective agents (*62*). Of course, further mechanisms may be involved for osmoregulation, but are unknown to date for myxobacteria. A list of general bacterial osmoregulation processes is given elsewhere (*63*).

4.2.1. Secondary metabolites from myxobacteria

Members of the order Myxococcales are famous for their ability to produce secondary metabolites of diverse chemical nature with the capability to exert different biological effects (*64, 65*). Detailed descriptions of myxobacteria-derived metabolites can be found in various detailed reports (*65, 64, 66–68*). The majority of these metabolites are either non-ribosomal peptides, *e.g.* cystobactamids **1-3** (*69*), polyketides, *e.g.* aurafuron A **4** (*70*), or hybrids thereof, *e.g.* corallopyronin A **5** (*71*).

Cystobactamid 507 **1**

Cystobactamid 919-1 **2**

Cystobactamid 919-2 **3**
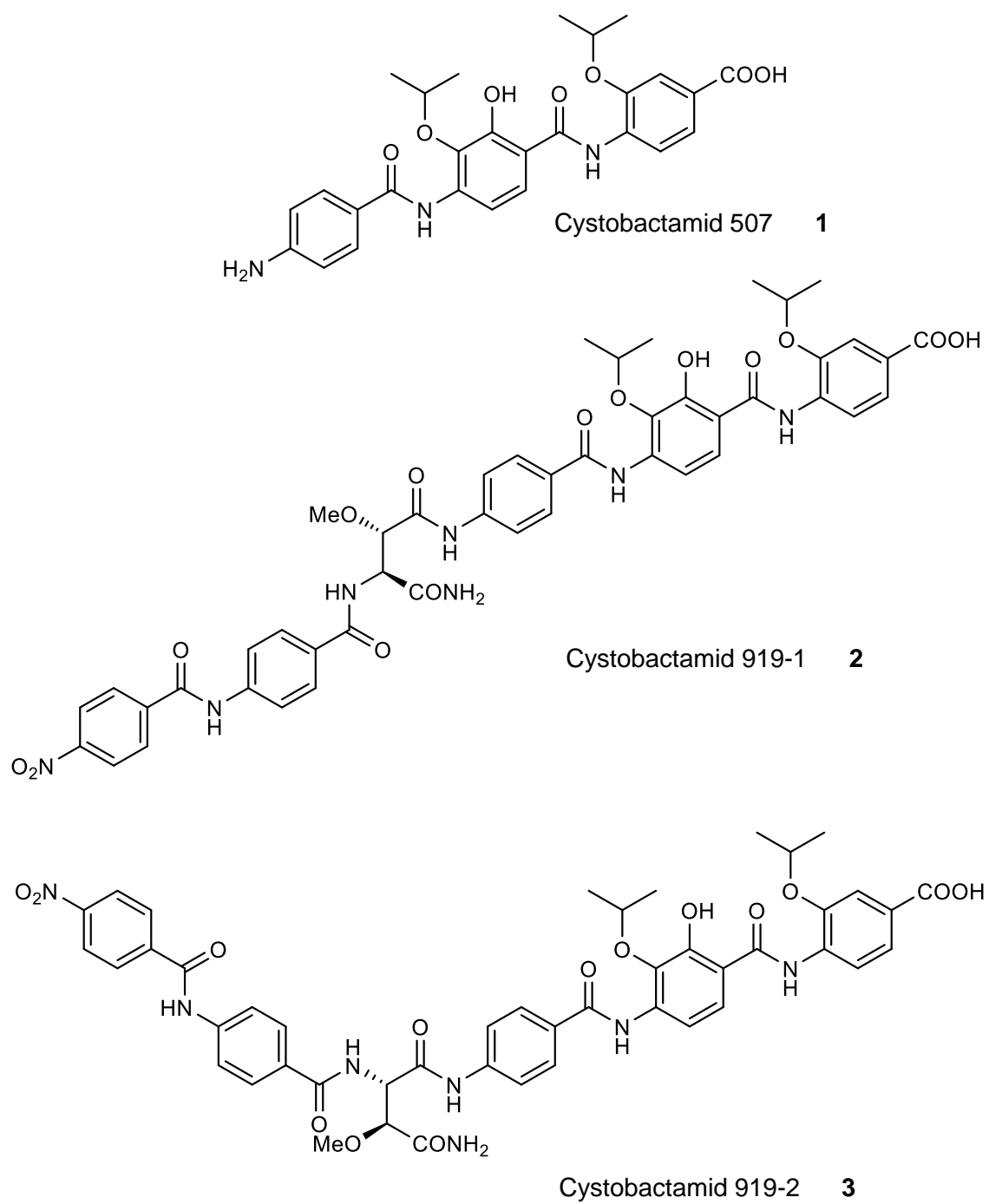
Figure 4-1 Structures of cystobactamids 507, 919-1 and 919-2.

Aurafuron A **4**
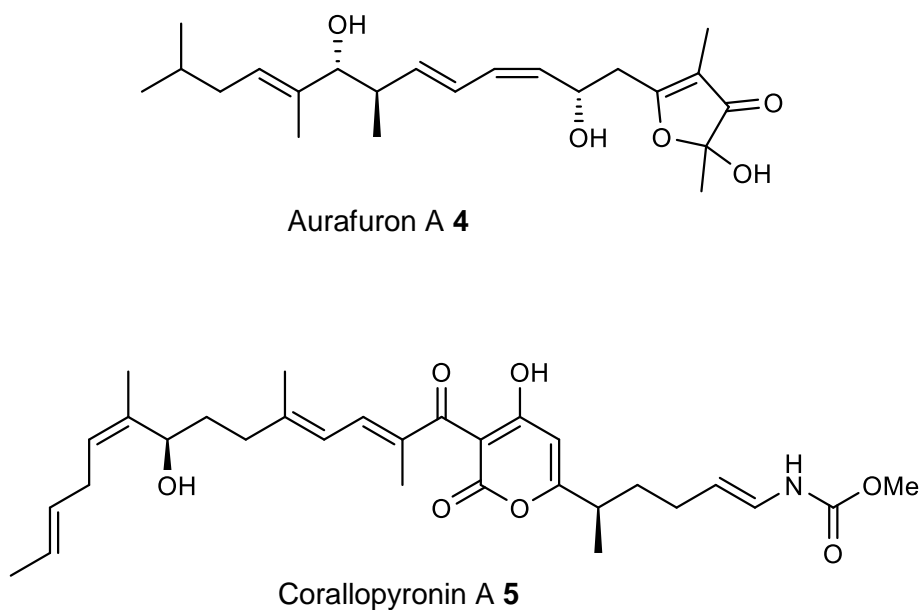
Corallopyronin A **5**

Figure 4-2 Structures of aurafuron A and corallopyronin

Interestingly, an ample amount of them was shown to work as antimicrobial agents, above all corallopyronin A. This is probably a reflection of their predatory habits (*72, 73*). A comprehensive description of antibiotics obtained from myxobacteria can be found in a previous review (*66*). One outstanding example of a biologically active PKS/NRPS-derived compound, produced by the terrestrial *S. cellulosum* is the microtubule stabilizer epothilone B. Its lactam analog, ixabepilone 6 is currently used together with capecitabine 7 in cancer therapy to improve the effectiveness of taxane-resistant metastatic breast cancer treatment, demonstrating the therapeutic potential of myxobacterial secondary metabolites (*74–76*). This drug has also been assessed as chemotherapeutic agent in pancreatic lymphoma showing promising results and tolerable toxicity (*77*).
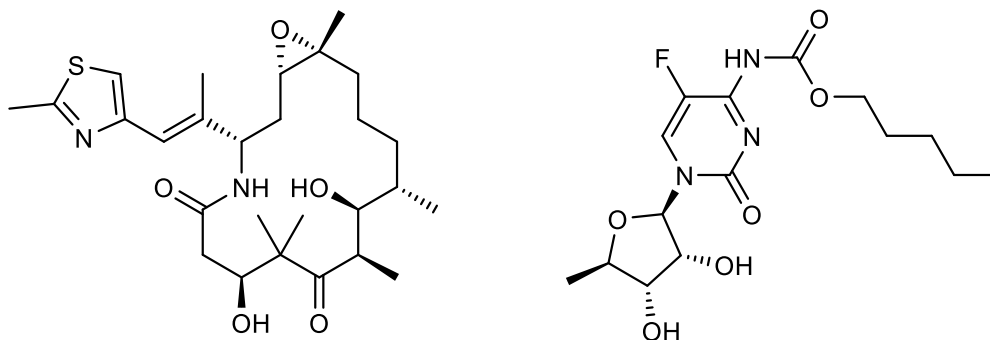
Ixabepilone **6** (Derived from the myxobacterial epothilone B (Hunt 2009)

Capecitabine **7**

Figure 4-3 Structures of ixabepilone and capecitabine.

Over time, different strategies have been designed to tackle the sometimes-cumbersome task of finding bioactive secondary metabolites of bacterial origin, *i.e.* mainly bioactivity- or chemistry-guided methods. An additional approach, complementary to the latter, arose in the late 1990s, when the first microbial genomes were sequenced, allowing genome mining. Thus, knowledge derived from bioinformatic analysis of microbial genomes paved the way to gain detailed insights into bacterial secondary metabolism. Since then, *in silico* methods for genome mining have enormously advanced, and effective experimental approaches for connecting genomic and metabolic information have been developed (*78–80*).

The terrestrial *Myxococcus xanthus* strain DK1622 was the first myxobacterium to have its 9.14 Mb genome sequenced, with the initial aim to study its swarming motility and fruiting body formation (*81*). At the same time, this work reinforced the notion that large genomes often correlate with the potential for prolific secondary metabolite production by revealing almost 8.6% of the genome to be possibly involved in the biosynthesis of secondary metabolites (*81*). Mining this genome for the presence of PKS and NRPS genes exposed 18 biosynthetic clusters, with a predominance of hybrid PKS-NRPS

systems (*82*). *M. xanthus* strain DK1622 is responsible for the synthesis of metabolites like DKxanthene-534 8, a pigment required for fruiting body formation and sporulation processes (*82*) and the siderophore myxochelin A 9, which belongs to a class of compounds that have recently been shown to have antiproliferative effects on leukemic K-562 cells (*72*).

Myxochelin A **9**
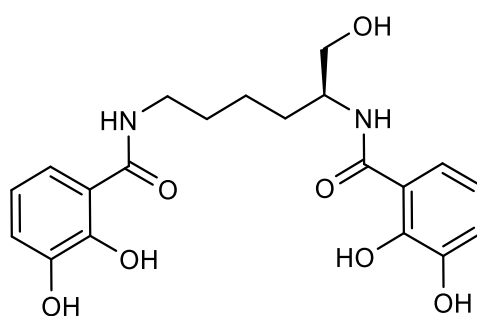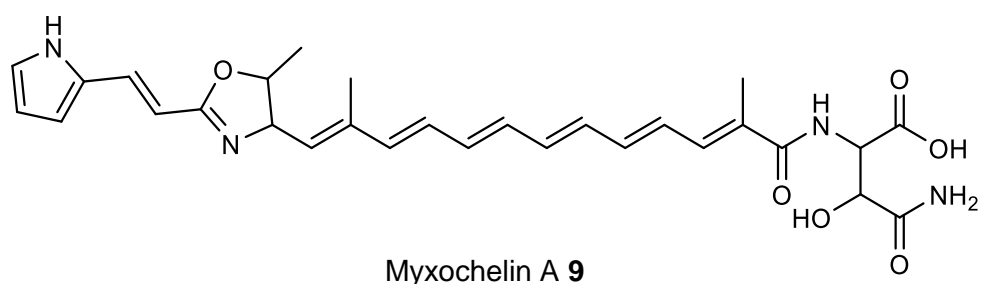
DKxanthene-534 **8**

Figure 4-4 Structures of DKxanthene-534 and myxochelin A.

.

Halotolerant and halophilic marine myxobacteria are poorly investigated regarding secondary metabolite production. Therefore, the pool of secondary metabolites isolated from organisms of this kind is very low to date, when compared to that of their terrestrial counterparts. This is mainly due to the difficulties that are encountered during isolation and cultivation processes of marine myxobacteria. However, herein we intend to show

that these organisms are a great research niche, which offers the opportunity to find novel bioactive compounds with the potential to become drug leads.

Regarding halotolerant myxobacteria, the 9 Mb genome of the *Myxococcus fulvus* strain HW-1 (ATCC BAA-855, suborder Cystobacterineae) was the first-of-its-kind to be sequenced (*83*). Genome mining performed in our group revealed that this organism displays, analogous to the previously discussed example *M. xanthus* strain DK1622, a plethora of cryptic gene clusters, *e.g.* five NRPS, four hybrid PKS-NRPS, one PKS-NRPS-lantipeptide, three lantipeptide and numerous bacteriocin- and terpene-encoding gene loci. A more detailed comparison revealed that both strains share the majority of their gene clusters, among them the aforementioned DKxanthene, the myxochromide (*65*) and myxoprincomide (*84*) pathways, besides other, yet uncharacterized loci. It is worth mentioning that no gene clusters involved in synthesis of osmolytes like betaine and ectoine were detected in the halotolerant bacterium.

4.3. Taxonomy, cultivation and secondary metabolite chemistry of marine-derived myxobacteria (Nannocystineae)

The following sections summarize features of three halotolerant and four marine-derived bacterial taxa clustered in the suborder Nannocystineae: Nannocystis, Haliangium, Enhygromyxa, Plesiocystis, Myxobacterium SMH-27-4 (*i.e.* Paraliomyxa) and Pseudenhygromyxa (see Figure 4-5).
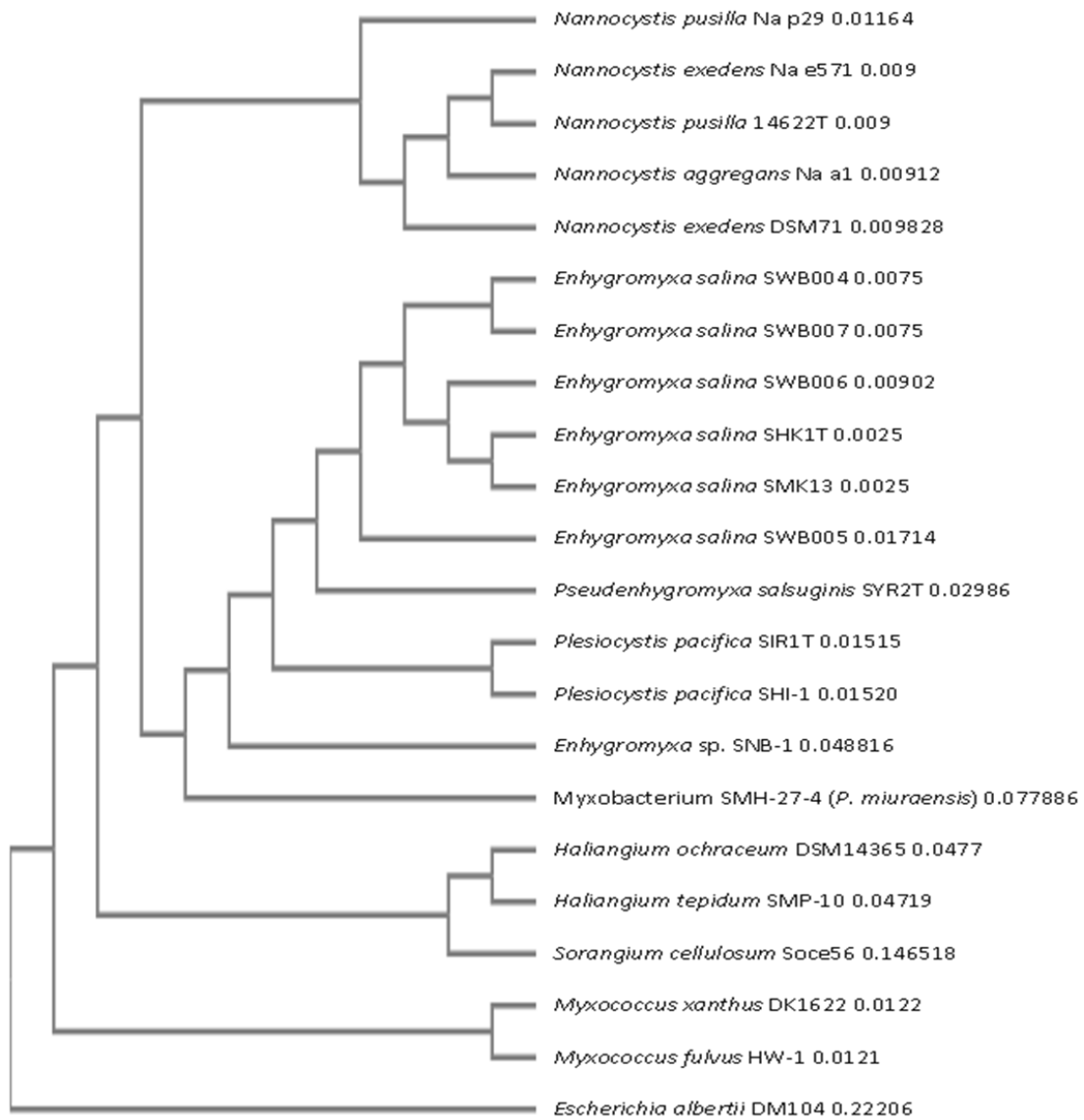
Figure 4-5 Phylogenetic tree of halotolerant and halophilic myxobacteria. The neighbor-joining tree is based on a multiple sequence alignment (MSA) of the 16S rDNA sequences. The terrestrial myxobacteria *Myxococcus xanthus* DK1622, *Sorangium cellulosum* Soce56as and *Escherichia albertii* DM104 are included for comparison. MSA was computed using MAFFT (Multiple Alignment using Fast Fourier Transform).

Information on strain isolation, culture conditions, phylogeny, genetics and hitherto isolated molecules will be provided, with an emphasis on structural details and biological activity of the metabolites. Additionally, putative gene clusters for secondary metabolite biosynthesis are included in this work. For this reason we were mining the four available

genomes from bacteria of the Nannocystineae using the antiSMASH (*42*)(see Table 4-1). The genome mining results are generated by feeding the software with the accession number (AN) of the annotated sequences. The databases are continuously updated, thus, results presented in this part of the work may vary in ulterior analyses. Our data, however, present a useful guide for future projects. For detailed information on terrestrial myxobacteria and other predatory bacteria, readers are referred to the review article from Korp (*85*).

Table 4-1 Summary of antiSMASH analysis (version 4.0.0) of the four available genomes of myxobacteria of the suborder Nannocystineae

	Halophilic/Halotolerant			Terrestrial
	Enhygromyxa salina DSM 15201	*Plesiocystis pacifica* SIR 1	*Haliangium ochraceum* DSM 14365	*Nannocystis exedens* ATCC 25963
Genome size (Mb)	10.44	10.59	9.45	11.61
GC%	67.4	70.7	69.5	72.2
Number of contigs	330	237	1	174
% of genome involved in secondary metabolism[1]	9.2	6.4	10.1	8.2
Total number of clusters	38	28	25	31
NRPS	2	1	3	1
PKS (including PKS hybrids)	13	11	2	2
NRPS/PKS hybrids	2	0	3	6
Terpene	7	6	3	10
Bacteriocin	6	6	5	3
Ribosomal peptides	0	0	4	1

Siderophore	2	1	0	2
Indole	1	0	0	0
Arylpolyene	2	1	0	2
Phenazine	0	0	0	2
Ectoine	0	0	1	0
Other	3	2	4	2

[1]Total bases of all detected antiSMASH secondary metabolite gene clusters divided by number of bases in the genome.

4.4. The genus *Nannocystis*

Bacteria of the genus Nannocystis are merely halotolerant and frequently isolated from terrestrial or intertidal regions. Back in the 1970s, the Reichenbach group informed on the isolation of a widely distributed soil-dwelling myxobacterium similar to members of the genus Sorangium in terms of cytology and growth pattern (*86*). After taxonomic studies, they proposed a new genus and species, *i.e. Nannocystis exedens*. Only recently, it has been recognized that members of this genus have a great potential as producers of metabolites with relevant biological activities. One striking example is the 2015 described nannocystin A **10**, a macrocyclic compound of NRPS-PKS origin with strong antiproliferative properties isolated from the terrestrial *Nannocystis sp.* ST201196 (DSM 18870) (*87*).
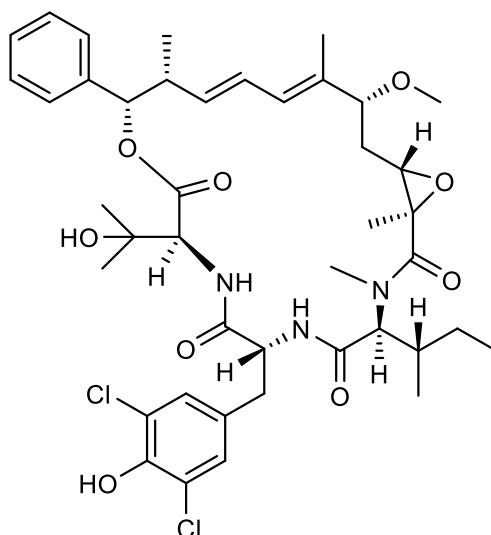
Nannocystin A **10**

Figure 4-6 Structure of nannocystin A.

It was subsequently shown that nannocystin A targets the eukaryotic translation elongation factor 1α, a promising novel target for cancer therapy (*87*). Regarding metabolites from halotolerant Nannocystis strains, the most outstanding examples are the phenylnannolones A-C **11-13**, molecules of polyketide nature with a phenylalanine-derived starter unit (*88*).
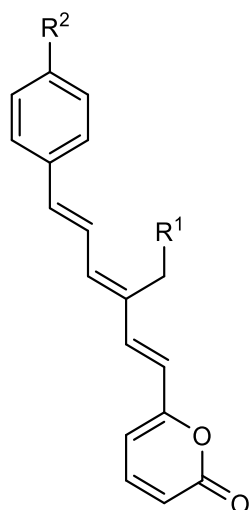
$R^1 = CH_3, R^2 = H$	Phenylnannolone A **11**
$R^1 = H, R^2 = H$	Phenylnannolone B **12**
$R^1 = CH_3, R^2 = OH$	Phenylnannolone C **13**

Figure 4-7 Structure of phenylnannolones A-C.

These compounds are synthesized by *N. exedens* strain 150, later reassigned to *N. pusilla,* isolated from the intertidal region of a beach in Crete (*88*). Cultivation of the regarding organism was carried out in liquid medium with the addition of adsorber resin. The adsorbed metabolites were then extracted and isolated via different chromatographic techniques. Phenylnannolone A **11** was found to be the main metabolite, which is accompanied by only minute amounts of the other derivatives **12** and **13**. Phenylnannolone A was proven to restore daunorubicin sensitivity in cancer cells by inhibiting P-glycoprotein (P-gp), an ATP-binding cassette transporter (ABC transporter). In tumor cells, P-gp serves as an efflux transporter of drugs, ultimately leading to treatment failure (*89*).

Apart from these polyketides, an array of nitrogen-containing metabolites was published recently by Jansen (*90*). They investigated three strains of *N. pusilla* isolated from coastal sediment samples - deemed halotolerant for this reason - for their secondary metabolite production. Two strains, Ari7 and Na a174 yielded a new class of halogenated pyrrole-oxazole compounds **14-18**. Pyrronazols A **14**, A2 **15** and B **16**, synthesized by Ari7, additionally include an α-pyrone-moiety (*91*).

This is worth noting, since the non-cyclic alkyl moiety in the pyrronazols C1 **17** and C2 **18**, found in strain Na a174, is supposed to be a result of degradation processes due to long-time cultivation. Additionally, the known compound 1, 6-dihydroxyphenazin **19** and its arabinofuranoside **20** were obtained.

To date, **14** has shown marginal antifungal activity towards *Mucor hiemalis* (DSM 2656) (MIC: 33.3 μg/mL) and **19** proved to have cytotoxic effects in the lower micromolar range against different cancer cell lines (*90*).
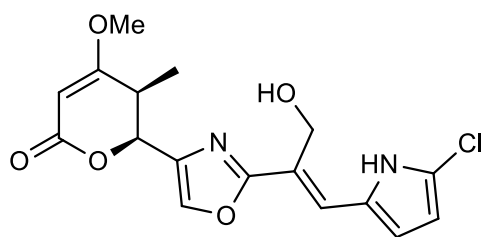
Pyrronazol A **14**
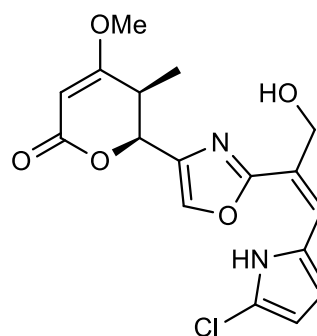
Pyrronazol A2 **15**
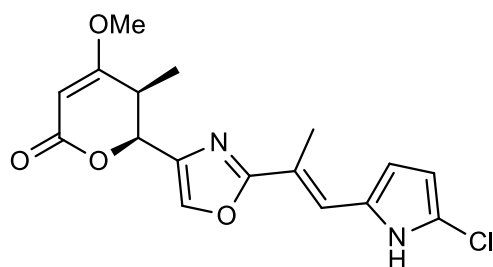
Pyrronazol B **16**
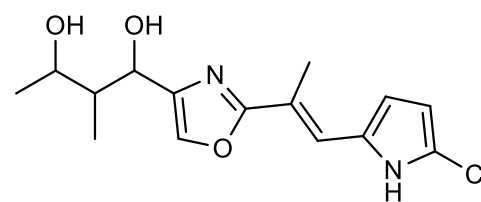
Pyrronazol C1 **17**
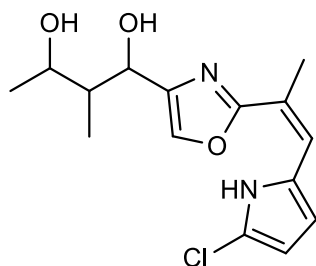
Pyrronazol C2 **18**
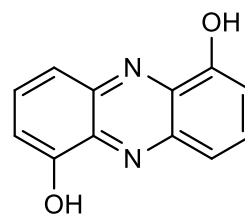
1,6-Dihydroxyphenazin **19**
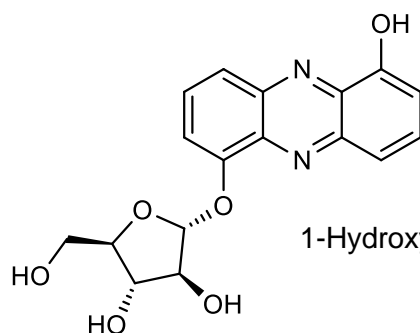
1-Hydroxyphenazin-6-yl-α-D-arabinofuranoside **20**

Figure 4-8 Structures of the pyrronazols, Dihydroxyphenazin and 1-hydroxyphenazin-6-yl-α-D-arabino-furanoside.

Nannozinones A 21 and B 22 are produced by *N. pusilla* strain MNa10913, isolated from a soil sample, collected in Mallorca, Spain (*92*). They represent novel pyrazinone type molecules. Additionally, the siderophore nannochelin A 23 also from other myxobacteria was isolated (*93*).

Nannozinone A **21**

Nannozinone B **22**
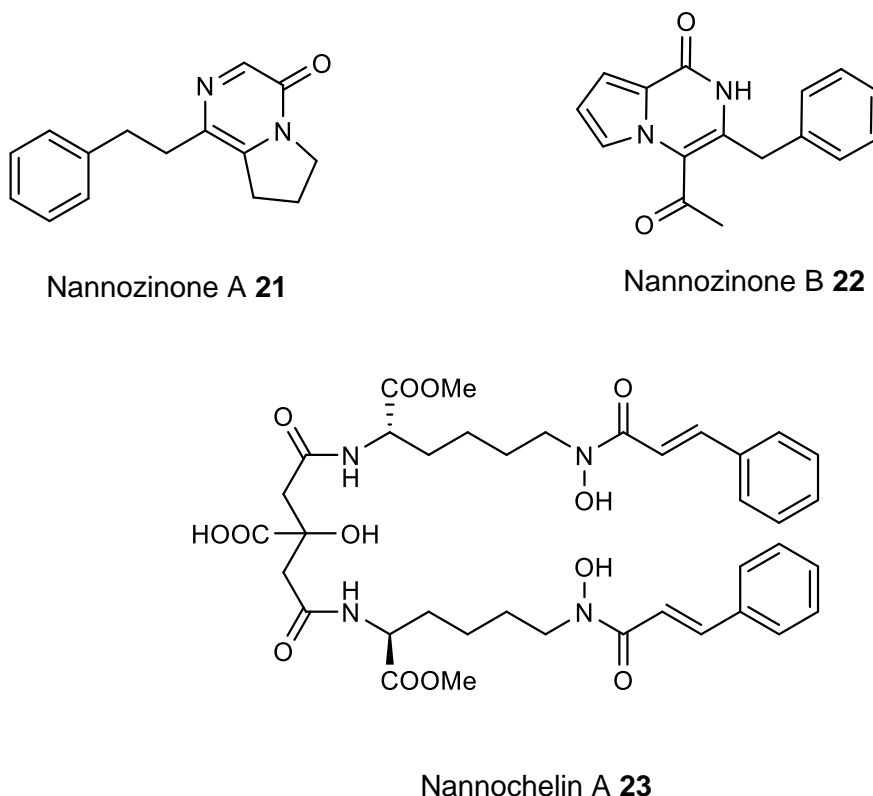
Nannochelin A **23**

Figure 4-9 Structures of nannozinones A + B and nannochelin A from *N. pusilla* strain MNa10913.

All three compounds were tested against a broad range of microorganisms and mammalian cell lines. The most relevant antimicrobial activity was shown by **21** towards *Mycobacterium diernhoferi* (DSM 43542), *Candida albicans* (DSM 1665) and *Mucor hiemalis* (DSM 2656) (33.3 μg mL^{-1} in each case). Significant cytotoxic activity was revealed for **22** towards SKOV-3 (IC$_{50}$ = 2.4 μM), KB3-1 (IC$_{50}$ = 5.3 μM), as well as A431 (IC$_{50}$ = 8.45 μM), while **23** showed remarkable cytotoxicity against cell lines HUVEC and KB3-1 (IC$_{50}$ = 50 nM).

So far, no genome sequence is publicly available for halotolerant strains of this genus. The only sequence found in the databases belongs to the terrestrial *N. exedens* ATCC 25963 (see Tabe 4-1). Remarkably, this genome encodes, among a considerable number of NRPS/PKS hybrids, 10 different terpene biosynthesis gene clusters.

4.5. The genus *Haliangium*

Haliangium ochraceum sp. nov. (Initially termed *H. luteum*, DSM 14365^T) and *H. tepidum* sp. nov. (DSM 14436^T) were isolated from seaweed and sea grass, respectively, with both samples being obtained from a sandy beach in Miura, Japan by Fudou in 2002 (*57*). The species were proposed to be of true marine origin according to their salt requirement for growth. Indeed, 2 to 3 % NaCl (w/v) and a pH of 7.5 are optimal for growth on yeast medium with artificial seawater solution. These conditions were established for routine isolation and cultivation. One particular feature worth mentioning is that the species have rather different optimal growth temperature intervals: 30-34 °C for *H. ochraceum* and 37-40 °C for *H. tepidum*. According to the original report, both strains share 95.5% of 16S rDNA sequence identity and have the terrestrial *Kofleria flava* (DSM 14601) as their closest relative (16S rDNA sequence identity lower than 95%). The GC content of *H. ochraceum* and *H. tepidum* is 67 and 69 mol%, respectively.

H. ochraceum was found by Fudou (*94*) to be a producer of secondary metabolites with antibacterial and antifungal activities. Further investigation led to the isolation and structure elucidation of the bioactive polyketide haliangicin **24**, which was the first myxobacterial metabolite of true marine origin.
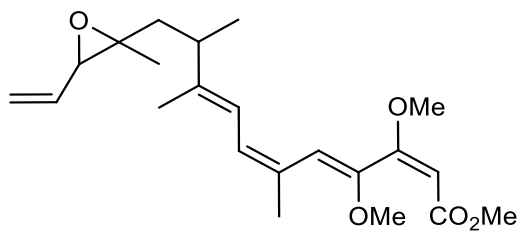
Haliangicin **24**

Figure 4-10 Structure of haliangicin from *H. ochraceum.*

It was found that this molecule comprised a β-methoxyacrylate sub-unit including a conjugated tetraene moiety (*95*). The complete structure was elucidated via 2D-NMR-techniques, while NOESY correlations were used to study the configuration of the double bonds. However, the configuration at the epoxide bearing carbon atoms could not be resolved at that time. In further work, Kundim (*96*) published three new haliangicin stereoisomers, which differed in the configuration of the three terminal double bonds in the tetraene moiety. Each of the isomers haliangicin, haliangicin B, haliangicin C and haliangicin D happened to be present with two different configurations around the epoxy group. The NOESY spectra showed correlations for the cis- and trans-configuration. However, the absolute configuration of the chiral centers could not be resolved yet. Moreover, the origin of the different isomers is not clear. Due to their alleged instability upon exposure to air and light, one could speculate that isomerization occurs during the purification process. Interestingly, the authors found a NaCl-dependent production of haliangicin (*94*). The optimal production range is at 2-3 % NaCl (w/v) in the medium, which is the same range as for optimal growth. Haliangicin showed activity against some fungal organisms, *e.g. Aspergillus niger* (AJ117374) (MIC: 12.5 μg mL^{-1}) and *Fusarium* sp. (AJ177167) (MIC: 6.3 μg mL^{-1}). These MIC values were in a similar range as those of known antifungal compounds such as amphotericin B or nystatin against the same fungi (MIC: 3.1 μg mL^{-1}for both compounds).

Recently, the 9.4 Mb genome of *H. ochraceum* (DSM 14365[T]) was completely sequenced and published (*97*). This was the first marine-derived myxobacterium to have its genome fully determined. We performed an antiSMASH analysis on the genome of *H. ochraceum* (DSM 14365[T]) (AN: CP001804.1). The results revealed the presence of 25 secondary metabolite gene clusters, among them three NRPS, two PKS, three NRPS/PKS and four ribosomal peptides (see Tabe 4-1). Apart from homologies to geosmin (100%), aurafuron (71%) and paneibactin (50%) biosynthetic genes, the gene clusters display a large degree of novelty. Recently, the biosynthetic gene cluster of haliangicin was heterologously expressed in *Myxococcus xanthus*, leading to tenfold higher haliangicin production than in the native producer. Insights into its biosynthesis were gained by feeding studies with labeled precursors and *in vitro* experiments. Additionally, unnatural haliangicin analogs that provided insights into the structure-activity-relationship of haliangicin were generated in this study (*98*).The huge potential to synthesize novel metabolites in the genus *Haliangium* is further corroborated by a PCR screening-based study for PKS sequences in *H. tepidum* among other myxobacteria (*99*). The authors found *H. tepidum* to contain the highest amount of novel PKS sequences in this array. Additionally, the indications at the genetic level are reinforced by the very recent discovery of a new compound produced by *H. ochraceum* SMP-2, *i.e.* haliamide 25. The authors also describe the corresponding hybrid PKS-NRPS machinery responsible for metabolite biosynthesis (*33*). The molecule was shown to have cytotoxic effects towards HeLa-S3 cells (IC$_{50}$ = 12 μM).
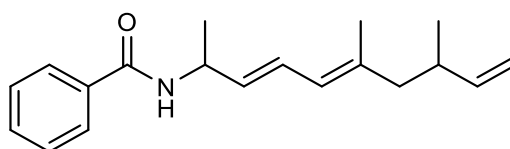
Haliamide **25**

Figure 4-11 Structure of haliamide from *H. ochraceum* SMP-2.

4.6. The genus *Enhygromyxa*

All Enhygromyxa species isolated to date are halophilic and considered as truly marine myxobacteria. The initial report on isolation, characterization and taxonomic classification of six strains of *E. salina*, SHK-1[T], SMK-1-1, SMK-1-3, SMK-10, SKK-2, and SMP-6, was published in 2003 by Iizuka (*59*). These organisms were obtained respectively from mud, sand and algal samples collected in marine environments around Japan. Later, four additional strains of *E. salina* were isolated by the group of König from marine-intertidal sediment samples collected at the West Coast of the USA, at German coasts and the Netherlands (*100, 101*). Recently, existance of strain SNB-1 was reported (*102*). This organism was isolated from a marine mud sample collected in 1998 at a beach in Kashiwazaki, Niigata (*102*).

As judged from these varied geographical occurrences a worldwide distribution of Enhygromyxa species is likely.

The prior mentioned groups reported 1-2 % NaCl (w/v) and a pH interval of 7.0-8.5 for optimal growth on yeast medium. The optimal temperature for growth was determined as 28-30 °C. In terms of gliding motility, fruiting body, and myxospore formation, these bacteria show the typical features of terrestrial myxobacteria. A salt-dependency and high G+C content ranging from 65.6 to 67.4 mol% (*59*) and 63.0 to 67.3 mol% (*101*) were also observed in some organisms. Based on 16S rDNA sequence alignments, *E. salina* SHK-1[T] (NR_024807) from Iizuka (*59*) was found to be most closely related to the *E. salina* strains from the König group (*101*). The 16SrDNA sequences of these strains share between 98% (SWB004, AN: HM769727) and 99% (SWB005, AN: HM769728; SWB006, AN: HM769729; SWB007, AN: KC818422) identity.

Some of the bacterial isolates were originally evaluated for their ability to produce PKS-type metabolites and for the biosynthesis of antimicrobials (*101*).

In these studies, PKS genes could be amplified, sequenced and compared with known sequences in the BLAST database. The potential of producing active molecules was established by using disc diffusion antibiotic activity testing of the bacterial extracts, whereby an inhibitory effect of the extracts of *E. salina* SWB005 on various test organisms, including the clinically relevant MRSA (methicillin resistant *Staphylococcus aureus*) strains LT1334, LT1338 and MRSE methicillin resistant *Staphylococcus epidermidis* strain LT1324 was observed (*101*).

To date, five structures of putative polyketide, shikimate and terpenoid origin have been described and classified as salimabromide **26** (*100*), produced by E. salina SWB007, enhygrolides **27**, **28** and salimyxins **31**, **32** produced by *E. salina* SWB005 (*103*). Recently, three novel structures have been isolated from *E. salina* SNB-1, namely deoxyenhygrolides **29**, **30** and enhygromic acid **33**, compounds of PKS and terpenoid nature, respectively (*102*). These structures are illustrated in Figure 4-12.

Salimabromide **26**

Enhygrolide A **27**

Enhygrolide B **28**

Z: deoxyenhygrolide A **29**

E: deoxyenhygrolide B **30**

Salimyxin A **31**
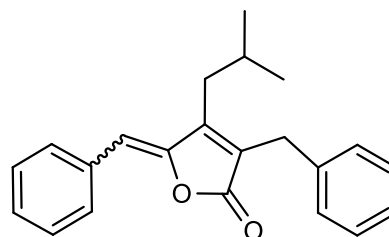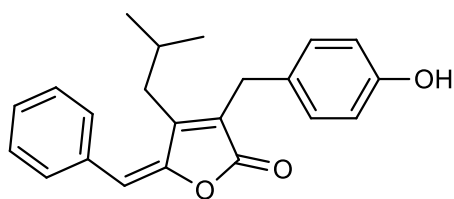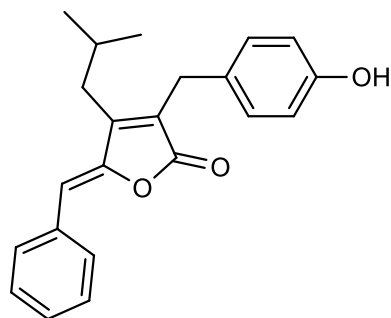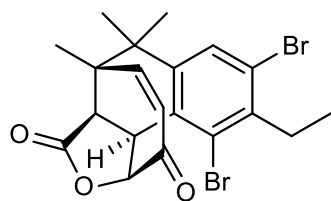
Salimyxin B **32**
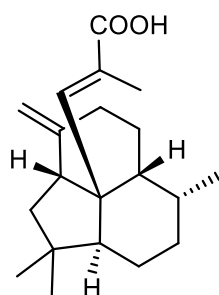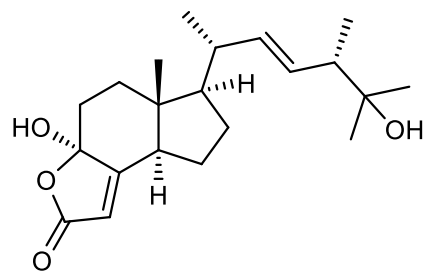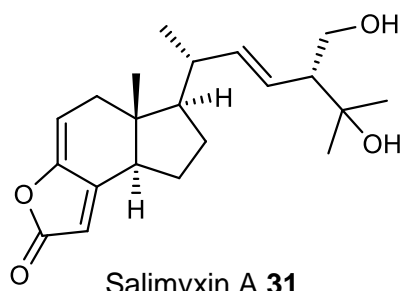
Enhygromic acid **33**

Figure 4-12 Structures of salimabromide, enhygrolides A + B, deoxyenhygrolides A + B, salimyxins A + B and enhygromic acid.

Salimabromide **26** is particularly interesting due to its unique halogenated tetracyclic core structure. Its biosynthesis is postulated to be carried out by a type III-PKS. Pure PKS-derived compounds are rare in myxobacteria, which together with the new carbon skeleton and the high bromination level makes this structure even more fascinating. Structure elucidation was achieved via extensive NMR-measurements. The absolute configuration of the chiral centers could be resolved through comparison of the experimental CD-spectrum with calculated data. This metabolite showed inhibitory activity towards the bacterium *Arthrobacter crystallopoietes* with an MIC value of 16 μg mL-1. Further bioactivity assays were impossible to carry out due to the minute amounts in which this metabolite is produced. Consequently, a synthetic approach has been utilized in order to overcome this problem, leading so far to the synthesis of the tricyclic core structure of the molecule. However, the complete natural product has not yet been synthesized (*104*).

The enhygrolide group of compounds comprises enhygrolide A **27** and B **28**. These molecules resemble cyanobacteria-derived metabolites, known as nostoclides and cyanobacterin, which also have a γ-lactone-moiety with a similar substitution pattern. In the myxobacterial metabolites an E-configuration was found at the benzylidene-unit, whereas the nostoclides and cyanobacterin have a Z-configuration. Only the anhydro form of cyanobacterin was found to isomerize from the Z- to the E-configured isomer in organic solvents upon light exposure (*105*). Deoxyenhygrolide A **29** and deoxyenhygrolide B **30** are analog structures to **27** and **28**, the only difference is the lack of –OH group on the *para* position of the aryl moiety. To date, no activities have been assigned to these compounds.

The salimyxins represent the third group of compounds, *i.e.* salimyxin A **31** and B **32**. These belong to a subgroup of terpenoids named incisterols, which were first discovered from the sponge *Dictyonella incisa* (*106*).

Their biosynthesis presumably involves oxidative degradation of a sterol, leading to the tricyclic core structure.

Compounds **27** and **30** have shown inhibitory activity towards *A. crystallopoietes* (MIC value of 8 and 4 μg mL-1, respectively).

Compound **33** represents a novel structure displaying a tricyclic skeleton linked to a α-meta acrylate acid chain. Bioinformatic-oriented investigations suggest a terpenoid biosynthetic origin (*102*). This research group conducted bioactivity tests whereby this compound exhibited cytotixic activity against B16 melanoma cells (IC$_{50}$ = 46 μM) and antimicrobial properties against the Gram-positive bacterium *Bacillus subtillis* (8 μg/mL).

Since salimabromide is a novel structure of putatively assigned PKS origin, our research group sequenced the genome of the producing strain SWB007. The results revealed a PKS III gene cluster adjacent to a halogenase sequence (unpublished data). Upon sequencing, primers for these genes were designed. Given the genetic proximity among the *E. salina* isolates, strains SWB004, SWB005 and SWB006 were screened with the PKS III and halogenase primers specific for the SWB007 sequence revealing the presence of close-to-identical sequences in their genomes (unpublished data), a clear suggestion that similar molecules may be also produced by the related strains.

Bioinformatic analysis was performed by us on the available genome of *E. salina* (DSM 15201) (AN: JMCC00000000.2) of which as to date, no reports on the isolation of compounds are available. However, the screening with antiSMASH revealed an ample amount of uncharacterized biosynthetic gene clusters, among them 17 gene clusters putatively responsible for the synthesis of NRPS, PKS and hybrid NRPS-PKS products (see Tabe 4-1). Apart from the geosmin biosynthesis genes, no gene cluster or fragment thereof shares an identity higher than 33% to any known gene cluster in the MiBIG database (*107*).

It should be noted that since this is a draft genome sequence, the actual amount of gene clusters might be slightly smaller since small contigs display only fragments of gene clusters.

4.7. The genus *Plesiocystis*

In 2003 Iizuka (*60*) proposed the genus and the species *Plesiocystis pacifica* for the myxobacterial strains SHI-1 (JCM 11592, DSM 14876) and SIR-1^T (JCM 11591^T, DSM 14875T). SHI-1 was retrieved from a sand sample of a Japanese coastal area, whilst strain SIR-1^T was isolated from a piece of dried marine grass (*Zostera* sp.). These strains require 2 - 3 % NaCl (w/v) and a pH of 7.4 for optimal growth on yeast medium with artificial seawater solution at 28 °C.

According to Iizuka (*60*) the isolates are closely related, sharing 99.5% 16S rDNA sequence identity between them. Their closest relative was reported to be *Nannocystis exedens* DSM 71T, with 89.3% sequence identity to SIR-1T and 89.4% to SHI-1. Regarding GC content, SIR-1T and SHI-1 were reported to have 69.3 and 70.0 mol%, respectively. Such a high GC content is a distinctive trait of all myxobacteria. To date, no reports on biological testing of extracts or of any metabolites isolated from these organisms have been published. The antiSMASH analysis was performed on the available draft genome of *P. pacifica* strain SIR-1 (AN: ABCS00000000.1). The analysis revealed the presence of 12 NRPS, PKS and hybrid NRPS-PKS gene clusters amongst many others (see Table 4-1), which should encourage researchers to isolate some of the predicted metabolites. Here, no gene clusters sharing more than 28 % identity to pathways of characterized molecules were detected. Again, many of the PKS and NRPS gene cluster appear to be fragmented to smaller contigs.

4.8. Myxobacterium SMH-27-4 (*Paraliomyxa miuraensis*)

In 2006, as a result of the remarkable efforts of Iizuka (*108*) a novel myxobacterium was isolated from a soil sample of a seashore area in Miura, Japan.

After genetic analysis, the new isolate was classified as strain SMH-27-4, tentatively named *Paraliomyxa miuraensis*. This strain is considered slightly halophilic. Yeast medium with only a low sea salt concentration was selected for isolation, whereas cultivation in NaBr-containing medium was selected for antibiotic production. The diminished strength of salinity in the medium implies an optimal salt range concentration for growth of 0.5-1 % (w/v), at pH = 7.2 and a temperature of 27 °C. Fermentation and the production of antibiotic compounds was performed at 27 °C at pH 7.3.

Surprisingly, the authors do not report fruiting body formation during the cultivation of myxobacterium SMH-27-4, which usually is a hallmark feature of myxobacteria. Phylogenetic analyses carried out by Iizuka (*108*) revealed that this organism shares 93.0% identity with *Nannocystis exedens* DSM 71^T (AB084253), 93.2 to 93.3% with *Enhygromyxa salina* JCM 11769^T (AB097590), and 91.3 to 91.5% with *Plesiocystis pacifica* JCM 11591^T (AB083432). No information on the GC content of the bacterial genome has been found. Myxobacterium SMH-27-4 (AN: AB252740) was investigated for the production of secondary metabolites (*108*). This work led to the isolation and structure elucidation of two compounds of peptidic nature called miuraenamide A **34** and B **35**. Two years later, the same research group published the structures of four additional derivatives, named miuraenamides C-F **36-39** (*109*).
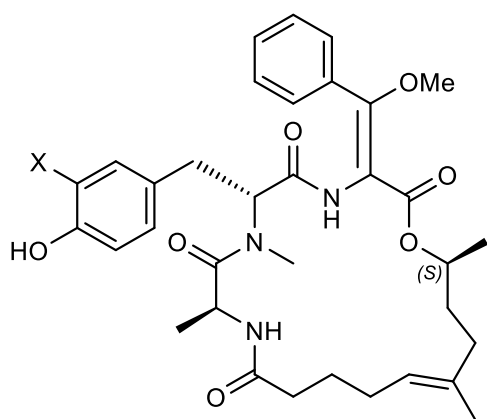
X = Br	Miuraenamide A **34**
X = I	Miuraenamide B **35**
X = Cl	Miuraenamide C **36**
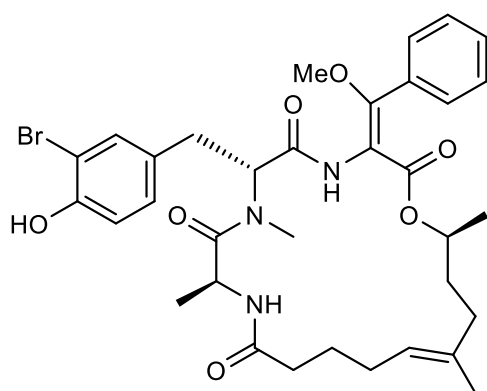
Miuraenamide D **37**
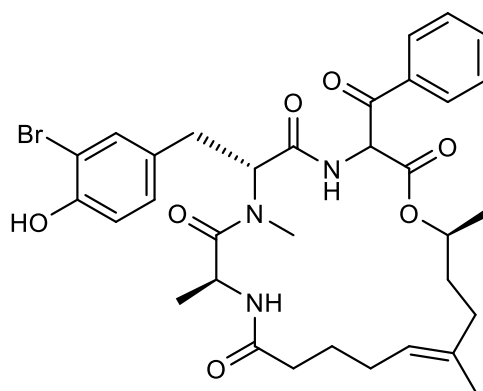
Miuraenamide E **38**
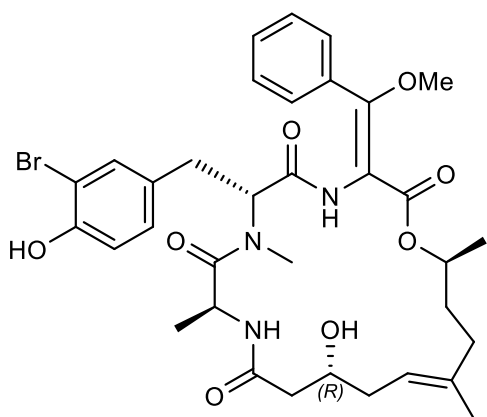
Miuraenamide F **39**

Figure 4-13 Structures of miuraenamides A-F from *P. miuraensis.*

The cyclic core structure of this compound class represents a halogenated depsipeptide with an additional polyketide-derived moiety. As in haliangicin, all miuraenamides, except E, contain a methoxyacrylate structural motif, which surely is important for the biological activity. For miuraenamide A **34** the absolute configuration was determined. Marfey´s method was employed to show that L-alanine and N-methyl D-tyrosine are present. Furthermore, after acid hydrolysis, methylation and application of modified Mosher´s method the absolute configuration at the oxygen-bearing C-9 was deduced as *S*. For miuraenamide F **39** the configuration at C-3 was found to be *R*, again using Mosher's method. For all the other chiral centers in compounds **35- 39** the authors conclude that they have the same configuration as determined for **34**. Further work led to semi-synthetic derivatives, which upon activity testing, revealed that the lactone moiety and the configuration of the methoxyacrylate partial structure are crucial for antifungal activity. The latter structural motif is well known from a range of antifungal compounds produced by fungi and myxobacteria, *e.g.* the strobilurins and the melithiazols (*110, 111*).

Miuraenamide A **34** was assayed against various fungal, yeast and bacterial organisms. It showed a remarkable inhibitory effect toward the fungal phytopathogen *Phytophthora capsici* NBRC 8386 (MIC: 0.4 mg mL^{-1}) and *Candida rugosa* AJ 14513 (MIC: 12.5 mg mL^{-1}). No inhibitory effect on selected bacteria was detected. The mode of action is proposed to be similar to other antifungals with a methoxyacrylate partial structure, *i.e.* inhibition of the mitochondrial cytochrome bc1 complex. Additionally, Miuraenamide A was shown to act as actin filament stabilizer in HeLa cells (*112*). The activity of miuraenamide B **35** was not assessed due to the minute amounts of the metabolite available.To date, there is no genome sequence available for this organism.

4.9. The genus Pseudenhygromyxa

Pseudenhygromyxa salsuginis is the latest example of a halotolerant myxobacterium, published in 2013 by Iizuka et al. (*113*). This organism was retrieved from mud samples of an estuarine marsh in a coastal area in Japan and termed SYR-2^T. Even though it is able to grow in the absence of salt, optimal growth was shown to occur within a concentration range of 0.2 - 1.0 % NaCl (w/v) and pH values from 7.0 - 7.5 on CY-S agar (bacto casitone, bacto yeast extract) in a temperature range of 30-35 °C. After alignment of 16S rDNA sequences, Iizuka et al. (*113*) found that *P. salsuginis* SYR-2^T showed 96.5% and 96.0% identity to *Enhygromyxa salina* SHK-1^T (NR_024807) and *Plesiocystis pacifica* SIR-1^T (NR_024795), respectively. The G+C content is 69.7 mol%, and thus slightly higher than for various *E. salina* strains described above.

To date, no reports on biological activities or any metabolites derived from *P. salsuginis* have been published. Nevertheless, the genetic proximity to *E. salina* and the fact that it belongs to the group of myxobacteria suggests that this organism may also possess a high potential as a producer of active molecules. To date, no genome sequence has been published.

5. CHAPTER 2: Cyclopropane-containing fatty acids isolated from *Labrenzia* sp. strain 011 (Ostsee6)

Marine microorganisms interact in a balanced coexistence, regulated to a high extent by chemicals, *e.g.* chemical warfare among fouling microorganisms and microbial symbionts or epibionts of a variety of macroscopic marine organisms with the capacity to produce antifouling compounds (*23, 114, 115*). Many of these interactions are dependent on secondary metabolism. Indeed, it has been established that epibiotic or symbiotic bacteria and metabolites produced by them play a major role in keeping their host healthy. A good example of these relations is the protective mechanism displayed by *Alteromonas* sp. I-2, which colonizes the embryos of the Caribbean shrimp *Palaemon macrodactylus* (*116*). This bacterium produces the antifungal agent 2,3-indolinedione, which prevents infection with the fungus *Lagenidium callinectes*, a frequent crustacean pathogen (*116*). In the same manner, embryos of the American lobster *Homarus americanus* were reported to be chemically protected against the same pathogen by the antifungal agent 4-hydroxyphenethyl alcohol, produced by the Gram-negative bacterium SG-76 (*117*).

Within this context, species of the genus *Labrenzia*, previously classified *Stappia* (*118*) have been suggested to be protective agents of mollusks, *e.g. Crassostrea virginica* against *Pseudoroseovarius crassostreae* (also *Aliiroseovarius crassostreae*), the causative agent of roseovarius oyster disease (*119–121*). This pathogen negatively impacts the ecology of the marine environment and economic activities related to aquaculture of these marine organisms (*122*). A secondary metabolite-mediated mechanism is thought to be involved in the putative protective role of *Labrenzia* spp.

To date, there is only one report of a pederine-analgous compound isolated from the genus *Labrenzia*, *i.e. Labrenzia* sp. PHM005 (Fig 5-1) (*25*).
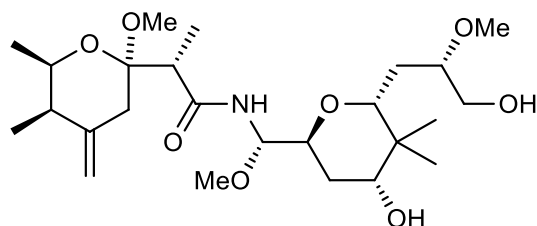
Figure 5-1 This pederin analog is produced by the halophilic *Labrenzia* sp. PHM005 (*25*). However, the ecological function of this interaction remains unknown. This molecule has been tested *in vitro*, showing cytotoxic activity against four different human cell lines: A549 (ATCC CCL-185) (lung carcinoma); HT-29 (ATCC HTB-38) (colon adenocarcinoma); MDA-MB-231 (ATCC HTB-26) (breast adenocarcinoma); and PSN-1 (ATCC CRL-3211) (pancreas adenocarcinoma) (*25*).

In this chapter, antimicrobial molecules produced by *Labrenzia* sp. strain 011 (Ostsee6) are described. These findings reinforce the idea that poses this bacterium as a biocontrol agent in the marine environment.

5.1. Investigation of *Labrenzia* sp. strain 011 (Ostsee6)

5.1.1. Isolation, taxonomy, and phenotype of *Labrenzia* sp. strain 011 (Ostsee6)

Labrenzia sp. strain 011 (Ostsee6) was retrieved as a free-living organism from a sample of marine sediment collected in August 2012 in the coastal area of Kronsgaard, Germany. The sample was air-dried and portions thereof were placed on WCX-ASW agar in Petri dishes. After 5 days of incubation at 30°C, creamy brownish colonies displaying gliding behavior on ASW-WCX agar were transferred to Petri dishes containing marine agar for isolation (Figure 5-2) (protocol described in section 3.2.1). Identification enabled by sequencing experiments revealed the identity of the isolate as a *Labrenzia* sp. strain 011 (Ostsee6).

Based on 16S rDNA alignments, it shares 99% identity with its closest relatives, namely *Labrenzia alba* strain 5OM6 (AN: NR_042378.1) and *Labrenzia aggregata* strain RMAR6-6 (AN: CP019630.1).
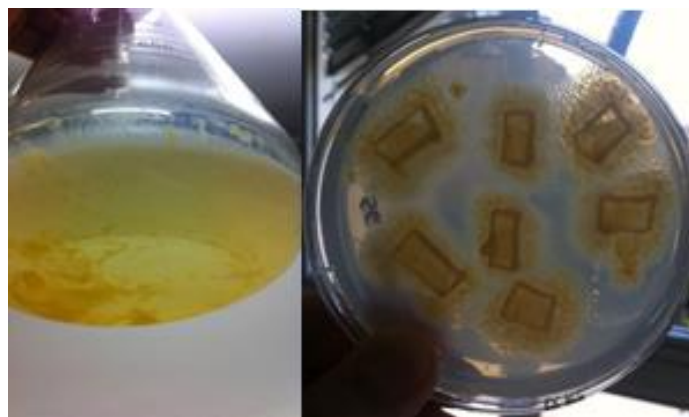
Figure 5-2 Colonies *of Labrenzia sp*. strain 011 (Ostsee6) on marine broth and marine agar respectively. This bacterium is motile by means of gliding, a trait often observed in heterotrophic organisms. The genus *Labrenzia* belongs to the α-proteobacteria group, family Rhodobacteraceae.

Once the isolate was identified, *in silico* genomic mining experiments on annotated sequences of *Labrenzia* species were conducted, as well as on the draft genome of *Labrenzia* sp. strain 011 (Ostsee6). The analyses revealed that the latter and its selected relatives harbor gene clusters putatively involved in the production of secondary metabolites (Table 5-1).

Table 5-1 The most relevant findings from the annotated genomes of three species of *Labrenzia* and the draft genome of *Labrenzia* sp. strain 011 (Ostsee) are presented. Genomic mining analyses were run on these sequences using the antiSMASH software version 4.0.0 (*42*). These results were decisive to orient the research endeavors towards *Labrenzia* sp. strain 011 (Ostsee6)

Organism	*Labrenzia* sp. 011 (Ostsee6)	*L. alexandri* DFL11	*Labrenzia* sp. CP4	*L. alba* CECT7551
Genome size (Mb)	5.1	5.5	6.1	5.9
Accession number	Not yet published	NZ_ACCU00000000.1	NZ_CP011927.1	NZ_CXTY00000000.1
GC %	60.3	56.4	58.9	53.8
% of genome involved in secondary metabolism[a]	1.51	2.05	2.06	1.32
Scaffolds	-	6	-	41
Total number of clusters	3	4	5	3
Type I PKS	1	1	1	1
NRPS	0	0	1	0
Terpene	1	2	2	0
Bacteriocin	1	1	1	1
Carotenoid	0	0	0	1

[a]Total bases of all secondary metabolite gene clusters detected by antiSMASH divided by number of bases in the genome (Genome size).

5.1.2. Unveiling the antimicrobial capabilities of *Labrenzia* sp. strain 011 (Ostsee6)

Cultivation was conducted according to sections 3.2.6 and 3.3.2. A crude extract was obtained by liquid-liquid extraction using ethyl acetate as organic solvent as described in section 3.3.1. The crude extract was fractionated as shown in section 3.3.3 (VLC). The fractions obtained from the VLC column were evaporated to dryness and resuspended in methanol to a final concentration of 1 mg/mL. Samples of 50 μL of each fraction equivalent to 50 μg were used for antimicrobial testing on disc diffusion tests (Table 5-2).

Table 5-2 Disc diffusion tests were applied for initial antimicrobial screening, using 50 μg of the solvent-fractionated extract of *Labrenzia* sp. strain 011 (Ostsee6). Codes in the table are FR1 = DCM fraction, FR2 = EtOAC fraction, FR3 = Acetone fraction, FR4 = MeOH fraction. T.i. = total inhibition, W.i. = weak inhibition. In these experiments, FR2 showed growth inhibition of a range of test microorganisms. Meanwhile, FR1, 3 and 4, did not show antimicrobial activity.

Test Organism	Test organism	Diameter of inhibition zone of fraction FR2
Bacillus megaterium DSM 32	Bacterium	3 mm (T.i.)
Escherichia coli DSM 498	Bacterium	<1 mm (W.i.)
Eurotium rubrum DSM 62631	Fungus	2 mm (T.i.)
Microbotryum violaceum MB#110229	Fungus	4 mm (T.i.)
Mycotypha microspora MB#271115	Fungus	<1 mm (W.i.)

Fraction 2 (FR2), eluted with ethyl acetate showed the most promising results in terms of microbial growth inhibition and a promising pattern in the ^{1}H-NMR spectrum (spectrum not shown). This fraction oriented the research efforts intended to identify the substances responsible for the antimicrobial activity described in the upcoming sections.

5.1.3. Metabolites isolated from *Labrenzia* sp. strain 011 (Ostsee6)

5.1.3.1. Large-scale cultivation of bacterium and isolation of metabolites

Cultures (12 L) were produced according to 3.2.6 in the experimental section. Metabolites were retrieved from marine broth according to section 3.3.2 utilizing 20 g of sepabeads 207/L of marine broth. After ten days of cultivation, the sepabeads were extracted with acetone for 24 hours as described in section 3.3.2. The crude extract obtained was 2.9 g of an oily dark residue, which was dissolved in 50 mL of aqueous methanol 60% and extracted three times with 60 mL of dichloromethane. The lipophilic phase was evaporated to dryness and yielded 617.9 mg of a dark oily extract. This extract was separated on a flash chromatography device. The fraction of interest (21.2 mg) was obtained by a linear gradient (0-3 min acetone/petroleum ether 0:100, 3-9 min up to 25% acetone, 9-10 min up to 100% acetone, ≈ 20 min 100% acetone at a constant flow rate of 30 mL/min), using a Reveleris silica column of 12 g (12 mg – 2.4 g sample load capacity, 12 μm). This fraction was collected between minute 5 and 6, evaporated under vacuum and resuspended in acetone. It was further fractionated by semi-preparative HPLC using a linear gradient (0-5 min acetonitrile/water 50:50, 5-20 minutes up to 100% acetonitrile, ≈ 50 min 100% acetonitrile, containing 0.01 M H_3PO_4 each solvent at a constant flow rate of 1 mL/min). The column YMC-triart C18 / S-5μm /12 nm (250 x 4.6 mm I.D) was employed for this step. Two oily colorless substances to [(**1**)**,** 1 mg; (**2**)**,** 6 mg] were obtained. Their retention time was respectively 22 (100% acetonitrile) and 17 min (90% acetonitrile) (Figures 9-1, 9-2 and 9-3 in the appendix).

5.1.4. Structure elucidation of metabolites isolated from *Labrenzia* sp. strain 011 (Ostsee6)

Two cyclopropane-containing fatty acids were isolated (CYPFA) (**1**, **2**, Figure 5-3). The structures of (**1**) and (**2**) were established by extensive NMR analyses (^{1}H, ^{13}C, COSY and HMBC, Table 5-3 and 5-4 respectively).

All chemical shifts were measured relative to the chloroform peak (7.26 ppm for ^{1}H-NMR, 77.16 ppm for ^{13}C-NMR).

cis - 4 - (2 - hexylcyclopropyl) - butanoic acid (1): the ^{13}C-NMR spectrum showed 12 resonances between 10 to 35 ppm attributable to an aliphatic compound (see Appendix, Figure 9-7). Furthermore, the resonance at 178.1 ppm suggested the presence of a carboxylic group (see Appendix, Figure 9-7). ^{1}H-^{13}C HMBC showed correlations from the α-methylene signal of H-2 (δ_H 2.40 ppm, t, J = 7.6 Hz, 2H) to the carboxyl signal C-1 (δ_C 178.1 ppm, C) and C-8 (δ_C 25.2 ppm, CH$_2$). β - methylene signal of H-8 (δ_H 1.75, p, J = 7.6 Hz, 2H) showed a mutual ^{1}H-^{1}H COSY correlation with splitted γ–methylene signals of H-7 (δ_H 1.46 ppm (a), m, H; δ_H 1.22 ppm (b), m, H). Further analysis of the ^{1}H-^{1}H COSY correlations showed that the splitted high-field methylene signals in the ^{1}H-NMR spectrum (see Appendix, Figure 9-6) H-13a/H-13b (δ_H -0.30 ppm (b), q, J = 4.6 Hz, H; δ_H 0.63 ppm (a), m, H) were coupled with methine signals H-10 (δ_H 0.66 ppm, m, H) and H-11 (δ_H 0.68 ppm, m, H). Finally, ^{1}H-^{13}C HMBC analysis showed a correlation of H-13a/H-13b with methine signals C-10 (δ_C 15.2 ppm, CH) and C-11 (δ_C 15.7 ppm, CH). The ^{1}H-^{1}H COSY and ^{1}H-^{13}C HMBC coupling patterns were assigned to a 1, 2 - disubstituted cyclopropane ring with three methylene groups between the ring and the carboxylic moiety. Five remaining methylene groups and one methyl group, namely H-3 (δ_H 1.27, m, 2H), H-4 (δ_H 1.35, m, 2H), H-5 (δ_H 1.27, m, 2H), H-6 (δ_H 1.35, m, 2H), H-9 (δ_H 1.28, m, 2H) and 12-H (δ_H 0.88, t, J = 6.8 Hz, 3H) were assigned as shown in Table 5-3. The chemical shift of H-13b (δ_H -0.30 ppm) suggested the *cis* stereochemistry of the three-membered ring, confirmed by comparison of ^{1}H-NMR chemical shifts of H-10, H-11, and H-13 with related reference compounds (*123*).

cis - 2 - (2 - hexylcyclopropyl) - acetic acid (2): the ^{13}C-NMR spectrum showed 10 resonance signals between 10 and 35 ppm (see Appendix, Figure 9-9) attributable to an aliphatic compound, suggesting a high similarity to (**1**). The ^{13}C-NMR signal at 180.2 ppm suggested the presence of the carboxylic moiety (see Appendix, Figure 9-9). ^{1}H-^{13}C HMBC correlations were observed from the splitted α-methylene signals of H-2 (δ_H 2.42 ppm (a), dd, J = 6.9, 16 Hz, H; δ_H 2.29 ppm (b), dd, J = 7.8, 16 Hz, H) to C-1 (δ_C 180.2 ppm, C). The splitted high-field signals in the ^{1}H-NMR spectrum (see Appendix, Figure 9-8) H-11a/H-11b (δ_H -0.13 ppm (b), q, J = 5.0 Hz, H; δ_H 0.75 ppm (a), dq, J = 8.4, 5.0, H) were coupled with methine protons H-8 (δ_H 0.81 ppm, m, H) and H-10 (δ_H 1.10 ppm, m, H,) according to ^{1}H-^{1}H COSY analysis. Correlations detected in ^{1}H-^{13}C HMBC of H-11a/H-11b with methine signals C-8 (δ_C 15.5 ppm, CH) and C-10 (δ_C 11.1 ppm, CH) suggested a cyclopropane ring configuration similar to (**1**). Five remaining methylene groups and one methyl group, namely H-3 (δ_H 1.26, m, 2H), H-4 (δ_H 1.37, m, 2H), H-5 (δ_H 1.29, m, 2H), H-6 (δ_H 1.35, m, 2H) H-7 (δ_H 1.29, m, 2H) and 9-H (δ_H 0.88, t, J = 7.3 Hz, 3H) were assigned as shown in Table 5-4. The coupling patterns were assigned to a 1, 2-disubstituted cyclopropane ring with only one methylene group between the ring and the carboxylic moiety. The chemical shift of H-11b (δ_H -0.13 ppm) suggested the *cis* stereochemistry of the three-membered ring, confirmed by comparison of ^{1}H-NMR chemical shifts of H-8, H-10 and H-11 with related reference compounds (*123*).

The lack of chromophores was evident from UV-data [(**1**) λ_{max} = 200 nm, (**2**) λ_{max} = 206 nm]. Structures were confirmed by HRESIMS measurements shown in 5.1.5 (chromatograms in appendix, Figure 9-4 and 9-5). Additionally, NMR spectroscopic data of compound (**2**) were equivalent to *cis* - cascarillic acid, an analogous structure to (**2**) (*124–126*) (see Appendix, Table 9-1). *cis* - cascarillic acid is known to occur in minute amounts in the acidic fraction of the essential oil of *Croton eluteria*, a medicinal shrub (*124*).

The main component of this fraction is *trans* - cascarillic acid (**3**, $[\alpha]_D$ = -8.9, in CHCl$_3$, Figure 5-3)(*124*).

The rotatory power of CYPFAs measured in our laboratory$[\alpha]_D^{20}$. The results of these measurements are shown in section 5.1.5. This is to the best of our knowledge, the first description of compound (**1**).

5.1.5. Spectroscopic characterization of *Labrenzia* sp. strain 011 (Ostsee6) metabolites

Compound 1: *cis* - 4 - (2 - hexylcyclopropyl) - butanoic acid; colorless oil; $[\alpha]_D^{20}$ -15 (c 0.1, CHCl$_3$); UV (acetonitrile) λ_{max} (ε) 207 nm (2366.42 M^{-1}cm^{-1}); ^{1}H- and ^{13}C-NMR (Table 5-3); (+) HRESIMS m/z 235.1660 [M+Na]$^+$ (calculated for C$_{13}$H$_{23}$O$_2$Na, 235.1629).

Compound 2: *cis* - 2 - (2 - hexylcyclopropyl) - acetic acid; colorless oil; $[\alpha]_D^{20}$ -1 (c 0.1, CHCl$_3$); UV (acetonitrile) λ_{max} (ε) 200 nm (1071.12 M^{-1}cm^{-1}); ^{1}H- and ^{13}C-NMR (Table 5-4); (+) HRESIMS m/z 207.1308 [M+Na]$^+$ (calculated for C$_{11}$H$_{19}$O$_2$Na, 207.1316).

cis - 4 - (2 - hexylcyclopropyl) - butanoic acid **1**

cis - 2 - (2 - hexylcyclopropyl) - acetic acid **2**

trans - cascarillic acid **3**
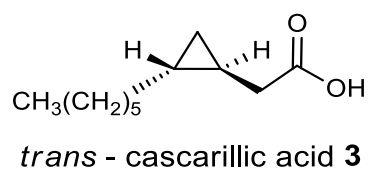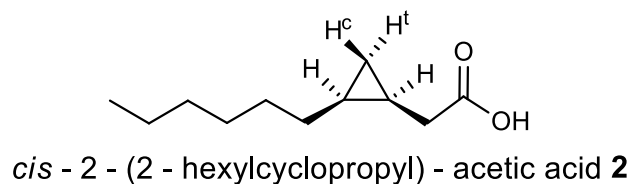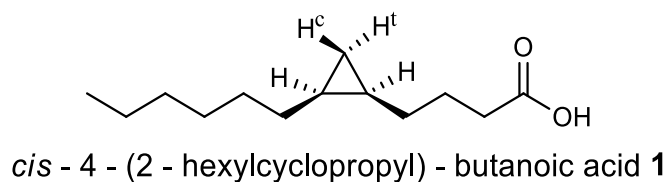
Figure 5-3 Proposed structures for (**1**) and (**2**)**,** cyclopropane fatty acids produced by the *Labrenzia* sp. strain 011 (Ostsee6).The *cis* (H^c) and *trans* (H^t) protons of the methylene group ^{13}C-CH$_2$ are shown. The absolute configuration of *trans*-cascarillic acid ([(1S,2R)-2-hexylcycloprop-1-yl]-acetic acid) (**3)** is presented as depicted by (126).

Table 5-3 1D and 2D NMR spectroscopic data (300 MHz, CDCl$_3$) of compound **1**.
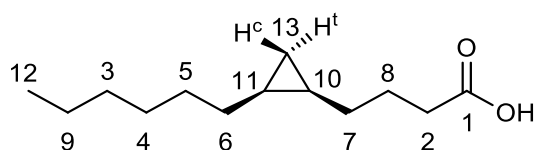
Position	δ$_C$, mult [ppm]	δ$_H$ (*J* in Hz) [ppm]	^{1}H-^{1}H COSY	^{1}H-^{13}C HMBC
1	178.1, C	-	-	
2	33.5, CH$_2$	2.40, t (7.6)	8	1, 7, 8
3	31.9, CH$_2$	1.27, m		
4	30.1, CH$_2$	1.35, m		
5	29.3, CH$_2$	1.25, m		
6	28.7, CH$_2$	1.35, m		
7	28.0, CH$_2$	a:1.46, m	7b, 8, 10	10
		b: 1.22, m	7a, 8, 10	10
8	25.2, CH$_2$	1.75, p (7.6)	2, 7	1, 2, 7, 10
9	22.7, CH$_2$	1.28, m	12	
10	15.2, CH	0.66, m	7a/b, 13a/b	
11	15.7, CH	0.68, m	6	
12	14.1, CH$_3$	0.88, t (6.8)	9	3, 9
13	10.9, CH$_2$	a^t: 0.63, m	10, 11, 13b	6, 7, 10, 11
		b^c: -0.30, q (4.6)	10, 11, 13a	6, 7, 10, 11

^{c}*cis*-configured proton; ^{t}*trans*-configured proton
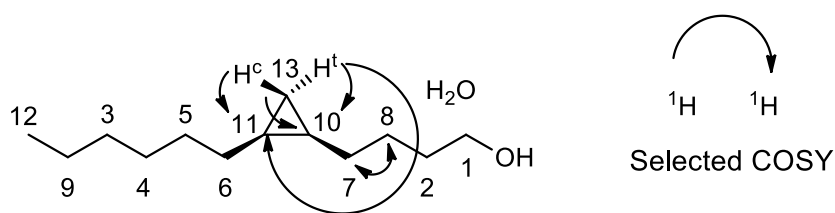
Figure 5-4 Graphic representation of ^{1}H-^{1}H COSY correlations of (**1**) detected in NMR spectroscopic studies. Correlations between H2-13a(^{c})/b(^{t}) with H1-10 and H1-11 were useful to determine the presence of a 1,2-disubstituted cyclopropane ring.
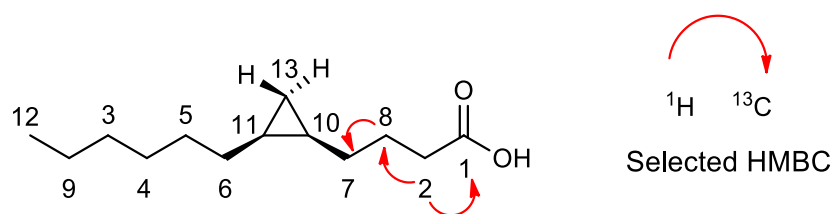
Figure 5-5 Graphic representation of ^{1}H-^{13}C HMBC correlations of (**1**) detected in NMR spectroscopic studies. The selected correlations were crucial to establish the number of carbons between the carboxylic moiety and the cyclopropane ring.

Table 5-4 1D and 2D NMR spectroscopic data (300 MHz, CDCl$_3$) of compound **2**.
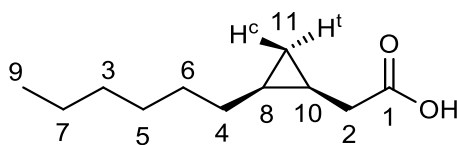
Position	δ_C, mult [ppm]	δ_H (*J* in Hz) [ppm]	^{1}H-^{1}H COSY	^{1}H-^{13}C HMBC
1	180.2, C	-	-	-
2	33.7, CH$_2$	a: 2.42, dd (6.9, 16.0) b: 2.29, dd (7.8, 16.0)	2b, 10 2a, 10	1, 8, 10, 11 1, 8, 10, 11
3	31.9, CH$_2$	1.26, m		
4	29.8, CH$_2$	1.37, m		
5	29.2, CH$_2$	1.29, m		
6	28.8, CH$_2$	1.35, m		
7	22.6, CH$_2$	1.29, m	9	
8	15.5, CH	0.81, m	10, 11a/b	
9	14.1, CH$_3$	0.88, t (7.3)	7	3, 7
10	11.1, CH	1.10, m	2, 8, 11a/b	
11	10.8, CH$_2$	a^t: 0.75, dq (8.4, 5.0) b^c: -0.13, q (5.0)	8, 10, 11b 8, 10, 11a	2, 4, 8, 10 2, 4, 8, 10

^{c}*cis*-configured proton; ^{t}*trans*-configured proton
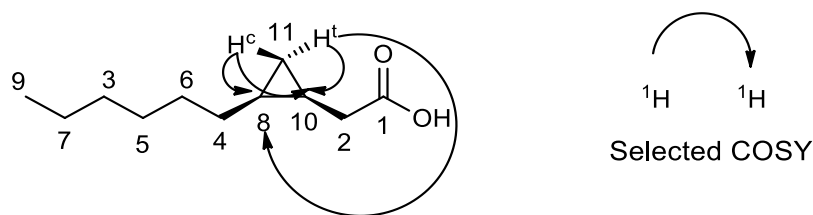
Figure 5-6 Graphic representation of ^{1}H-^{1}H COSY correlations of (**2**) detected in NMR spectroscopic studies. Correlations between H2-11a(c)/b(t) with H1-10 and H1-8 were useful to determine the presence of a 1,2-disubstituted cyclopropane ring.
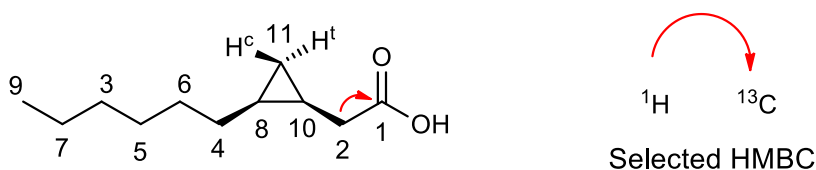
Figure 5-7 Graphic representation of ^{1}H-^{13}C HMBC correlations of (**2**) detected in NMR spectroscopic studies. The selected correlation was crucial to establish that, unlike compound (**1**), compound (**2**) presents only one carbon atom between the carboxylic moiety and the cyclopropane ring.

5.1.6. Bioactivity assessment

5.1.6.1. Antimicrobial properties

Antimicrobial capacities of (**1**) and (**2**) were assessed revealing remarkable growth inhibition of a range of bacterial and fungal organisms in disc diffusion tests (DDT) (Table 5-5). Furthermore, cytotoxic activity of compound (**2**) was tested, displaying no effect against the human cell line selected for this purpose (Table 5-5).

Table 5-5 Summary of bioactivities attributed to the compounds (**1**) and (**2**) in disc diffusion and cytotoxicity testing. For the antimicrobial evaluation, 50 μg of each compound and positive control were utilized. Values presented are inhibition zones in mm. Different concentrations at a micromolar level for the cytotoxicity assay (max. 50 μM). Streptomycin was used as the antibacterial positive control; meanwhile, miconazole as the antifungal positive control. Etoposide worked as the positive control in cytotoxicity test.

Antibacterial activity			
Organism	**1**	**2**	**Streptomycin (+)**
Escherichia coli DSM 498	2	3	6
Bacillus megaterium DSM 32	NA	10	9
Pseudoroseovarius crassostreae DSM 16950^T	5	5	6
Antifungal activity			
Organism	**1**	**2**	**Miconazole (+)**
Eurotium rubrum DSM 62631	NA	10	8.5
Mycotypha microspora MB#271115	3	6	9
Microbotryum violaceum MB#110229	8	10	6
Citotoxic activity			
		2	**Etoposide (+)**
HEK293 embryonic kidney cell line		>50 μM	50 μM 40% cell viability

NA: no activity

Due to efficient growth inhibition exhibited by compound (**2**), it was selected to evaluate its antimicrobial properties against pathogens of human concern (Table 5-6).

Table 5-6 Disc diffusion test panel for the evaluation of compound (**2**) against multidrug-resistant bacteria. The values shown correspond to inhibition zone in mm. The amount of substance evaluated was 3 μg. No positive controls for the selected organism were available. DMSO was used as negative control. These experiments were kindly conducted by MTA Michaele Josten at the Institute for Medical Microbiology of the University of Bonn.
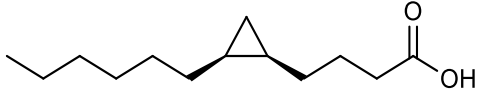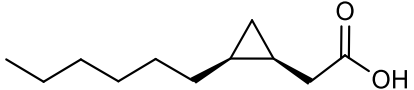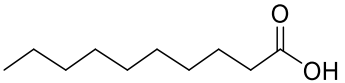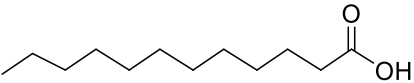
Organism	(2)
Echerichia coli I-11276b	2
Echerichia coli O-19592	2
Klebsiella pneumoniae subsp. *ozeanae* I-10910	2
Listeria welchimeri DSM 20650	2
MRSA LT-1338	2
MRSA LT-1334	2
MSSA 5185	2
MSSA I-11574	2
Staphylococcus aureus 133	3
Staphylococcus aureus SG 511	3
Stenotrophomonas maltophilia I-10717	2

5.1.6.2. Effect of compounds 1 and 2 at the G$_i$ protein-coupled receptor GPCR84.

The G protein-coupled receptor (GPCR) 84 (GPR84) is a pro-inflammatory Gi protein-coupled class A GPCR which is highly expressed in the bone marrow, lung tissue, microglial cells, peripheral leucocytes (*127–130*). It has been demonstrated that medium-chain fatty acids (9-14 carbon atoms) exert agonistic-mediated pro-inflammatory activities promoted by this receptor (*125, 130, 129, 128*). Wang et al demonstrated that undecanoic acid (11C) induced this effect (*128*). Later research concluded that 2- and 3- hydroxylated undecanoic acid are more potent agonists than the non-hydroxylated molecule (*130*). This particular fact leads us to theorize that the carboxylic acid end, spanning the cyclopropyl moieties adjacent to the carbon 4 of (**1**) and carbon 2 of (**2**), may be crucial for the affinity and the interaction with this receptor.

To date, the isolated fatty acid derivatives (**1**) and (**2**) were investigated in radioligand binding assays at the human GPR84 receptor expressed in Chinse Ovarian Hamster cells. The experiments were kindly conducted in collaborative work in the research unit under the responsibility of Prof. Dr. Christa Müller and supervised by Dr. Meryem Köse. Their work produced the following results:

Table 5-7 *In vitro* potencies of fatty acid derivatives (**1**) and (**2**) at GPR84 expressed in Chinese hamster ovary cells (CHO).

cis - 4 - (2 - hexylcyclopropyl) - butanoic acid (**1**)   *cis* - 2 - (2 - hexylcyclopropyl) - acetic acid (**2**)

Decanoic acid   Dodecanoic acid

	Human GPRC84		
Compound	**Binding Assay**	**cAMP assay**[a]	**β-arrestin assay**
	$K_i \pm$ SEM (µM) vs. [^{3}H]PSB-1584 (or % inhibition $\pm$ SEM at 100 µM) (n=3)	$EC_{50} \pm$ SEM (µM) (or % receptor activation $\pm$ SEM at 100 µM) (n=3)	$EC_{50} \pm$ SEM (µM) (or % receptor activation $\pm$ SEM at 30 µM) [*efficacy*][b] (n=5)
Decanoic acid	**3.18** ± 0.51[4]	**7.42** ±0.40 [*100%*][5]	**6.08** ± 0.36 [*92%*][5]
Dodecanoic acid	**3.62** ± 0.49[4]	**8.87** ± 0.75[4]	**2.84** ± 0.31[4c]
1	> **100** (11%)	>> **100** (0%)	> **30** (17 %)
2	**13.3** ± 2.0 (88%)	> **100** (24%)	**0.114** ± 0.060 [*54%*]

[a]Inhibition of forskolin- (10 µM) -induced decrease in cAMP accumulation
[b]Efficacy (E_{max}) relative to the maximal effect of the full agonist embelin (10 µM) (=100%)
[c]n=3

Compound (**2**) showed an affinity for GPR84 with a K_i value of 13.3 µM (Table 5-7, Figure 5-8), which is in about the same range (about 4-fold higher) as that of the physiological agonists decanoic acid (capric acid) and dodecanoic acid (lauric acid). Compound (**1**) did not show any affinity for GPR84 at concentrations up to 100 µM.
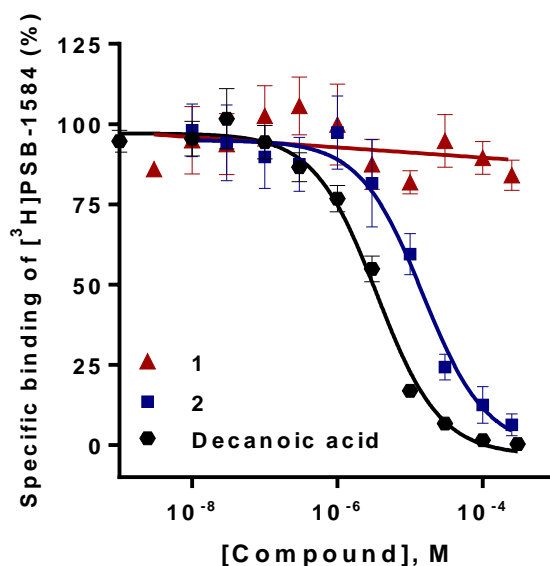
Figure 5-8 Competition binding experiments at membrane preparations of CHO cells recombinantly expressing the human GPR84. The experiments were performed at 25 °C (150 min) using 2 nM [^{3}H]PSB-1584 and 10 µg protein/vial in 50 mM TRIS buffer, pH 7.4, 10 mM MgCl$_2$, 0.05 % fatty acid free BSA. A K_i value of 13.3 ± 2.0 µM was calculated for compound (**2**) and a K_i value of 3.18 ± 0.51 µM for the known agonist decanoic acid. Data points represent means ± SEM from 3 independent experiments, each performed in duplicates.

GPR84 agonistic properties were evaluated in two different assays: (1) cAMP accumulation assays determining the compounds' potency to inhibit forskolin-induced cAMP accumulation in Chinese hamster ovary (CHO) cells stably expressing the G_i protein-coupled human GPR84, and (2) β-arrestin recruitment assays using the enzyme complementation technology.

Compound (**1)** was inactive in both assays in agreement with results obtained in radioligand binding experiments. Compound (**2**) did neither induce nor block G_i-mediated signalling; however, it showed a concentration-dependent activation of β-arrestin

recruitment with an EC_{50} value of 114 nM being 53-fold more potent than decanoic acid (EC_{50} = 6.08 µM) and 25-fold more potent than dodecanoic acid (EC_{50} = 2.84 µM) in that assay (Table 5-7, Figure 5-9). The efficacy was determined to be 54 % compared to the full agonist embelin. This indicates that compound (**2**) is a partial agonist of GPR84 biased towards β-arrestin recruitment.
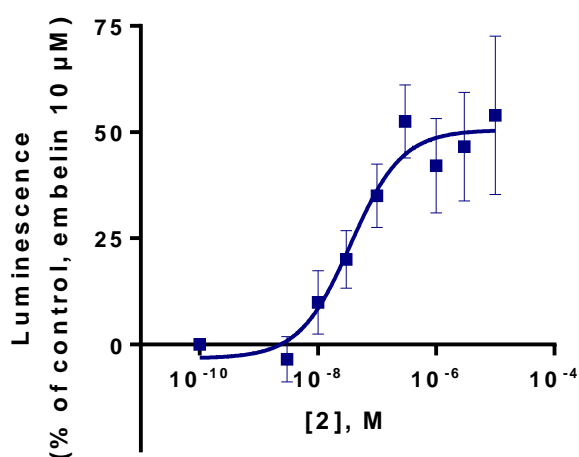
Figure 5-9 Concentration-response curve of (2) determined in β-arrestin assays using the β-galactosidase complementation technology. The maximal luminescence induced by the full agonist embelin (10 µM) was defined as 100 %. The buffer control was defined as 0 %. An EC_{50} value of 114 ± 60 nM was calculated for (**2**). Mean values ± SEM from 5 independent experiments performed in duplicates are shown.

6. CHAPTER 3: Bioactivity assessment of bacteria isolated from the German North Sea

6.1. Background

Supporting our efforts to find bioactive compounds from microbial producers, the research group of Prof. Dr. Thorsten Brinkoff (Oldenburg University) kindly provided our group with marine environmental samples collected in the German coastal area of Neuharlingersiel, from which we isolated bacterial strains.

Bacteria were isolated applying the protocol described in section 3.2.1. The most promising organisms in terms of potential production of bioactive metabolites are listed in Table 6-1 together with some of their most relevant phenotypic traits. Preliminary strain identification was done by 16S rDNA Sanger sequencing experiments. The corresponding sequences are shown in the appendix (A9.2 - A9.4).

Table 6-1 Phenotypic profiling of the bacteria isolated from marine environmental samples. The nomenclature of each organism (**Siel #L**) was randomly assigned and hold no implications of any kind with the experimental observations.

Isolate	Siel 3m	Siel 4n	Siel 7n	Siel 8n
16S rDNA-based identity	94 % Uncultured bacterium (AN: GU118051)	97 % Uncultured bacterium (AN: GQ867431)	97 % *Lysobacter* sp. (AN: JQ716253)	99 % *Myxococcus xanthus* (AN: NR_074873)
Origin	Clam shell	Sediment	Sediment	Sediment
Lytic activity	Yeast	Yeast, bacteria	Yeast, bacteria	Yeast, bacteria
Approximate length (μm)	15-20	3-7	5-10	5-10
Temperature growth range (°C)	4-37	20-37	20-37	20-37

The following phenotypic traits are common for the 4 isolates: Gram-negative staining, rod shape, halotolerance, aerobic metabolism, and gliding motility. Isolates Siel 4n, 7n and 8n were capable to lyse *E. coli* bacterial spots (section 3.2.1) and *S. cerevisiae*. The latter feature was observed in broth ASW-VY/4. The broth is turbid due to the *S. cerevisiae* suspension, thus its clearance after bacterial growth was taken as positive lytic activity on yeast. Siel 3m lysed exclusively these cells.

Sequencing results of 16S rDNA sequences allowed preliminary identification of the isolates. Additionally, Siel 8n exhibited the typical yellow pigmentation and fruiting body formation features of the genus *Myxococcus* (*48, 50*), further confirming the sequencing results.

6.1.1. Biological assessment of the bacterial isolates

In order to confirm the first observations in terms of bioactivity, and further characterize the organisms, a deeper biochemical profiling was done and a bioactivity-screening panel was designed to test the metabolites produced by the isolated bacteria (*131*). Such work is supplementary to this doctoral thesis and includes detailed descriptions of methods and materials employed in the evaluation of the isolates.

The lytic behavior displayed by the organisms may be a reflection of predatory habits and presumably, of potential production of chemical bioactive substances. Hereby we present the biochemical profile of the isolates and lytic behavior on cyanobacteria, *E. coli* and *S. cereviseae* assays (Table 6-2).

Table 6-2 Summary of bioactivities and phenotypic traits of the bacteria isolated from environmental samples.

Isolate	Siel 3m	Siel 4n	Siel 7n	Siel 8n
Fischerella ambigua lysis	-	+	-	-
Nostoc sp. lysis	-	+	-	+
Nostoc insulare lysis	-	-	-	-
Oscillatoria sp. lysis	-	+	-	+
Tychonema sp. lysis	-	-	-	-
E. coli lysis	-	+	+	+
S. cerevisiae lysis	+	+	+	+
Haemolysis	β	β	γ	(-)
Chitosanase	-	-	-	-
Cellulase	-	-	-	-
Agarase	+	-	-	-
Amylase	-	-	+	-
Gelatinase	+	+	-	+
Caseinase	-	-	+	+

β-galactosidase	+ (g)	+ (g)	+	(-)
Catalas	+	+	+	+

+ = Lysis or enzyme activity; – = No lysis or no enzyme activity; (–) = No growth; β = β-haemolytic;

γ = γ-haemolytic; (g) = Gas production

6.1.1.1. Production of bacterial crude extracts

Bacteria were grown in ASW-VY/4 and casitone broth. Extracts of each culture were

obtained by liquid-liquid extraction using ethyl acetate as described in 3.3.1. Extracts

were evaluated in agar diffusion tests (Table 6-3).

Table 6-3 Disc diffusion test of extracts obtained from the bacterial culture. A volume equivalent to 50 μg of each extract was used for the evaluation. Values shown correspond to mm of growth inhibition on the test strains. Ampicillin and miconazole (50 μg) were used as positive control, respectively against bacteria and fungi.

Antibacterial activity				
Organism	**Siel 3m**	**Siel 4n**	**Siel 7n**	**Siel 8n**	**Ampicillin (+)**
Escherichia coli DSM 498	NA	NA	NA	NA	13
Bacillus megaterium DSM 32	3	NA	NA	NA	15
Antifungal activity				
Organism	**Siel 3m**	**Siel 4n**	**Siel 7n**	**Siel 8n**	**Miconazole (+)**
Eurotium rubrum DSM 62631	NA	NA	NA	NA	8
Mycotypha microspora (this study)	NA	NA	NA	NA	9
Microbotrium violaceum (this study)	2.5	NA	NA	NA	9

NA: no activity

7. SUMMARY

Bacteria are the source of many biotechnologically produced drugs, *e.g.* the antibacterial antibiotics daptomycin and vancomycin, the antifungal antibiotic amphotericin B, and chemotherapeutic anticancer agents, *e.g.* doxorubicin. For decades, such bacteria were isolated from terrestrial sources, above all from soil samples. Thus, the immunosuppressive drug tacrolimus, biosynthesized by the bacterium *Streptomyces tsukubaensis* was obtained from a soil sample collected in Japan, and is today administrated to patients with organ transplants with the aim to decrease the risk of immune-mediated rejection of the organs received. It has been proposed that microorganisms produce such secondary metabolites for ecological purposes, *e.g.* to weaken or kill competitors for nutrients.

The current project focuses on marine-derived bacteria as a novel source of compounds with a presumably high degree of structural novelty. Indeed, marine actinomycetes were found to be producers of highly bioactive compounds, *e.g. Salinispora tropica* as the source of salinosporamide A, a selective proteasome inhibitor currently undergoing clinical studies as anticancer drug. The objective of the current study is to assess the biosynthetic capabilities of marine-derived bacteria, either through a genome-mining approach and/or through the isolation of bioactive products.

The first group of bacteria investigated was marine myxobacteria, an overlooked source of bioactive compounds. Interestingly, some of the chemistry known from these bacteria, *e.g.* salimabromide from *Enhygromyxa salina* SWB007 was unprecedented. To date, many bacterial genomes are publicly available. Among such genomes are also some from marine myxobacteria. Using bioinformatic tools like antiSMASH, genomes of marine myxobacteria, namely *Haliangium*, *Enhygromyxa*, Myxobacterium SMH-27-4 (*Paraliomyxa*), *Plesiocystis* and *Pseudenhygromyxa* were analysed. These works

revealed numerous putative gene clusters encoding enzymes for secondary metabolites in each strain analysed. Among the most relevant findings are the 38 biosynthetic gene clusters detected in Enhygromyxa salina DSM 15201, 28 gene clusters in *Plesiocystis pacifica* SIR 1, and 25 in Haliangium ochraceum DSM 14365. Mostly, the gene clusters detected correspond to hybrids of polyketide synthase and non-ribosomal peptides. Additionally, the putative gene cluster encoding the cytotoxic drug haliangicin (cytotoxicity, HeLa-S3 cell line, $IC_{50} = 12 \mu M$) produced by *H. ochraceum* was envisioned. The prospective research possibilities offered by these organisms concerning the potential secondary metabolite production is vindicated.

Five bacterial strains were isolated from German coastal areas. The most remarkable activities were shown by one unclassified isolate labeled Siel 3m and *Labrenzia* sp. strain 011 (Ostsee6). These bacteria were respectively isolated from a seashell collected in Neuharlingersiel, and marine sediment retrieved from the shallows of Kronsgaard, Germany.

Extracts of the bacterium Siel 3m showed growth inhibition of bacteria and fungi in disc diffusion tests (mm of inhibition at 50 μg). Susceptible organisms were the bacterium *Bacillus megaterium* DSM 32 (3 mm) and the fungus *Microbotrium violaceum* (2.5 mm). Additionally, the growing bacterium Siel 3m displayed lytic activity against *Saccharomyces cereviseae*. To date, no metabolites responsible for these activities have been identified.

Concerning *Labrenzia* sp. strain 011 (Ostsee6), experiments to identify metabolites of biological interest were conducted. Antimicrobial-oriented evaluation of bacterial extracts showed growth inhibition of fungi and bacteria. Fractionation and purification of the extracts yielded two metabolites of lipid nature, namely (**1**) cis - 4 - (2 - hexylcyclopropyl) - butanoic acid and (**2**) cis - 2 - (2 - hexylcyclopropyl) - acetic acid; (**1**) exhibiting a novel structure.

Summary

The structures were deduced by extensive 1H-, 13C- and 2D-NMR analyses. Interpretation of NMR spectra revealed aliphatic compounds, showing resonance signals in the upfield regions of the ^{1}H-NMR spectrum with negative ppm values, consistent with the typical resonances of protons of cyclopropane moieties. NMR studies together with UPLC-HRMS confirmed the structures of the compounds presented below:
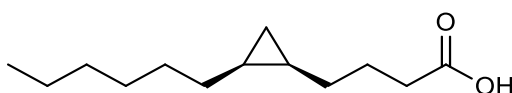
cis - 4 - (2 - hexylcyclopropyl) - butanoic acid (**1**)
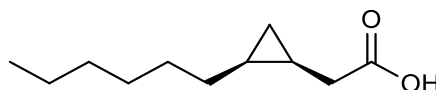
cis - 2 - (2 - hexylcyclopropyl) - acetic acid (**2**)

Antimicrobial activities of (**1**) and (**2**) were assessed revealing remarkable growth suppression of a range of bacteria and fungi. The activity spectrum of compound (**2**) assessed in disc diffusion tests included bacterial pathogens, *e.g.* methicillin-resistant *Staphylococcus aureus* strain LT-1338 (2 mm diameter inhibition, 3 µg/disc).

It has been proposed that species of the genus *Labrenzia* play important ecological roles in the marine habitat. This notion originates from previous research works where it was observed that colonization of the oyster *Crassostrea virginica* by species of the genus *Labrenzia* prevented infection by the bacterial oyster pathogen *Pseudoroseovarius crassostreae*. In the present work, the antimicrobial compounds (**1**) and (**2**) isolated from *Labrenzia* sp. strain 011 (Ostsee6) were tested against *P. crassostreae* strain DSM 16950.

Summary

These experiments revealed remarkable growth inhibition of *P. crassostreae* DSM 16950 in disc diffusion tests (**1** and **2**, 5 mm diameter inhibition; streptomycin as positive control, 6 mm diameter inhibition, 50 μg/disc). These results add up to the aforementioned notion that posed bacteria of the genus *Labrenzia* as biocotrol agents in the marine environment.

Due to similarities among compounds (**1**) and (**2**) with medium-chain fatty acids, both compounds were evaluated as ligands at the medium-chain fatty acid receptor GPCR 84 (collaboration with Prof. Dr. Christa Müller), which is upregulated in inflammatory processes. In this context, it is of interest that compounds similar to (**1**) and (**2**) were also isolated from *Croton eleuteria*, a plant whose aqueous extracts have been used as inhalants in folk medicine to palliate the inflammatory symptoms of respiratory ailments. Compound (**1**) did not show affinity towards this receptor (Ki > 100 μM), unlike compound (**2**), which indeed showed affinity (Ki = 13.3 ± 2.0 μM). Analyses of the latter interaction revealed that compound (**2**) is a partial agonist at this receptor biased to β-arrestin accumulation (cAMP assay, EC_{50} > 100 μM; β-arrestin assay, EC_{50} = 0.114 ± 0.06 μM). These results suggest that (**2**) may affect inflammatory processes *in vivo*.

In conclusion, this work vindicates unusual bacterial sources as efficient producers of bioactive metabolites with the potential to become lead compounds. Interestingly, genomic explorations revealed that microorganisms like myxobacteria are an underexplored source of promising compounds, comparing the number of gene clusters harbored in their genomes and the compounds isolated hitherto. Furthermore, substances isolated from the halophilic bacterium *Labrenzia* sp. strain 011 (Ostsee6) showed that the growth of resistant bacterial pathogens can be inhibited, *e.g. Escherichia coli* I-11276b, *Escherichia coli* O-19592, MRSA LT-1338, MRSA LT-1334, *Staphylococcus aureus* SG 511. Altogether, genomic and chemical studies performed during the current project point towards a rich resource of chemical structures that may be investigated in the search for new bioactive molecules.

8. DISCUSSION AND CONCLUSIONS

Bacteria produce many of the antibiotics currently used, *e.g.* the antibacterial daptomycin, vancomycin, the antifungal amfotericin B, and drugs used to treat cancer, *e.g* doxorubicin (*132–135*). For decades, such bacteria were isolated from terrestrial sources, above all soil samples. It has been proposed that microorganisms produce this class of compounds as secondary metabolites for ecological purposes, *e.g* weaken or kill competitors for nutrients and living preys in their environments.

The current project focuses on marine-derived bacteria as a novel source of compounds with a high degree of structural novelty. The objective is to discover new compounds in order to tackle the phenomenon of antimicrobial resistance.

The marine bacteria investigated in this work are, on one hand, myxobacteria, some of them marine obligates and, on the other hand the strictly halophilic α-proteobacterium *Labrenzia* sp. strain 011 (Ostsee6). The myxobacteria were analysed *in silico* and *L. aggregata* experimentaly, yielding two bioactive molecules (**1** and **2**) with antimicrobial and possibly, anti-inflammatory properties which will be discussed in the following sections.

8.1. Marine-derived myxobacteria

Geographically, halophilic and halotolerant myxobacteria are widely distributed as evidenced by some of the bacterial isolates described in chapter 4, originating, *e.g.* from German, Japanese and US American marine environments. This observation is supported by the investigation of myxobacteria-enriched libraries of 16S rRNA gene sequences revealing myxobacteria-related sequences in mud samples taken around Japan (*136*). The latter sequences were phylogeographically clearly distinct from those of terrestrial myxobacteria (*136*).

A further report also states that myxobacteria capable of thriving in ocean-like conditions exhibit a worldwide distribution (*137*).

The quantitative presence of myxobacteria in marine environments can hardly be judged. Based on the isolation success one may suggest that the frequency is much lower (*e.g.* only 6 isolates from 90 coastal samples (*57, 59*)) than in terrestrial habitats, but this may simply represent the less-than-perfect isolation and cultivation conditions used today. Indeed, the currently applied isolation protocols for marine myxobacteria are only slightly altered in terms of the addition of sea salt, when compared to those for terrestrial strains, *e.g.* terrestrial *Escherichia coli* is still used as prey. In addition, it is difficult to recognize marine myxobacterial colonies after isolation, because their morphological features may deviate from the ones of terrestrial strains. Thus, in order to use marine-derived myxobacteria as a source of bioactive metabolites, in-depth studies of their morphology and physiology are necessary.

From the available genetic and chemical data, the potential of halotolerant and halophilic myxobacteria as producers of chemically diverse secondary metabolites is out of question. Salimabromide **26** from *E. salina* is an outstanding example of such a molecule having a most unusual new carbon skeleton (*100*). The number of molecules obtained so far, however, is very low (Table 8-1), especially when compared with the expected metabolites envisioned after bioinformatic analysis of the four available genomes of myxobacteria in the suborder Nannocystineae. All strains harbor at least 25 biosynthetic gene clusters (Chapter 4, table 4-1), most of them bearing no or very little homology to known biosynthetic genes. Compared to *Myxococcus xanthus* DK1622, the so far sequenced strains dedicate a similar or even larger portion of their genome of up to 10% to secondary metabolism.

Table 8-1 Metabolites reported to date from myxobacteria grouped into the suborder Nannocystineae and their bioactivities.

Genus	Classification according to salt requirements for growth	Metabolites	Metabolite [No] Bioactivity
Nannocystis	Terrestrial	Nannocystin A **10**	**10** Antiproliferative activity, MDA-MB231 and its related drug resistant MDA-A1 (IC_{50} = 6.5 and 12 nM respectively), HCT116 (IC_{50} = 1.2 nM) and PC3 (IC_{50} = 1.0 nM)
	Halotolerant	Phenylnannolone A, B, C **11-13**, Pyrronazol A, A2, B, C1, C2 **14-18**, Nannozinone A, B 21, 22, Nannochelin A **23**	**11** Reversing drug-resistance of tumor cells **21** *Mycobacterium diernhoferi*, *Candida albicans*, *Mucor hiemalis*, MICs: 33.3 μgmL^{-1} in each case **22** Cytotoxicity, SKOV-3 IC_{50} = 2.4 μM, KB3-1 IC_{50} = 5.3 μM and A431 IC_{50} = 8.45 μM **23** Cytotoxicity, HUVEC and KB3-1 IC_{50} = 50 nM
Haliangium	Moderately halophilic	Haliangicin **24** Haliamide **25**	**24** *Aspergillus niger*, MIC: 12.5 μgmL^{-1}, *Phytophthora capsici,* MIC: 0.4 μgmL^{-1}; **25** Cytotoxicity, HeLa-S3, IC_{50} =12 μM
Enhygromyxa	Halophilic	Salimabromide **26**	**26, 27, 32**

		Enhygrolide A, B **27, 28** Deoxyenhygrolide A, B **29, 30** Salimyxin A, B **31, 32** Enhygromic acid **33**	*Arthrobacter crystallopoietes*, MICs: 16, 8 and 4 μgmL^{-1} respectively; **33** Cytotoxicity, melanoma B16, IC$_{50}$=46 μM; *Bacillus subtillis*, MIC: 8 μgmL^{-1}
Myxobacterium SMH-27-4 (*Paraliomyxa*)	Slightly halophilic	Miuraenamide A-F **34-39**	**34** *Trichophyton mentagrophytes*, MIC: 12.5 μgmL^{-1}
Plesiocystis	Halophilic	No metabolites described	-
Pseudenhygro-myxa	Halotolerant	No metabolites described	-

These "cryptic" or "silent" gene clusters may be addressed with different strategies (*138*), *e.g.* the OSMAC (one strain, many compounds) approach (*139*) or co-culturing and elicitation techniques (*140–142*). Mass spectrometric analysis (*143–146*), dereplication procedures (*80, 144*), bioinformatic analysis and genetic experiments allow a direct connection of metabolites and gene clusters (*78, 79, 145*). On the other hand, recent advances in the direct cloning of gene clusters and their heterologous expression (*147–150*) may enable researchers to select their "favorite" gene cluster and express and manipulate it in heterologous hosts for rational secondary metabolite discovery. These techniques offer the chance for an effective metabolomics-guided natural product and genome-mining platform.

It can be concluded that the application of these promising state-of-the-art approaches to marine myxobacteria should expand our knowledge on novel secondary metabolites

in these organisms, and help to unveil systematically the chemistry encoded in their genomes.

8.2. Discussion of metabolites isolated from the halophilic bacterium *Labrenzia* sp. strain 011 (Ostsee6)

Apart from marine myxobacteria, different groups of sea-dwelling bacteria should be investigated as producers of secondary metabolites. A reason for this is provided by the findings derived from the investigations conducted on the halophilic bacterium *Labrenzia* sp. strain 011 (Ostsee6). Species of the genus *Labrenzia* were previously thought to be protective agents of the oyster *Crassostrea virginica* against the halophilic bacterium *Pseudoroseovarius crassostreae*, a frequent oyster pathogen (*119*). In this work, the antimicrobial compounds (**1**) and (**2**) isolated from *L. aggregata* sp. strain 011 (Ostsee6) were tested against *P. crassostreae* strain DSM 16950. Both compounds (**1**) and (**2**) revealed remarkable growth inhibition of the oyster pathogen in disc diffusion tests (**1** and **2**, 5 mm diameter inhibition, 50 µg/disc). The structures are shown in figure 8-1.
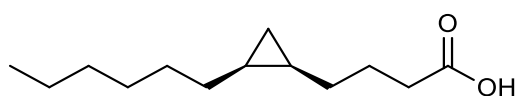
cis - 4 - (2 - hexylcyclopropyl) - butanoic acid (**1**)
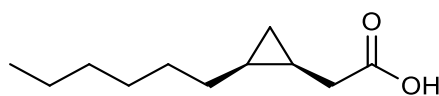
cis - 2-(2 - hexylcyclopropyl) - acetic acid (**2**)

Figure 8-1 Fatty acid-derivatives containing cyclopropyl groups were isolated from the halophilic bacterium *Labrenzia* sp. strain 011 (Ostsee6). Both compounds display remarkable antibacterial and antifungal activities.

These results add up to the aforementioned notion that posed bacteria of the genus *Labrenzia* as biocontrol agents in the marine environment. Additionally, (**1**) and (**2**) exhibited antimicrobial properties against a range of fungi and bacteria, and compound

(**2**), interaction with the GPCR84 receptor *in vitro*. These aspects will be discussed in the upcoming sections.

8.2.1. Hints on the biosynthetic origins of the cyclopropane-containing fatty acids derived from *Labrenzia* sp. strain 011 (Ostsee6)

The biosynthetic origin of (**1**) and (**2**) remains unclear. However, studies on cyclopropane-containing fatty acids were performed earlier and found that these structures are typically produced in the cell membrane of an ample number of bacterial genera, hence functioning as structural components (*151*). The reaction involved is methylation of double bonds of unsaturated phospholipids via a fatty acid cyclopropane fatty acid synthase (CFAS)-mediated activity (CFAS, with S-adenosylmethionine (AdoMet) as a methyl donor (Figure 8-2)(*151*).

S-Adenosyl-L-methionine   S-Adenosyl-L-homocysteine
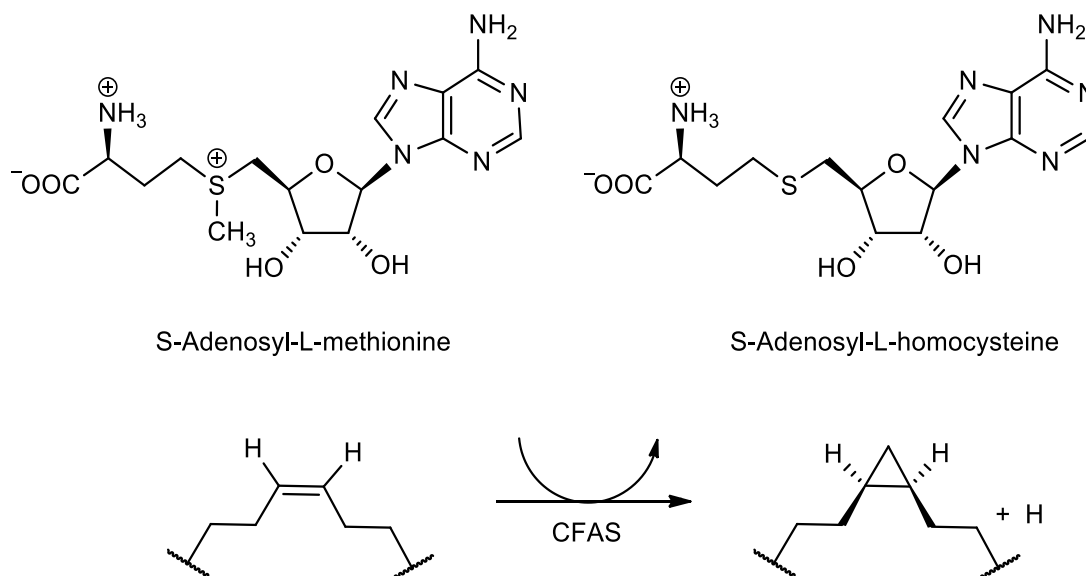
Figure 8-2 Typical cyclopropanation mechanism observed in bacteria, *e.g. Escherichia coli* modified from (*152*). The substrates of the cyclopropane fatty acid synthase (CFAS) are usually unsaturated phospholipids. An alternative mechanism is observed in the genus *Mycobacterium* -efficient producers of cyclopropane fatty acids-*,* where the unsaturated alkyl chain is probably bound to an acyl carrier protein (*152*), suggesting the involvement of biosynthetic gene clusters in the production of this compund class.

Biebl et al. (*118*) conducted extensive profiling of structural fatty acids of various species comprised within the genus *Labrenzia*. Their work revealed unusual structures, predominantly 11-methyl 20:1ω6t, and 11-methyl 18:1ω6t, which reflect the capacity of these organisms to methylate unsaturated phospholipids. Additionally, genomic analyses conducted on the BRENDA system detected putative cyclopropane-fatty-acyl-phospholipid synthase and class I SAM-dependent methyltransferases in annotated genomes of *Labrenzia* spp. (Data not shown). Therefore, one possible biosynthetic origin of (**1**) and (**2**) would be the cyclopropanation of unsaturated phospholipids in the membrane (Figure 8-2), subsequently cleaved to be released into the bacterial environment.

Interestingly, CFAS are thought to be incapable to methylate regions close to the carboxylic end of the alkyl chains of phospholipids (*151*). Thus, it is worthwhile to investigate the biosynthetic origin of (**1**) and (**2**).

8.2.2. Antimicrobial capacities of 1 and 2

It is known that certain fatty acids are capable to exert notorious antimicrobial activities by inhibiting the synthesis of structural fatty acids in microorganisms or generating disturbances and instability in their cell membranes (*153*). Specifically, modified fatty acids with antifungal properties have been isolated from marine organisms in the past (*154*). The capacity of producing antimicrobial metabolites is a relevant feature for the hosts of *Labrenzia*, *e.g.* mollusks may harness to be protected against pathogens if *Labrenzia* metabolites (**1**) and (**2**) are produced in the natural environment. Experiments of Graça et al. (*155*) suggest that protection by *Labrenzia* is also provided to organisms like corals. They retrieved one organism of the genus *Labrenzia* from coral surfaces, whose extracts inhibited bacterial growth *in vitro*.

It is thought that producers of antimicrobial compounds generate such substances to suppress competitors for nutrients and to kill or weaken living microbial preys of bacteria

that exhibit heterotrophic behavior, *e.g.* myxobacteria and *Labrenzia* spp. (*118, 36, 101, 25, 156*).

Particularly striking in the present work was the efficient growth inhibition caused by (**1**) and (**2**) of the pathogen *Pseudoroseovarius crassostreae* DSM 16950^T in disc diffusion tests, in which 50 μg of (**1**) and (**2**) respectively produced a 5 mm inhibition zone, comparable to the 6 mm shown by 50 μg of the positive control streptomycin. This fact strengthens the assumption of (*118*) regarding the protective role of bacteria of the genus *Labrenzia* against the roseovarius oyster disease. Probably, these antimicrobial compounds would provide protection against a wide range of microorganisms, considering the growth inhibition observed of test organisms of bacterial and fungal origin in disc diffusion testing.

The factors triggering the production of antimicrobial CYPFAs should be a subject of deeper investigation, but microbial competition for nutrients could be a good reason to produce substances intended to overcome rivalry in the marine environment. This assumption makes sense if we consider that stress factors, *e.g.* nutrient deprivation, exposure to toxic entities and oxygen depletion stimulate the production of structural cyclopropanated fatty acids on the membranes of various bacterial genera under *in vitro* conditions (*151, 157–159*). This correlates with the fact that we observed the production of these compounds only after one week of cultivation.

Additionally, it is reasonable to think that a few amount of gene clusters involved in secondary metabolism may suggest the performance of very specific tasks. This is reasonable if we consider the putative PKS, NRPS nature of the clusters found in our in silico screening, and knowing that molecules of this nature often display antimicrobial activities (*66, 65, 67, 68*). Bacteriocins, antimicrobial polypeptides, and proteins (*160*) are putatively produced by *Labrenzia* species according to the genome mining analyses.

It is worthwhile to keep in mind that these peptides may also mediate biological control by suppressing microbial diversification.

To date, isolation of *Labrenzia* species has been reported in coastal areas with contrasting climate conditions: the Mediterranean region in Spain by (*161*), and German North Sea (this work). Furthermore, additional strains of *Labrenzia aggregata* and *Labrenzia alexandrii* were also isolated in our group from marine samples collected in the Peruvian Pacific Coast (data not shown). This suggests successful adaptability and presumably, a worldwide distribution.

8.2.3. Effect of metabolites 1 and 2 on GPRC84

Agonistic-mediated activation by medium-chain fatty acids (9-14 carbon chain length) as well as by the respective 2- or 3-hydroxy-fatty acids of GPCR84 lead to enhanced cytokine (IL-12 p40, IL-8, and TNF-α) production in myeloid cells (*130, 128, 162*). Additionally, the natural products embelin (3,3-diindolylmethane [DIM]), originally isolated from the plant *Embelia ribes* Rumb (Primulaceae), as well as the synthetic compound 6-octylaminouracil were found to act as GPR84 full agonists (*163, 130*). Surprisingly, recent works have proven embelin to ameliorate the symptoms of acute respiratory distress syndrome in murine models (*163*). This finds congruence with the demonstration that some agonistic agents are capable of exerting different effects according to the kind of agonism they exhibit, *e.g.* biased agonism or inverse agonism (*164*). Particularly, it has been observed that biased agonists are capable of inducing competitive- and noncompetitive-like antagonistic effects in the presence of agonists (*165*). Probably, inflammation promoters, *e.g.* decanoic acid (10C), dodecanoic acid (12C), and related compounds may promote inflammation by impeding the intracellular recruitment of cAMP and favoring the accumulation of β-arrestins in accordance to our assays.

If the latter is true, it can be expected a GPR84-dependant anti-inflammatory effect mediated by the biased-agonist (**2**) considering that selectively favors β-arrestins recruitment (cAMP assay, $EC_{50} > 100$ μM; β-arrestin assay, $EC_{50} = 0.114 \pm 0.06$ μM), a phenomenon that leads to desensitization of agonist occupied-GPCR receptors (*166, 167*). Furthermore, *in vivo* experiments have shown that accumulation of cAMP is involved in anti-inflammatory mechanisms in certain models of inflammation (*168*). Hence, it is likely to expect downregulation of GPR84, hence mitigation of inflammatory processes by (**2**) *in vivo*. This effect should not be surprising, since certain fatty acids (Ω-monounsaturated) competitively inhibit the proinflammatory eicosanoid derivatives, *e.g.* leukotrienes, thus leading to mitigation of inflammatory response (*169*). Probably, cascarillic acid, analogous to (**2**) present in the tropical Caribbean shrub *Croton eluteria*, utilized in folk medicine to palliate the inflammatory symptoms of respiratory ailments, may be responsible for this putative medicinal effect (*124–126*).

In spite of the evidence generated, further research is required to prove these hypotheses. Aspects to investigate future works are: i) evaluate the interaction of (**2**) with proinflammatory agonists of GPR84 and different proinflammatory receptors, ii) characterize ligand affinity of (**2**) towards different GPR-expressing tissues/cells in order to gain mechanistic insights, iii) assess anti-inflammatory activity using *in vivo* models, iiii) characterize the mechanisms of receptor attenuation (if any) and pathways activated by (**2**).

The divergence among the *in vitro* biological effects of (**1**) and (**2**) may be explained by the relative position of the cyclopropyl structure relative to the carboxylic moiety of the hydrocarbon chains; also, the chain length seems to have an influence on the effects of the ligands according to the differences observed between C10 and C12. Lastly, the relative position of the ring in the hydrocarbon chain is decisive for the affinity of the compounds for the GPR84.

Although not fully understood, previous research suggests the involvement of the GPR84 receptor in neuroinflammatory processes as well, *e.g.*, multiple sclerosis and Alzheimer disease (*170, 127*). In this regard, the search for ligands affine to this receptor deserves particular attention in order to elucidate its function.

8.3. Bacteria isolated from the German North Sea

Bacteria isolated were capable of lysing microorganisms, probably due to the production of enzymes with the correspondent activity. This is a trait observed also in some other bacteria isolated from terrestrial and marine environments when exposed to alien organisms (125, 126). Bacterium Siel 3m was chosen for secondary metabolite isolation due to the growth inhibition shown in the domestic antimicrobial disc diffusion testing on a range of microorganisms, *e.g. Bacillus megaterium* DSM 32 (3 mm) and the fungus *Microbotrium violaceum* (2.5 mm). Additionally, the living organism displayed lytic activity against *Saccharomyces sereviseae* under co-culture conditions. To date, no metabolites responsible for any of the mentioned activities have been identified. Unfortunately, this organism lost its growth capacity under laboratory conditions in the development of this project, thus hindering assessment of further bioactivities. It would be desirable to reestablish the viability of this bacterium due to potential production of natural inhibitors. Extracts from this organism showed similar behavior of those of the bacterial mixture described in chapter 2 in terms of antimicrobial growth inhibition. Furthermore, ^{1}H spectrum of crude extracts obtained by liquid-liquid extraction from liquid cultures showed signals similar to the ones produced by cyclopropyl groups of metabolites described in the previous chapter (Appendix, Figure 9-10). The activities displayed by the bacteria isolated is a reflection of the infinite possibilities of finding unknown organisms as well as novel compounds. It is especially notorious that conventional screening and isolation techniques remain to be useful tools to increase the stock of microorganisms with potential use for clinical purposes.

8.4. Closing remarks

This work contributes to widening the reservoir of natural sources of bioactive compounds. Previous reports had focused mainly on terrestrial organisms as a source of bioactive metabolites (*171, 110, 49, 172, 173, 66, 72, 67, 68*). However, marine-derived organisms have been proven to be an underexplored source of interesting substances (*101, 36, 174, 57, 60, 108*). Furthermore, it was demonstrated that bioinformatics orient the classic experimental approaches in the isolation of metabolites of interest, or at least is helpful to determine whether it is worthwhile to put research efforts on a certain organism. Myxobacteria are excellent examples to illustrate the virtues of natural product research (*66, 101, 77, 67, 68*). These organisms are producers of compounds with most diverse bioactivities, and the possibilities to find novel structures is huge. To date, just a handful of these extraordinary bacteria has been isolated and the number of so far-isolated compounds in comparison to the ones putatively encoded in the genomes is minimum. Deeper investigations on the topic are available in recent works comprehending marine myxobacteria (*36*), but the low ratio isolated/encoded is also true for their terrestrial counterparts according to several bioinformatic analyses conducted in our lab and elsewhere. Factors hindering the isolation of new microorganism must be urgently overcome in order to accelerate the pace of discovery of novel drugs with the potential to become lead compounds.

PUBLICATIONS

Davila-Cespedes, A., Hufendiek, P., Crusemann, M., Schaberle, T. F., & Konig, G. M. (2016). Marine-derived myxobacteria of the suborder Nannocystineae: An underexplored source of structurally intriguing and biologically active metabolites. Beilstein journal of organic chemistry, 12, 969–984. https://doi.org/10.3762/bjoc.12.96

Dávila-Céspedes, A., Juárez-Flores, B. I., Pinos-Rodríguez, J. M., Aguirre-Rivera, J. R., Oros-Ovalle, A. C., Loyola-Martínez, E. D., & Andrade-Zaldívar, H. (2014). Protective effect of *Agave salmiana* fructans in azoxymethane- induced colon cancer in Wistar rats. Natural product communications, 9 (10), 1503–1506.

Dávila-Céspedes, A., M., Kehraus, S., Köse, M., Neu, E. & König, G.M. (In preparation). Cyclopropane-containing fatty acids isolated from *Labrenzia* sp. 011 (Ostsee6) inhibit the roseovarius oyster disease pathogen *Pseudoroseovarius crassostreae* DSM 16950.

Amiri Moghaddam, J., **Dávila-Céspedes, A.** et al. (In preparation). Comparative genomic and metabolomic analysis of marine myxobacteria reveals high potential for biosynthesis of novel natural products.

9. References

1. Woese, C. R. Bacterial evolution. *Microbiological Reviews [Online]* **1987,** *51* (2), 221–271.

2. Zhang, Y.-Q.; Li, Y.-Z.; Wang, B.; Wu, Z.-H.; Zhang, C.-Y.; Gong, X.; Qiu, Z.-J.; Zhang, Y. Characteristics and living patterns of marine myxobacterial isolates. *Applied and environmental microbiology [Online]* **2005,** *71* (6), 3331–3336.

3. Battistuzzi, F. U.; Hedges, S. B. A major clade of prokaryotes with ancient adaptations to life on land. *Molecular biology and evolution [Online]* **2009,** *26* (2), 335–343.

4. Pomeroy, L. R.; Wiebe, W. J. Temperature and substrates as interactive limiting factors for marine heterotrophic bacteria. *Aquatic Microbial Ecology [Online]* **2001,** *23* (2), 187–204. http://www.int-res.com/articles/ame/23/a023p187.pdf.

5. Davila-Cespedes, A.; Juarez-Flores, B. I.; Pinos-Rodriguezc, J. M.; Aguirre-Riverab, J. R.; Oros-Ovalled, A. C.; Loyola-Martinez, E. D.; Andrade-Zaldivar, H. Protective effect ofAgave salmiana fructans in azoxymethane- induced colon cancer in Wistar rats. *Natural product communications [Online]* **2014,** *9* (10), 1503–1506.

6. Bakun, A. Wasp-waist populations and marine ecosystem dynamics: Navigating the "predator pit" topographies. *Progress in Oceanography [Online]* **2006,** *68* (2-4), 271–288.

7. CHENG, T. C. Marine molluscs as hosts for symbioses, with a review of known parasites of commercially important species. *Advances in Marine Biology* **1967,** *5*.

8. Thakur, N. L.; Müller, W. E. G. Sponge-bacteria association: A useful model to explore symbiosis in marine invertebrates. *Symbiosis (Rehovot) [Online]* **2005,** *39* (3), 109–116.

9. HENRY, S. M. Symbiosis. Vol. I. Associations of microorganisms, plants, and marine organisms. *Symbiosis. Vol. I. Associations of microorganisms, plants, and marine organisms. [Online]* **1966**.

10. Clay, K. Defensive symbiosis: A microbial perspective. *Functional Ecology [Online]* **2014,** *28* (2), 293–298. http://onlinelibrary.wiley.com/doi/10.1111/1365-2435.12258/full.

11. Desriac, F.; Defer, D.; Bourgougnon, N.; Brillet, B.; Le Chevalier, P.; Fleury, Y. Bacteriocin as weapons in the marine animal-associated bacteria warfare: Inventory and potential applications as an aquaculture probiotic. *Mar Drugs [Online]* **2010,** *8* (4), 1153–1177.

12. Cotter, P. D.; Ross, R. P.; Hill, C. Bacteriocins — a viable alternative to antibiotics? *Nature Reviews Microbiology [Online]* **2012,** *11* (2), nrmicro2937. https://www.nature.com/articles/nrmicro2937.pdf.

13. Phelan, R. W.; Barret, M.; Cotter, P. D.; O'Connor, P. M.; Chen, R.; Morrissey, J. P.; Dobson, A. D. W.; O'Gara, F.; Barbosa, T. M. Subtilomycin: A new lantibiotic from Bacillus subtilis strain MMA7 isolated from the marine sponge Haliclona simulans. *Mar Drugs [Online]* **2013,** *11* (6), 1878–1898.

14. Singh, R. D.; Mody, S. K.; Patel, H. B.; Devi, S.; Sarvaiya, V. N.; Patel, H. A.; Patel, B. R. Antimicrobial Drug Discovery: Evident Shifting from Terrestrial to Marine Micro-organisms. *Int.J.Curr.Microbiol.App.Sci [Online]* **2017,** *6* (5), 2322–2327.

15. Montaser, R.; Luesch, H. Marine natural products: a new wave of drugs? *Future medicinal chemistry [Online]* **2011,** *3* (12), 1475–1489.

16. Lam, K. S. Discovery of novel metabolites from marine actinomycetes. *Current opinion in microbiology [Online]* **2006,** *9* (3), 245–251.

17. Jensen, P. R.; Mincer, T. J.; Williams, P. G.; Fenical, W. Marine actinomycete diversity and natural product discovery. *Antonie van Leeuwenhoek [Online]* **2005,** *87* (1), 43–48.

18. Sathiyanarayanan, G.; Saibaba, G.; Kiran, G. S.; Yang, Y.-H.; Selvin, J. Marine sponge-associated bacteria as a potential source for polyhydroxyalkanoates. *Critical reviews in microbiology [Online]* **2017,** *43* (3), 294–312.

19. Lee, Y.; Phat, C.; Hong, S.-C. Structural diversity of marine cyclic peptides and their molecular mechanisms for anticancer, antibacterial, antifungal, and other clinical applications. *Peptides [Online]* **2017**.

20. Ruiz-Torres, V.; Encinar, J. A.; Herranz-López, M.; Pérez-Sánchez, A.; Galiano, V.; Barrajón-Catalán, E.; Micol, V. An Updated Review on Marine Anticancer Compounds: The Use of Virtual Screening for the Discovery of Small-Molecule Cancer Drugs. *Molecules (Basel, Switzerland)* **2017,** *22* (7). DOI: 10.3390/molecules22071037.

21. Mayer, A. M.; Nguyen, M.; Kalwajtys, P.; Kerns, H.; Newman, D. J.; Glaser, K. B. The Marine Pharmacology and Pharmaceuticals Pipeline in 2016. *FASEB J [Online]* **2017,** *31* (1 Supplement), 818.1-818.1.

22. Newman, D. J.; Cragg, G. M. Drugs and Drug Candidates from Marine Sources: An Assessment of the Current "State of Play". *Planta medica [Online]* **2016,** *82* (9-10), 775–789.

23. Boyd, K. G.; Adams, D. R.; Burgess, J. G. Antibacterial and repellent activities of marine bacteria associated with algal surfaces. *Biofouling [Online]* **1999,** *14* (3), 227–236.

24. Böhringer, N.; Fisch, K. M.; Schillo, D.; Bara, R.; Hertzer, C.; Grein, F.; Eisenbarth, J.-H.; Kaligis, F.; Schneider, T.; Wägele, H.; König, G. M.; Schäberle, T. F. Antimicrobial Potential of Bacteria Associated with Marine Sea Slugs from North Sulawesi, Indonesia. *Frontiers in microbiology [Online]* **2017,** *8*, 1092.

25. Schleissner, C.; Cañedo, L. M.; Rodríguez, P.; Crespo, C.; Zúñiga, P.; Peñalver, A.; La Calle, F. de; Cuevas, C. Bacterial Production of a Pederin Analogue by a Free-Living Marine Alphaproteobacterium. *J. Nat. Prod. [Online]* **2017,** *80* (7), 2170–2173.

26. Winter, J. M.; Behnken, S.; Hertweck, C. Genomics-inspired discovery of natural products. *Curr Opin Chem Biol [Online]* **2011,** *15* (1), 22–31.

27. Udwary, D. W.; Zeigler, L.; Asolkar, R. N.; Singan, V.; Lapidus, A.; Fenical, W.; Jensen, P. R.; Moore, B. S. Genome sequencing reveals complex secondary metabolome in the marine actinomycete Salinispora tropica. *PNAS [Online]* **2007,** *104* (25), 10376–10381. http://www.pnas.org/content/104/25/10376.full.

28. Machado, H.; Sonnenschein, E. C.; Melchiorsen, J.; Gram, L. Genome mining reveals unlocked bioactive potential of marine Gram-negative bacteria. *BMC Genomics [Online]* **2015,** *16* (1), 158. https://bmcgenomics.biomedcentral.com/track/pdf/10.1186/s12864-015-1365-z?site=bmcgenomics.biomedcentral.com.

29. Fisch, K. M.; Gurgui, C.; Heycke, N.; Sar, Sonia A van der; Anderson, S. A.; Webb, V. L.; Taudien, S.; Platzer, M.; Rubio, B. K.; Robinson, S. J.; Crews, P.; Piel, J. Polyketide assembly lines of uncultivated sponge symbionts from structure-based gene targeting. *Nature chemical biology [Online]* **2009,** *5* (7), nchembio.176. https://www.nature.com/articles/nchembio.176.pdf.

30. Cardani, C.; Ghiringhelli, D.; Mondelli, R.; Quilico, A. The structure of Pederin. *Tetrahedron Letters [Online]* **1965,** *6* (29), 2537–2545.

31. Kellner, R. L.L. Molecular identification of an endosymbiotic bacterium associated with pederin biosynthesis in Paederus sabaeus (Coleoptera: Staphylinidae). *Insect Biochemistry and Molecular Biology [Online]* **2002,** *32* (4), 389–395.

32. Greule, A.; Marolt, M.; Deubel, D.; Peintner, I.; Zhang, S.; Jessen-Trefzer, C.; Ford, C. de; Burschel, S.; Li, S.-M.; Friedrich, T.; Merfort, I.; Lüdeke, S.; Bisel, P.; Müller, M.; Paululat, T.; Bechthold, A. Wide Distribution of Foxicin Biosynthetic Gene Clusters in Streptomyces Strains - An Unusual Secondary Metabolite with Various Properties. *Frontiers in microbiology [Online]* **2017,** *8*, 221.

33. Sun, Y.; Tomura, T.; Sato, J.; IIZUKA, T.; FUDOU, R.; Ojika, M. Isolation and Biosynthetic Analysis of Haliamide, a New PKS-NRPS Hybrid Metabolite from the Marine Myxobacterium Haliangium ochraceum. *Molecules (Basel, Switzerland) [Online]* **2016,** *21* (1), 59.

34. Zarins-Tutt, J. S.; Barberi, T. T.; Gao, H.; Mearns-Spragg, A.; Zhang, L.; Newman, D. J.; Goss, R. J. M. Prospecting for new bacterial metabolites: a glossary of approaches for inducing, activating and upregulating the biosynthesis of bacterial cryptic or silent natural products. *Natural product reports [Online]* **2016,** *33* (1), 54–72.

35. Scherlach, K.; Hertweck, C. Triggering cryptic natural product biosynthesis in microorganisms. *Organic & biomolecular chemistry [Online]* **2009,** *7* (9), 1753–1760.

36. Davila-Cespedes, A.; Hufendiek, P.; Crusemann, M.; Schaberle, T. F.; Konig, G. M. Marine-derived myxobacteria of the suborder Nannocystineae: An underexplored source of structurally intriguing and biologically active metabolites. *Beilstein journal of organic chemistry [Online]* **2016,** *12*, 969–984.

37. Lowy, F. D. Antimicrobial resistance: The example of Staphylococcus aureus. *Journal of Clinical Investigation [Online]* **2003,** *111* (9), 1265–1273.

38. Ventola, C. L. The Antibiotic Resistance Crisis: Part 1: Causes and Threats. *Pharmacy and Therapeutics [Online]* **2015,** *40* (4), 277–283.

39. Barriere, S. L. Clinical, economic and societal impact of antibiotic resistance. *Expert Opinion on Pharmacotherapy [Online]* **2015,** *16* (2), 151–153.

40. McGowan, J. E. *Economic Impact of Antimicrobial Resistance - Volume 7, Number 2—April 2001 - Emerging Infectious Disease journal - CDC*.

41. Altschul, S. F.; Gish, W.; Miller, W.; Myers, E. W.; Lipman, D. J. Basic local alignment search tool. *Journal of molecular biology [Online]* **1990,** *215* (3), 403–410.

42. Blin, K.; Medema, M. H.; Kottmann, R.; Lee, S. Y.; Weber, T. The antiSMASH database, a comprehensive database of microbial secondary metabolite biosynthetic gene clusters. *Nucleic acids research [Online]* **2017,** *45* (D1), D555-D559.

43. Li, W.; Cowley, A.; Uludag, M.; Gur, T.; McWilliam, H.; Squizzato, S.; Park, Y. M.; Buso, N.; Lopez, R. The EMBL-EBI bioinformatics web and programmatic tools framework. *Nucleic Acids Res [Online]* **2015,** *43* (W1), W580-4.

44. Schmieder, R.; Edwards, R. Quality control and preprocessing of metagenomic datasets. *Bioinformatics (Oxford, England) [Online]* **2011,** *27* (6), 863–864.

45. Matheson, M. Gram Stain. *Community Eye Health [Online]* **1999,** *12* (30), 24.

46. Schulz, B.; Sucker, J.; Aust, H. J.; Krohn, K.; Ludewig, K.; Jones, P. G.; Döring, D. Biologically active secondary metabolites of endophytic Pezicula species. *Mycological Research [Online]* **1995,** *99* (8), 1007–1015.

47. Han, K.; Li, Z.-f.; Peng, R.; Zhu, L.-p.; Zhou, T.; Wang, L.-g.; Li, S.-g.; Zhang, X.-b.; Hu, W.; Wu, Z.-H.; Qin, N.; Li, Y.-Z. Extraordinary expansion of a Sorangium cellulosum genome from an alkaline milieu. *Sci Rep [Online]* **2013,** *3*, 2101.

48. Reichenbach, H. The ecology of the myxobacteria. *Environ. Microbiol. [Online]* **1999,** *1* (1), 15–21.

49. Cao, P.; Dey, A.; Vassallo, C. N.; Wall, D. How Myxobacteria Cooperate. *Journal of molecular biology [Online]* **2015,** *427* (23), 3709–3721.

50. Reichenbach, H. Myxobacteria: A Most Peculiar Group of Social Prokaryotes. In *Myxobacteria*; Rich, A., Rosenberg, E., Eds.; Springer Series in Molecular Biology; Springer New York: New York, NY, 1984; pp 1–50.

51. Sanford, R. A.; Cole, J. R.; Tiedje, J. M. Characterization and description of Anaeromyxobacter dehalogenans gen. nov., sp. nov., an aryl-halorespiring facultative anaerobic myxobacterium. *Appl. Environ. Microbiol. [Online]* **2002,** *68* (2), 893–900.

52. *Myxobacteria;* Rich, A., Rosenberg, E., Eds.; Springer Series in Molecular Biology; Springer New York: New York, NY, 1984.

53. Dworkin, M. Recent advances in the social and developmental biology of the myxobacteria. *Microbiological Reviews [Online]* **1996,** *60* (1), 70–102.

54. Wang, B.; Hu, W.; Liu, H.; Zhang, C.-Y.; Zhao, J.-y.; Jiang, D.-m.; Wu, Z.-H.; Li, Y.-Z. Adaptation of salt-tolerant Myxococcus strains and their motility systems to the ocean conditions. *Microb. Ecol. [Online]* **2007,** *54* (1), 43–51.

55. Pan, H.-W.; Tan, Z.-G.; Liu, H.; Li, Z.-f.; Zhang, C.-Y.; Li, C.-Y.; Li, J.; Li, Y.-Z. Hdsp, a horizontally transferred gene required for social behavior and halotolerance in salt-tolerant Myxococcus fulvus HW-1. *The ISME journal [Online]* **2010,** *4* (10), 1282–1289.

56. Li, Y. Z.; Hu, W.; Zhang, Y. Q.; Qiu, Z. j.; Zhang, Y.; Wu, B. H. A simple method to isolate salt-tolerant myxobacteria from marine samples. *J. Microbiol. Methods [Online]* **2002,** *50* (2), 205–209.

57. FUDOU, R.; Jojima, Y.; IIZUKA, T.; YAMANAKA, S. Haliangium ochraceum gen. nov., sp. nov. and Haliangium tepidum sp. nov.: novel moderately halophilic myxobacteria isolated from coastal saline environments. *J. Gen. Appl. Microbiol. [Online]* **2002,** *48* (2), 109–116.

58. Iizuka, T.; Jojima, Y.; Fudou, R.; Yamanaka, S. Isolation of myxobacteria from the marine environment. *FEMS Microbiol. Lett. [Online]* **1998,** *169* (2), 317–322.

59. IIZUKA, T.; Jojima, Y.; FUDOU, R.; Tokura, M.; Hiraishi, A.; YAMANAKA, S. Enhygromyxa salina gen. nov., sp. nov., a slightly halophilic myxobacterium isolated from the coastal areas of Japan. *Syst. Appl. Microbiol. [Online]* **2003,** *26* (2), 189–196.

60. IIZUKA, T.; Jojima, Y.; FUDOU, R.; Hiraishi, A.; Ahn, J.-W.; YAMANAKA, S. Plesiocystis pacifica gen. nov., sp. nov., a marine myxobacterium that contains dihydrogenated menaquinone, isolated from the Pacific coasts of Japan. *Int. J. Syst. Evol. Microbiol. [Online]* **2003,** *53* (Pt 1), 189–195.

61. Kimura, Y.; Kawasaki, S.; Yoshimoto, H.; Takegawa, K. Glycine betaine biosynthesized from glycine provides an osmolyte for cell growth and spore germination during osmotic stress in Myxococcus xanthus. *Journal of bacteriology [Online]* **2010,** *192* (5), 1467–1470.

62. Amiri Moghaddam, J.; Boehringer, N.; Burdziak, A.; Kunte, H.-J.; Galinski, E. A.; Schäberle, T. F. Different strategies of osmoadaptation in the closely related marine myxobacteria Enhygromyxa salina SWB007 and Plesiocystis pacifica SIR-1. *Microbiology (Reading, England) [Online]* **2016**.

63. Sleator, R. Bacterial osmoadaptation: The role of osmolytes in bacterial stress and virulence. *FEMS Microbiology Reviews [Online]* **2001,** *25* (5), 0.

64. Still, P. C.; Johnson, T. A.; Theodore, C. M.; Loveridge, S. T.; Crews, P. Scrutinizing the scaffolds of marine biosynthetics from different source organisms: Gram-negative cultured bacterial products enter center stage. *J. Nat. Prod. [Online]* **2014,** *77* (3), 690–702.

65. Wenzel, S. C.; Müller, R. The biosynthetic potential of myxobacteria and their impact in drug discovery. *Curr Opin Drug Discov Devel [Online]* **2009,** *12* (2), 220–230.

66. Schaberle, T. F.; Lohr, F.; Schmitz, A.; Konig, G. M. Antibiotics from myxobacteria. *Natural product reports [Online]* **2014,** *31* (7), 953–972.

67. Weissman, K. J.; Müller, R. A brief tour of myxobacterial secondary metabolism. *Bioorg. Med. Chem. [Online]* **2009,** *17* (6), 2121–2136.

68. Weissman, K. J.; Müller, R. Myxobacterial secondary metabolites: bioactivities and modes-of-action. *Natural product reports [Online]* **2010,** *27* (9), 1276–1295.

69. Baumann, S.; Herrmann, J.; Raju, R.; Steinmetz, H.; Mohr, K. I.; Huttel, S.; Harmrolfs, K.; Stadler, M.; Muller, R. Cystobactamids: Myxobacterial topoisomerase inhibitors exhibiting potent antibacterial activity. *Angewandte Chemie (International ed. in English) [Online]* **2014,** *53* (52), 14605–14609.

70. Frank, B.; Wenzel, S. C.; Bode, H. B.; Scharfe, M.; Blocker, H.; Muller, R. From genetic diversity to metabolic unity: Studies on the biosynthesis of aurafurones and aurafuron-like structures in myxobacteria and streptomycetes. *Journal of molecular biology [Online]* **2007,** *374* (1), 24–38.

71. Erol, O.; Schaberle, T. F.; Schmitz, A.; Rachid, S.; Gurgui, C.; El Omari, M.; Lohr, F.; Kehraus, S.; Piel, J.; Muller, R.; Konig, G. M. Biosynthesis of the myxobacterial antibiotic corallopyronin A. *Chembiochem [Online]* **2010,** *11* (9), 1253–1265.

72. Schieferdecker, S.; König, S.; Koeberle, A.; Dahse, H.-M.; Werz, O.; Nett, M. Myxochelins target human 5-lipoxygenase. *J. Nat. Prod. [Online]* **2015,** *78* (2), 335–338.

73. Xiao, Y.; Wei, X.; Ebright, R.; Wall, D. Antibiotic production by myxobacteria plays a role in predation. *Journal of bacteriology [Online]* **2011,** *193* (18), 4626–4633.

74. Thomas, E.; Tabernero, J.; Fornier, M.; Conté, P.; Fumoleau, P.; Lluch, A.; Vahdat, L. T.; Bunnell, C. A.; Burris, H. A.; Viens, P.; Baselga, J.; Rivera, E.; Guarneri, V.; Poulart, V.; Klimovsky, J.; Lebwohl, D.; Martin, M. Phase II clinical trial of ixabepilone (BMS-247550), an epothilone B analog, in patients with taxane-resistant metastatic breast cancer. *J. Clin. Oncol. [Online]* **2007,** *25* (23), 3399–3406.

75. Thomas, E. S.; Gomez, H. L.; Li, R. K.; Chung, H.-C.; Fein, L. E.; Chan, V. F.; Jassem, J.; Pivot, X. B.; Klimovsky, J. V.; Mendoza, F. H. de; Xu, B.; Campone, M.; Lerzo, G. L.; Peck, R. A.; Mukhopadhyay, P.; Vahdat, L. T.; Roché, H. H. Ixabepilone plus capecitabine for metastatic breast cancer progressing after anthracycline and taxane treatment. *J. Clin. Oncol. [Online]* **2007,** *25* (33), 5210–5217.

76. Hunt, J. T. Discovery of ixabepilone. *Molecular cancer therapeutics [Online]* **2009,** *8* (2), 275–281.

77. Smaglo, B. G.; Pishvaian, M. J. Profile and potential of ixabepilone in the treatment of pancreatic cancer. *Drug Des Devel Ther [Online]* **2014,** *8*, 923–930.

78. Kersten, R. D.; Yang, Y.-L.; Xu, Y.; Cimermancic, P.; Nam, S.-J.; Fenical, W.; Fischbach, M. A.; Moore, B. S.; Dorrestein, P. C. A mass spectrometry-guided genome mining approach for natural product peptidogenomics. *Nature chemical biology [Online]* **2011,** *7* (11), 794–802.

79. Kersten, R. D.; Ziemert, N.; Gonzalez, D. J.; Duggan, B. M.; Nizet, V.; Dorrestein, P. C.; Moore, B. S. Glycogenomics as a mass spectrometry-guided genome-mining method for microbial glycosylated molecules. *Proceedings of the National Academy of Sciences of the United States of America [Online]* **2013,** *110* (47), E4407-16.

80. Nguyen, D. D. et al. MS/MS networking guided analysis of molecule and gene cluster families. *Proceedings of the National Academy of Sciences of the United States of America [Online]* **2013,** *110* (28), E2611-20.

81. Goldman, B. S.et al. Evolution of sensory complexity recorded in a myxobacterial genome. *Proceedings of the National Academy of Sciences of the United States of America [Online]* **2006,** *103* (41), 15200–15205.

82. Krug, D.; Zurek, G.; Revermann, O.; Vos, M.; Velicer, G. J.; Müller, R. Discovering the hidden secondary metabolome of Myxococcus xanthus: a study of intraspecific diversity. *Appl. Environ. Microbiol. [Online]* **2008,** *74* (10), 3058–3068.

83. Li, Z.-f.; Li, X.; Liu, H.; Liu, X.; Han, K.; Wu, Z.-H.; Hu, W.; Li, F.-F.; Li, Y.-Z. Genome sequence of the halotolerant marine bacterium Myxococcus fulvus HW-1. *J. Bacteriol. [Online]* **2011,** *193* (18), 5015–5016.

84. Cortina, N. S.; Krug, D.; Plaza, A.; Revermann, O.; Muller, R. Myxoprincomide: A natural product from Myxococcus xanthus discovered by comprehensive analysis of the secondary metabolome. *Angewandte Chemie (International ed. in English) [Online]* **2012,** *51* (3), 811–816.

85. Korp, J.; Vela Gurovic, M. S.; Nett, M. Antibiotics from predatory bacteria. *Beilstein journal of organic chemistry [Online]* **2016,** *12*, 594–607.

86. Reichenbach, H. Nannocystis exedens gen. nov., spec. nov., a new myxobacterium of the family Sorangiaceae. *Arch Mikrobiol [Online]* **1970,** *70* (2), 119–138.

87. Hoffmann, H.et al. Discovery, Structure Elucidation, and Biological Characterization of Nannocystin A, a Macrocyclic Myxobacterial Metabolite with Potent Antiproliferative Properties. *Angewandte Chemie (International ed. in English) [Online]* **2015,** *54* (35), 10145–10148.

88. Ohlendorf, B.; Leyers, S.; Krick, A.; Kehraus, S.; Wiese, M.; König, G. M. Phenylnannolones A-C: biosynthesis of new secondary metabolites from the myxobacterium Nannocystis exedens. *Chembiochem [Online]* **2008,** *9* (18), 2997–3003.

89. Bouhired, S. M.; Crüsemann, M.; Almeida, C.; Weber, T.; Piel, J.; Schäberle, T. F.; König, G. M. Biosynthesis of phenylnannolone A, a multidrug resistance reversal agent from the halotolerant myxobacterium Nannocystis pusilla B150. *Chembiochem : a European journal of chemical biology [Online]* **2014,** *15* (5), 757–765.

90. Jansen, R.; Sood, S.; Huch, V.; Kunze, B.; Stadler, M.; Müller, R. Pyrronazols, metabolites from the myxobacteria Nannocystis pusilla and N. exedens, are unusual chlorinated pyrone-oxazole-pyrroles. *J. Nat. Prod. [Online]* **2014,** *77* (2), 320–326.

91. Schäberle, T. F. Biosynthesis of α-pyrones. *Beilstein J. Org. Chem. [Online]* **2016,** *12*, 571–588.

92. Jansen, R.; Sood, S.; Mohr, K. I.; Kunze, B.; Irschik, H.; Stadler, M.; Müller, R. Nannozinones and sorazinones, unprecedented pyrazinones from myxobacteria. *J. Nat. Prod. [Online]* **2014,** *77* (11), 2545–2552.

93. Kunze, B.; TROWITZSCH-KIENAST, W.; Höfle, G.; Reichenbach, H. Nannochelins A, B and C, new iron-chelating compounds from Nannocystis exedens (myxobacteria). Production, isolation,physico-chemical and biological properties. *J. Antibiot. [Online]* **1992,** *45* (2), 147–150.

94. Fudou, R.; Iizuka, T.; Yamanaka, S. Haliangicin, a novel antifungal metabolite produced by a marine myxobacterium. 1. Fermentation and biological characteristics. *J. Antibiot. [Online]* **2001,** *54* (2), 149–152.

95. Fudou, R.; Iizuka, T.; Sato, S.; Ando, T.; Shimba, N.; Yamanaka, S. Haliangicin, a novel antifungal metabolite produced by a marine myxobacterium. 2. Isolation and structural elucidation. *J. Antibiot. [Online]* **2001,** *54* (2), 153–156.

96. Kundim, B. A.; Itou, Y.; Sakagami, Y.; FUDOU, R.; IIZUKA, T.; YAMANAKA, S.; Ojika, M. New haliangicin isomers, potent antifungal metabolites produced by a marine myxobacterium. *J. Antibiot. [Online]* **2003,** *56* (7), 630–638.

97. Ivanova, N.et al. Complete genome sequence of Haliangium ochraceum type strain (SMP-2). *Stand Genomic Sci [Online]* **2010,** *2* (1), 96–106.

98. Sun, Y.; Feng, Z.; Tomura, T.; Suzuki, A.; Miyano, S.; Tsuge, T.; Mori, H.; Suh, J.-W.; IIZUKA, T.; FUDOU, R.; Ojika, M. Heterologous Production of the Marine Myxobacterial Antibiotic Haliangicin and Its Unnatural Analogues Generated by Engineering of the Biochemical Pathway. *Sci. Rep. [Online]* **2016,** *6*, 22091.

99. Komaki, H.; Fudou, R.; Iizuka, T.; Nakajima, D.; Okazaki, K.; Shibata, D.; Ojika, M.; Harayama, S. PCR Detection of Type I Polyketide Synthase Genes in Myxobacteria. *Applied and environmental microbiology [Online]* **2008,** *74* (17), 5571–5574.

100. Felder, S.; Dreisigacker, S.; Kehraus, S.; Neu, E.; Bierbaum, G.; Wright, P. R.; Menche, D.; Schäberle, T. F.; König, G. M. Salimabromide: unexpected chemistry from the obligate marine myxobacterium Enhygromxya salina. *Chemistry [Online]* **2013,** *19* (28), 9319–9324.

References

101. Schäberle, T. F.; Goralski, E.; Neu, E.; Erol, O.; Hölzl, G.; Dörmann, P.; Bierbaum, G.; König, G. M. Marine myxobacteria as a source of antibiotics--comparison of physiology, polyketide-type genes and antibiotic production of three new isolates of Enhygromyxa salina. *Mar Drugs [Online]* **2010,** *8* (9), 2466–2479.

102. Tomura, T.; Nagashima, S.; Yamazaki, S.; IIZUKA, T.; FUDOU, R.; Ojika, M. An Unusual Diterpene-Enhygromic Acid and Deoxyenhygrolides from a Marine Myxobacterium, Enhygromyxa sp. *Mar Drugs* **2017,** *15* (4). DOI: 10.3390/md15040109.

103. Felder, S.; Kehraus, S.; Neu, E.; Bierbaum, G.; Schäberle, T. F.; König, G. M. Salimyxins and enhygrolides: antibiotic, sponge-related metabolites from the obligate marine myxobacterium Enhygromyxa salina. *Chembiochem [Online]* **2013,** *14* (11), 1363–1371.

104. Schmalzbauer, B.; Menche, D. Concise Synthesis of the Tricyclic Core of Salimabromide. *Organic letters [Online]* **2015,** *17* (12), 2956–2959.

105. Pignatello, J. J.; Porwoll, J.; Carlson, R. E.; Xavier, A.; Gleason, F. K.; Wood, J. M. Structure of the antibiotic cyanobacterin, a chlorine-containing .gamma.-lactone from the freshwater cyanobacterium Scytonema hofmanni. *J. Org. Chem. [Online]* **1983,** *48* (22), 4035–4038.

106. Ciminiello, P.; Fattorusso, E.; Magno, S.; Mangoni, A.; Pansini, M. Incisterols, a new class of highly degraded sterols from the marine sponge Dictyonella incisa. *J. Am. Chem. Soc. [Online]* **1990,** *112* (9), 3505–3509.

107. Medema, M. H. et al. Minimum Information about a Biosynthetic Gene cluster. *Nature chemical biology [Online]* **2015,** *11* (9), 625–631.

108. IIZUKA, T.; FUDOU, R.; Jojima, Y.; Ogawa, S.; YAMANAKA, S.; Inukai, Y.; Ojika, M. Miuraenamides A and B, novel antimicrobial cyclic depsipeptides from a new slightly halophilic myxobacterium: taxonomy, production, and biological properties. *J. Antibiot. [Online]* **2006,** *59* (7), 385–391.

109. Ojika, M.; Inukai, Y.; Kito, Y.; Hirata, M.; IIZUKA, T.; FUDOU, R. Miuraenamides: antimicrobial cyclic depsipeptides isolated from a rare and slightly halophilic myxobacterium. *Chem Asian J [Online]* **2008,** *3* (1), 126–133.

110. Bartlett, D. W.; Clough, J. M.; Godwin, J. R.; Hall, A. A.; Hamer, M.; Parr-Dobrzanski, B. The strobilurin fungicides. *Pest Manag. Sci. [Online]* **2002,** *58* (7), 649–662.

111. Böhlendorf, B.; Herrmann, M.; Hecht, H.-J.; Sasse, F.; Forche, E.; Kunze, B.; Reichenbach, H.; Höfle, G. Melithiazols A–N: New Antifungal β-Methoxyacrylates from Myxobacteria. *Eur. J. Org. Chem. [Online]* **1999,** *1999* (10), 2601–2608.

112. Sumiya, E.; Shimogawa, H.; Sasaki, H.; Tsutsumi, M.; Yoshita, K.'i.; Ojika, M.; Suenaga, K.; Uesugi, M. Cell-morphology profiling of a natural product library identifies bisebromoamide and miuraenamide A as actin filament stabilizers. *ACS chemical biology [Online]* **2011,** *6* (5), 425–431.

113. IIZUKA, T.; Jojima, Y.; Hayakawa, A.; Fujii, T.; YAMANAKA, S.; FUDOU, R. Pseudenhygromyxa salsuginis gen. nov., sp. nov., a myxobacterium isolated from an estuarine marsh. *Int. J. Syst. Evol. Microbiol. [Online]* **2013,** *63* (Pt 4), 1360–1369.

114. Ganapiriya, V.; Maharajan, A.; Kumarasamy, P. Antifouling effect of bioactive compounds from marine sponge Acanthella elongata and different species of bacterial film on larval attachment of Balanus amphitrite (cirripedia, crustacea). *Braz. arch. biol. technol. [Online]* **2012,** *55* (3), 395–402.

115. Clare, A. Marine natural product antifoulants: Status and potential. *Biofouling [Online]* **1996,** *9* (3), 211–229.

116. Gil-Turnes, M. S.; Hay, M. E.; Fenical, W. Symbiotic marine bacteria chemically defend crustacean embryos from a pathogenic fungus. *Science (New York, N.Y.) [Online]* **1989,** *246* (4926), 116–118.

117. Gil-Turnes, M. S.; Fenical, W. Embryos of Homarus americanus are Protected by Epibiotic Bacteria. *The Biological Bulletin [Online]* **1992,** *182* (1), 105–108.

118. Biebl, H.; Pukall, R.; Lunsdorf, H.; Schulz, S.; Allgaier, M.; Tindall, B. J.; Wagner-Dobler, I. Description of Labrenzia alexandrii gen. nov., sp. nov., a novel alphaproteobacterium containing bacteriochlorophyll a, and a proposal for reclassification of Stappia aggregata as Labrenzia aggregata comb. nov., of Stappia marina as Labrenzia marina comb. nov. and of Stappia alba as Labrenzia alba comb. nov., and emended descriptions of the genera Pannonibacter, Stappia and Roseibium, and of the species Roseibium denhamense and Roseibium hamelinense. *International journal of systematic and evolutionary microbiology [Online]* **2007,** *57* (Pt 5), 1095–1107.

119. Boettcher, K. J. Additional evidence that juvenile oyster disease is caused by a member of the Roseobacter group and colonization of nonacted animals by Stappia stellulata-like strains.

120. Maloy, A. P.; Ford, S. E.; Karney, R. C.; Boettcher, K. J. Roseovarius crassostreae, the etiological agent of Juvenile Oyster Disease (now to be known as Roseovarius Oyster Disease) in Crassostrea virginica. *Aquaculture [Online]* **2007,** *269* (1-4), 71–83.

121. Pujalte, M. J. Stappia alba sp. nov., isolated from Mediterranean oysters.

122. Romalde, J. L.; Barja, J. L. Bacteria in molluscs: good and bad guys [Online] **2010**.

123. Knothe, G. NMR characterization of dihydrosterculic acid and its methyl ester. *Lipids [Online],* *41* (4), 393–396. http://link.springer.com/content/pdf/10.1007/s11745-006-5110-x.pdf.

124. Motl, O.; Amin, M.; Sedmera, P. The structure of cascarillic acid from cascarilla essential oil. *Phytochemistry [Online]* **1972,** *11* (1), 407–408.

125. Roberts, I. O.; Baird, M. S.; Liu, Y. The absolute stereochemistry of cascarillic acid. *Tetrahedron Letters [Online]* **2004,** *45* (47), 8685–8686.

126. Wilson, S. R.; Prodan, K. A. The synthesis and stereochemistry of cascarillic acid. *Tetrahedron Letters [Online]* **1976,** *17* (47), 4231–4234.

127. Bouchard, C.; Page, J.; Bedard, A.; Tremblay, P.; Vallieres, L. G protein-coupled receptor 84, a microglia-associated protein expressed in neuroinflammatory conditions. *Glia [Online]* **2007,** *55* (8), 790–800.

128. Wang, J.; Wu, X.; Simonavicius, N.; Tian, H.; Ling, L. Medium-chain fatty acids as ligands for orphan G protein-coupled receptor GPR84. *The Journal of biological chemistry [Online]* **2006,** *281* (45), 34457–34464.

129. Venkataraman, C.; Kuo, F. The G-protein coupled receptor, GPR84 regulates IL-4 production by T lymphocytes in response to CD3 crosslinking. *Immunology letters [Online]* **2005,** *101* (2), 144–153.

130. Suzuki, M.; Takaishi, S.; Nagasaki, M.; Onozawa, Y.; Iino, I.; Maeda, H.; Komai, T.; Oda, T. Medium-chain fatty acid-sensing receptor, GPR84, is a proinflammatory receptor. *The Journal of biological chemistry [Online]* **2013,** *288* (15), 10684–10691.

131. Thieme, F. Characterization of gliding marine bacteria. Bachelor of Science in Applied Biology; University of Applied Sciences, Bonn, Germany, 2014.

132. Rocha, D.; Ruiz-Villafán, B.; Manzo, M.; Rodríguez-Sanoja, R.; Sánchez, S. Development of an efficient conjugal DNA transfer system between Escherichia coli and a non-sporulating Streptomyces strain. *J. Microbiol. Methods [Online]* **2017,** *144*, 60–66.

133. Reynolds, P. E. Structure, biochemistry and mechanism of action of glycopeptide antibiotics. *European journal of clinical microbiology & infectious diseases : official publication of the European Society of Clinical Microbiology [Online]* **1989,** *8* (11), 943–950.

134. Steenbergen, J. N.; Alder, J.; Thorne, G. M.; Tally, F. P. Daptomycin: A lipopeptide antibiotic for the treatment of serious Gram-positive infections. *The Journal of antimicrobial chemotherapy [Online]* **2005,** *55* (3), 283–288.

135. Zhang, B.; Zhang, H.-D.; Zhou, Y.-T.; Huang, K.; Liu, Z.-Q.; Zheng, Y.-G. Improvement of amphotericin B production by a newly isolated Streptomyces nodosus mutant. *Biotechnology and Applied Biochemistry*.

136. Jiang, D.-m.; Kato, C.; Zhou, X.-W.; Wu, Z.-H.; Sato, T.; Li, Y.-Z. Phylogeographic separation of marine and soil myxobacteria at high levels of classification. *The ISME journal [Online]* **2010,** *4* (12), 1520–1530.

137. Brinkhoff, T.; Fischer, D.; Vollmers, J.; Voget, S.; Beardsley, C.; Thole, S.; Mussmann, M.; Kunze, B.; Wagner-Döbler, I.; Daniel, R.; Simon, M. Biogeography and phylogenetic diversity of a cluster of exclusively marine myxobacteria. *ISME J [Online]* **2012,** *6* (6), 1260–1272.

138. Zarins-Tutt, J. S.; Barberi, T. T.; Gao, H.; Mearns-Spragg, A.; Zhang, L.; Newman, D. J.; Goss, R. J. M. Prospecting for new bacterial metabolites: A glossary of approaches for inducing, activating and upregulating the biosynthesis of bacterial cryptic or silent natural products. *Nat. Prod. Rep. [Online]* **2016**.

139. Bode, H. B.; Bethe, B.; Hofs, R.; Zeeck, A. Big effects from small changes: possible ways to explore nature's chemical diversity. *Chembiochem : a European journal of chemical biology [Online]* **2002,** *3* (7), 619–627.

140. Pimentel-Elardo, S. M.; Sørensen, D.; Ho, L.; Ziko, M.; Bueler, S. A.; Lu, S.; Tao, J.; Moser, A.; Lee, R.; Agard, D.; Fairn, G.; Rubinstein, J. L.; Shoichet, B. K.; Nodwell, J. R. Activity-Independent Discovery of Secondary Metabolites Using Chemical Elicitation and Cheminformatic Inference. *ACS chemical biology [Online]* **2015,** *10* (11), 2616–2623.

141. Seyedsayamdost, M. R. High-throughput platform for the discovery of elicitors of silent bacterial gene clusters. *Proceedings of the National Academy of Sciences of the United States of America [Online]* **2014,** *111* (20), 7266–7271.

142. Derewacz, D. K.; Covington, B. C.; McLean, J. A.; Bachmann, B. O. Mapping Microbial Response Metabolomes for Induced Natural Product Discovery. *ACS chemical biology [Online]* **2015,** *10* (9), 1998–2006.

143. Watrous, J.; Roach, P.; Alexandrov, T.; Heath, B. S.; Yang, J. Y.; Kersten, R. D.; van der Voort, M.; Pogliano, K.; Gross, H.; Raaijmakers, J. M.; Moore, B. S.; Laskin, J.; Bandeira, N.; Dorrestein, P. C. Mass spectral molecular networking of living microbial colonies. *Proceedings of the National Academy of Sciences of the United States of America [Online]* **2012,** *109* (26), E1743-52.

144. Yang, J. Y.; Sanchez, L. M.; Rath, C. M.; Liu, X.; Boudreau, P. D.; Bruns, N.; Glukhov, E.; Wodtke, A.; Felicio, R. de; Fenner, A.; Wong, W. R.; Linington, R. G.; Zhang, L.; Debonsi, H. M.; Gerwick, W. H.; Dorrestein, P. C. Molecular networking as a dereplication strategy. *Journal of natural products [Online]* **2013,** *76* (9), 1686–1699.

145. Johnston, C. W.; Skinnider, M. A.; Wyatt, M. A.; Li, X.; Ranieri, M. R. M.; Yang, L.; Zechel, D. L.; Ma, B.; Magarvey, N. A. An automated Genomes-to-Natural Products platform (GNP) for the discovery of modular natural products. *Nature communications [Online]* **2015,** *6,* 8421.

146. Duncan, K. R.; Crüsemann, M.; Lechner, A.; Sarkar, A.; Li, J.; Ziemert, N.; Wang, M.; Bandeira, N.; Moore, B. S.; Dorrestein, P. C.; Jensen, P. R. Molecular networking and pattern-based genome mining improves discovery of biosynthetic gene clusters and their products from Salinispora species. *Chemistry & biology [Online]* **2015,** *22* (4), 460–471.

147. Tang, X.; Li, J.; Millan-Aguinaga, N.; Zhang, J. J.; O'Neill, E. C.; Ugalde, J. A.; Jensen, P. R.; Mantovani, S. M.; Moore, B. S. Identification of Thiotetronic Acid Antibiotic Biosynthetic Pathways by Target-directed Genome Mining. *ACS chemical biology [Online]* **2015**.

148. Yamanaka, K.; Reynolds, K. A.; Kersten, R. D.; Ryan, K. S.; Gonzalez, D. J.; Nizet, V.; Dorrestein, P. C.; Moore, B. S. Direct cloning and refactoring of a silent lipopeptide biosynthetic gene cluster yields the antibiotic taromycin A. *Proceedings of the National Academy of Sciences of the United States of America [Online]* **2014,** *111* (5), 1957–1962.

149. Jiang, W.; Zhao, X.; Gabrieli, T.; Lou, C.; Ebenstein, Y.; Zhu, T. F. Cas9-Assisted Targeting of CHromosome segments CATCH enables one-step targeted cloning of large gene clusters. *Nature communications [Online]* **2015,** *6,* 8101.

150. Ongley, S. E.; Bian, X.; Neilan, B. A.; Müller, R. Recent advances in the heterologous expression of microbial natural product biosynthetic pathways. *Natural product reports [Online]* **2013,** *30* (8), 1121–1138.

151. Grogan, D. W.; Cronan, J. E. Cyclopropane ring formation in membrane lipids of bacteria. *Microbiol. Mol. Biol. Rev. [Online]* **1997,** *61* (4), 429–441. http://mmbr.asm.org/content/61/4/429.full.pdf.

152. Courtois, F.; Guérard, C.; Thomas, X.; Ploux, O. Escherichia coli cyclopropane fatty acid synthase. *European Journal of Biochemistry* **2004,** *271. DOI:* 10.1111/j.1432-1033.2004.04441.x.

153. Pohl, C. H.; Kock, J. L. F.; Thibane, V. S. Antifungal free fatty acids: a review [Online].

154. Macmillan, J. B.; Molinski, T. F. Majusculoic acid, a brominated cyclopropyl fatty acid from a marine cyanobacterial mat assemblage. *J. Nat. Prod. [Online]* **2005,** *68* (4), 604–606.

155. Graca, A. P.; Bondoso, J.; Gaspar, H.; Xavier, J. R.; Monteiro, M. C.; La Cruz, M. de; Oves-Costales, D.; Vicente, F.; Lage, O. M. Antimicrobial activity of heterotrophic bacterial communities from the marine sponge Erylus discophorus (Astrophorida, Geodiidae). *PloS one [Online]* **2013,** *8* (11), e78992.

156. Yee, B.; Oertli, G. E.; Fuerst, J. A.; Staley, J. T. Reclassification of the polyphyletic genus Prosthecomicrobium to form two novel genera, Vasilyevaea gen. nov. and Bauldia gen. nov. with four new combinations: Vasilyevaea enhydra comb. nov., Vasilyevaea mishustinii comb. nov., Bauldia consociata comb. nov. and Bauldia litoralis comb. nov. *International journal of systematic and evolutionary microbiology [Online]* **2010,** *60* (Pt 12), 2960–2966.

157. Lee, H. J.; Rho, J. K.; Yoon, S.C. , E-mail: scyoon@nongae.gsnu.ac.kr. Growth Temperature-Dependent Conversion of De novo-Synthesized Unsaturated Fatty Acids into Polyhydroxyalkanoic Acid and Membrane Cyclopropane Fatty Acids in the Psychrotrophic Bacterium Pseudomonas fluorescens BM07. *Journal of Microbiology and Biotechnology [Online]* **2004**.

158. Montanari, C.; Sado Kamdem, S. L.; Serrazanetti, D. I.; Etoa, F.-X.; Guerzoni, M. E. Synthesis of cyclopropane fatty acids in Lactobacillus helveticus and Lactobacillus sanfranciscensis and their cellular fatty acids changes following short term acid and cold stresses. *Food Microbiology [Online]* **2010,** *27* (4), 493–502.

159. Yu, X.-H.; Prakash, R. R.; Sweet, M.; Shanklin, J. Coexpressing Escherichia coli cyclopropane synthase with Sterculia foetida Lysophosphatidic acid acyltransferase enhances cyclopropane fatty acid accumulation. *Plant physiology [Online]* **2014,** *164* (1), 455–465.

160. Bakkal, S.; M., S.; A., M. Bacteriocins of Aquatic Microorganisms and Their Potential Applications in the Seafood Industry. In *The Atlantic Salmon (Salmo salar) Vertebra and Cellular Pathways to Vertebral Deformities*; Elisabeth Ytteborg, Grete Baeverfjord, Harald Takle, Jacob Torgersen, Eds.; INTECH Open Access Publisher, 2012.

161. Pujalte, M. J. Stappia alba sp. nov., isolated from Mediterranean oysters.

162. Oh, D. Y.; Lagakos, W. S. The role of G-protein-coupled receptors in mediating the effect of fatty acids on inflammation and insulin sensitivity. *Current opinion in clinical nutrition and metabolic care [Online]* **2011,** *14* (4), 322–327.

163. Shirole, R. L.; Shirole, N. L.; Saraf, M. N. Embelia ribes ameliorates lipopolysaccharide-induced acute respiratory distress syndrome. *Journal of Ethnopharmacology [Online]* **2015,** *168*, 356–363.

164. Makita, N.; Iiri, T. Biased agonism: A novel paradigm in G protein-coupled receptor signaling observed in acquired hypocalciuric hypercalcemia [Review]. *Endocrine Journal [Online]* **2014,** *61* (4), 303–309. https://www.jstage.jst.go.jp/article/endocrj/61/4/61_EJ13-0453/_pdf.

165. Zhu, B. T. Mechanistic explanation for the unique pharmacologic properties of receptor partial agonists. *Biomedicine & pharmacotherapy = Biomedecine & pharmacotherapie [Online]* **2005,** *59* (3), 76–89.

166. Expanding roles for β-arrestins as scaffolds and adapters in GPCR signaling and trafficking. *Current Opinion in Cell Biology [Online]* **2001,** *13* (2), 139–145.

167. Rankovic, Z.; Brust, T. F.; Bohn, L. M. Biased agonism: An emerging paradigm in GPCR drug discovery. *Bioorganic & medicinal chemistry letters [Online]* **2016,** *26* (2), 241–250.

168. Moore, A. R.; Willoughby, D. A. *The role of cAMP regulation in controlling inflammation*: England, 1995 Sep.

169. Fritsche, K. Fatty acids as modulators of the immune response. *Annual review of nutrition [Online]* **2006,** *26*, 45–73.

170. Audoy-Rémus, J.; Bozoyan, L.; Dumas, A.; Filali, M.; Lecours, C.; Lacroix, S.; Rivest, S.; Tremblay, M.-E.; Vallières, L. GPR84 deficiency reduces microgliosis, but accelerates dendritic degeneration and cognitive decline in a mouse model of Alzheimer's disease. *Brain, behavior, and immunity [Online]* **2015,** *46*, 112–120.

171. Bentley, S. D.et al. Complete genome sequence of the model actinomycete Streptomyces coelicolor A3(2). *Nature [Online]* **2002,** *417* (6885), 141–147.

172. Challis, G. L. Genome mining for novel natural product discovery. *J. Med. Chem. [Online]* **2008,** *51* (9), 2618–2628.

173. Corre, C.; Challis, G. L. New natural product biosynthetic chemistry discovered by genome mining. *Nat Prod Rep [Online]* **2009,** *26* (8), 977–986.

174. FUDOU, R.; IIZUKA, T.; YAMANAKA, S. Haliangicin, a Novel Antifungal Metabolite Produced by a Marine Myxobacterium. 1. Fermentation and Biological Characteristics. *J. Antibiot. [Online]* **2001,** *54* (2), 149–152.

Manuscripts in preparation used as reference:

(A) Köse, M.; Pillaiyar, M.; De Filippo, E.; Sylvester, K.; Namasivayam, V.; Müller, C.E.

(B) Pillaiyar, T.; Köse, M.; Sylvester, K.; Weighardt, H.; Thimm, D.; Borges, G.; Förster, I.; von Kügelgen, I.; Müller, C.E Diindolylmethane derivatives: Potent agonists of the immunostimulatory orphan G protein-coupled receptor GPR84. *J. Med. Chem.* **2017**, *60*, 3636-3655.

(C) Pillaiyar, T.; Köse, M.; Namasivayam, V.; Sylvester, K.; Borges, G. ; Thimm, D.; von Kügelgen, I.; Müller, C

10. APPENDIX

10.1. A1. 16S rDNA Sequence of *Labrenzia* sp. strain 011 (Ostsee6)

CGCATGCTCCGGCCGCCATGGCCGCGGGATTAAGGAGGTGATCCAGCCCCAGGTTCCCCTAGGGCTACCTTGTTA
CGACTTCACCCCAGTCGCTGAGCCTACCGTGGTCAGCTGCCTCCTTGCGGTTAGCGCACTGCCTTCGGGTAAACC
CAACTCCCATGGTGTGACGGGCGGTGTGTACAAGGCCCGGGAACGTATTCACCGCGTCATGCTGTTACGCGATTA
CTAGCGATTCCAACTTCATGCTCTCGAGTTGCAGAGAACAATCCGAACTGAGACGGCTTTTGGAGATTAGCTCCCT
CTCGCGAGTTCGCTGCCCACTGTCACCGCCATTGTAGCACGTGTGTAGCCCAGCCCGTAAGGGCCATGAGGACTT
GACGTCATCCCCACCTTCCTCTCGGCTTATCACCGGCAGTCCCCCTAGAGTGCCCAACTTAATGCTGGCAACTAAG
GGCGAGGGTTGCGCTCGTTGCGGGACTTAACCCAACATCTCACGACACGAGCTGACGACAGCCATGCAGCACCTG
TCCTGGCGTCCCCGAAGGGAACAATCGGTCTCCCGATCTAGCACCAAATGTCAAGGGCTGGTAAGGTTCTGCGCG
TTGCTTCGAATTAAACCACATGCTCCACCGCTTGTGCGGGCCCCCGTCAATTCCTTTGAGTTTTAATCTTGCGACCG
TACTCCCCAGGCGGGAAGCTTAATGCGTTAGCTGCGCCACCAAATAGCATGCTACCTGACGGCTAGCTTCCATCGT
TTACGGCGTGGACTACCAGGGTATCTAATCCTGTTTGCTCCCCACGCTTTCGCACCTCAGCGTCAGTACCGAGCCA
GTGAGCCGCCTTCGCCACTGGTGTTCTTCCGAATATCTACGAATTTCGCCTCTACACTCGGAGTTCCACTCACCTCT
CTCGGTCTCAAGACTGACAGTATCAAAGGCAGTTCCGGGGGTTGAGCCCCGGGATTTCACCCCTGACTGATCAGTC
CGCCTACGTGCGCTTTACGCCCAGTGATTCCGAACAACGCTAGCCCCCTTCGTATTACCGCGGCTGCTGGCACGA
AGTTAGCCGGGGCTTCTTCTGCGAGTAACGTCATTATCCTCCTCGCTGAAAGAGCTTTACAACCCTAGGGCCTTCA
TCACTCACGCGGCATGGCTGGATCAGGGTTGCCCCCATTGTCCAATATTCCCCACTGCTGCCTCCCGTAGGAGTCT
GGGCCGTGTCTCAGTCCCAGTGTGGCTGATCATCCTCTCAGACCAGCTATGGATCGTCGCCTTGGTAGGCCATTA
CCCCACCAACTAGCTAATCCAACGCGGGCCCATCCTTAGGCGATAAATCTTCCCCCCATAGGGCACATACGGTATT
AGCAGTCGTTTCCAACTGTTGTTCCGTACCTAAAGGTAGGTTCCCACGCGTTACTCACCCGTCTGCCACTAACTCC
GAAGAGTTCGTTCGACTTGCATGTGTTAAGCCTGCCGCCAGCGTTCGTTCTGAGCCAGGATCAAACTCTAATCACT
AGTGCGGCCGCCTGCAGGTCGACCATATGGGAGAGCTCCCAACGCGTGA

10.2. A2. 16s rDNA sequence of Siel 3m

GCTCCCGGCCGCCATGGCCGCGGGATTAGAGTTTGATCCTGGCTCAGGATGAACGCTAGCGGCAGGCCTAATACA
TGCAAGTCGAGGGGGCAGCATTCACTTCGGTGAGATGGCGACCGGCGAACGGGTGCGTAACGCGTATGCAACCTG
CCCCTTACCGGGGGATAGCCCAGAGAAATTTGGATTAACACCCCATAGCCCCGCGAGAAGGCATCTTCTTTCGGG
TAAATACTAAGGTAAGGGATGGGCATGCGTGCCATTAGTTAGTTGGCGGGGTAACGGCCCACCAAGGCAACGATG
GCTAGGGGTTCTGAGAGGATGATCCCCCACACTGGCACTGAGATACGGGCCAGACTCCTACGGGAGGCAGCAGT
AGGGAATATTGGTCAATGGGCGAGAGCCTGAACCAGCCATGCCGCGTGCAGGAAGACGGCCTTCTGGGTTGTAAA
CTGCTTTTACCAGGGAACAAAAGGCCCACGCGTGGGAGATTGCGTGTACCTGGGGGATAAGCACCGGCTAACTCC
GTGCCAGCAGCCGCGGTAANACGGAGGGTGCAAGCGTTGTCCGGATTTATTGGGTTTAAAGGGTGCGTAGGCGG
CCCGTTAAGTCAGGGGTGAAATCCCACAGCTCAACTGTGGAACTGCCCTTGATACTGGCGGGCTTGAGTACAGAC
GAGGTAGGCGGAATTTATGGTGTAGCGGTGAAATGCATAGATACCATAAAGAACACCGATAGCGAAGGCAGCTTAC
TGGACTGTAACTGACGCTGATGCACGAAAGCGTGGGTAGCGAACAGGATTAGATACCCTGGTAGTCCACGCCGTA

AACGATGATCACTCGATGTGTGCGACATTACTGTACGCGTCCAAGCGAAAGCGTTAAGTGATCCACCTGGGGAGTA
CGCCCGCAAGGGTGAAACTCAAAGGAATTGACGGGGGTCCGCACAAGCGGTGGAGCATGTGGTTTAATTCGATGA
TACGCGAGGAACCTTACCTGGGCTAGAATGTGATTGCCATCCCCGGAGACGGGGAGTTCTTCGGACATGAAACAA
GGTGCTGCATGGCTGTCGTCAGCTCGTGCCGTGAGGTGTTGGGTTAAGTCCCGCAACGAGCGCAACCCCTACTGT
TAGTTGCCAGCACGTCAAGGTGGGGACTCTAACAGGACTGCCTGCGCAAGCAGAGAGGAAGGAGGGGACGACGT
CAAGTCATCATGGCCCTTACGCCCAGGGCTACACACGTGCTACAATGGGGGGGTACAGCGGGTAGCTACCACGCAA
GTGGATGCCAATCTCAAAAAGCCCCTCTCAGTTCGGATCGTGGCCTGCAACTCGGCCACGTGAAGTTGGAATCGC
TAGTAATCGCGCATCAGCAATGGCGCGGTGAATACGTTCCCGGACCTTGTACACACCGCCCGTCAAGCCATGGAA
GTTGGGAGGACCTGAAGGCAGTAGCCTAGCGGCGCTGTTTAGGGTTATACCAGTAACTAGGGCTAAGTCGTAACA
AGGTAGCCGTACCGGAAGGTGGGGCTGGATCACCTCCTTAA
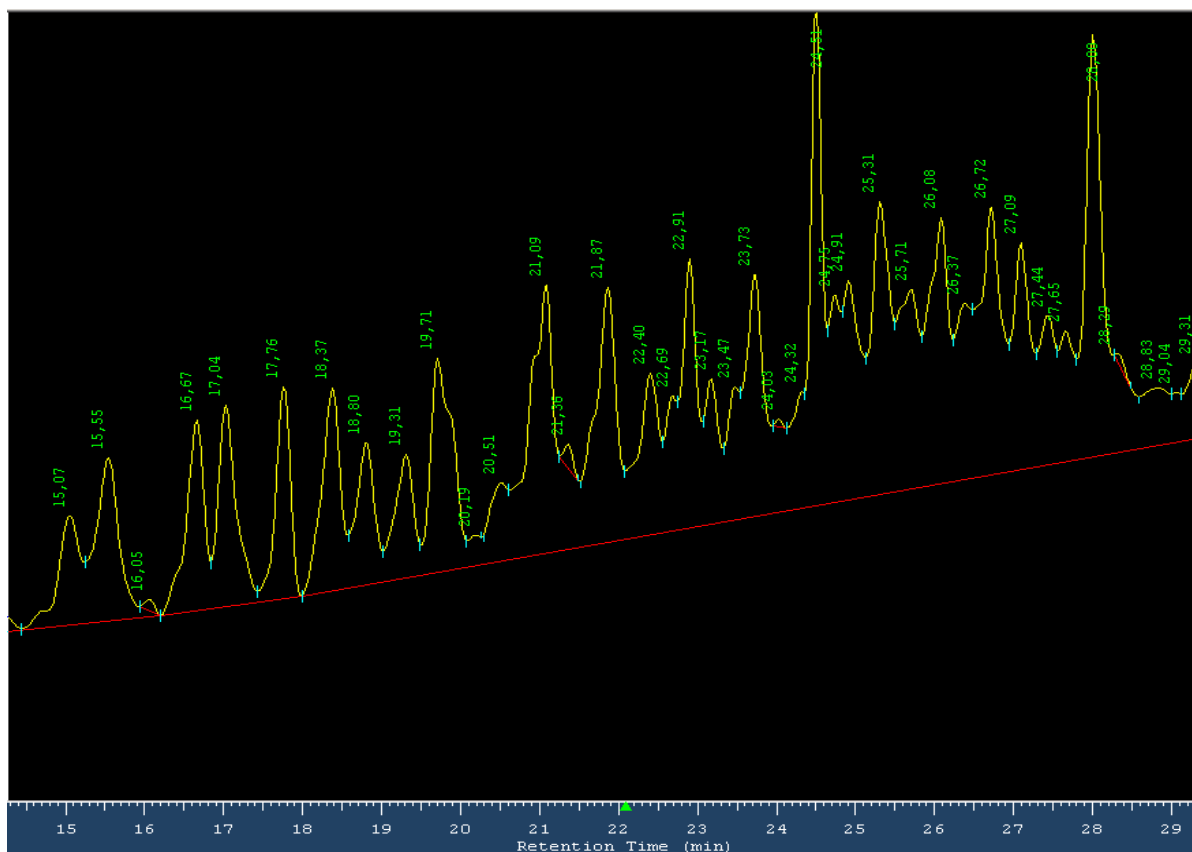
Figure 10-1 The figure shows the behavior of **1** and **2** during the HPLC run. The wavelength used was 230 nm. The retention times 17.76 min and 21.87 min indicate the signals of **2** and **1** respectively. The longer chain length of compound **1** determined a belayed retention time with respect to **2** in the reverse phase column.
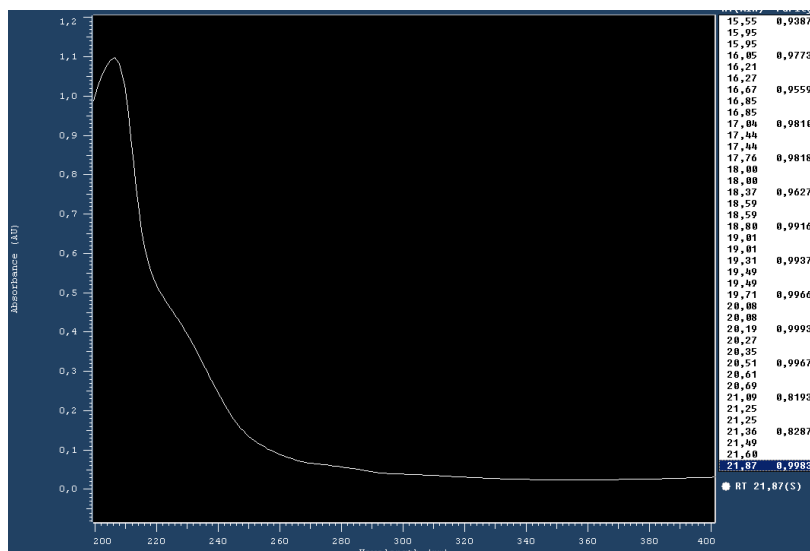
Figure 10-2 The figure shows the UV spectrum of compound **1** at retention time 21.87 min. The maximum absorbption for this molecule occurs at around 206 nm.
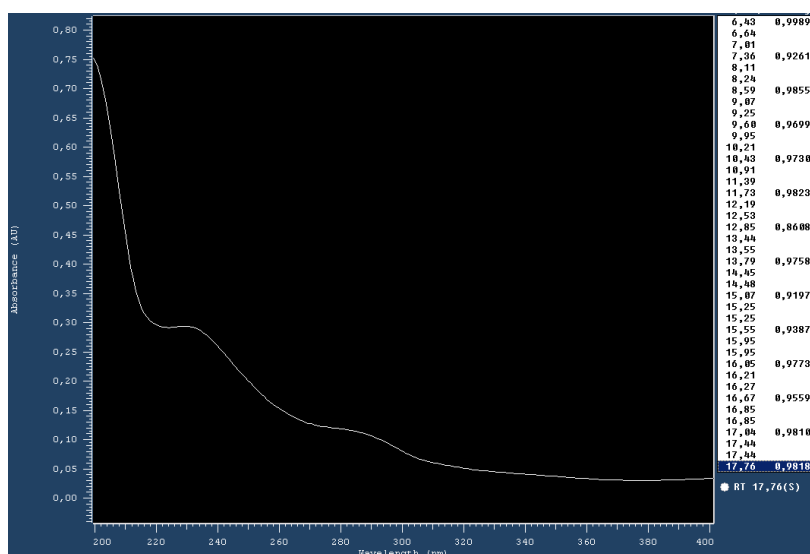
Figure 10-3 The figure shows the UV spectrum of compound **2** at retention time 17.76 min. The maximum absorpbtion for this molecule is around 200 nm.
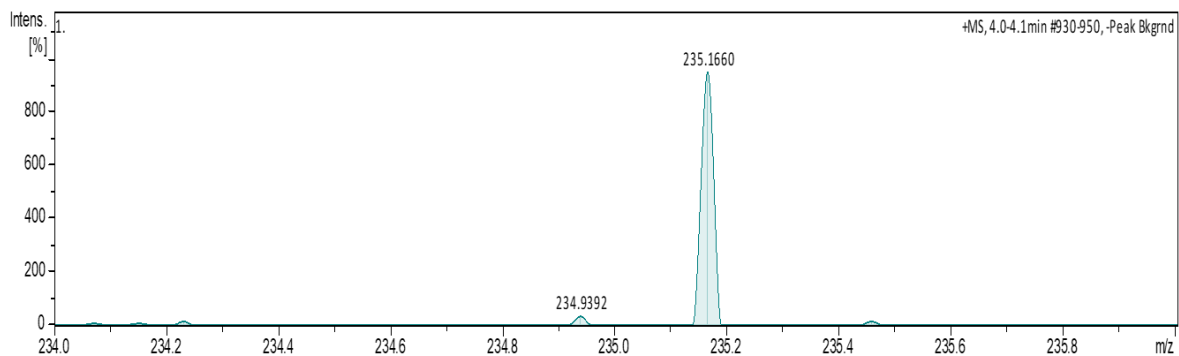
Figure 10-4 (+) HRMS spectrum of compound (**1**). The mass (m/z) is presented as Na adduct (Calculated: 235.1629 / Measured: 235.1660).
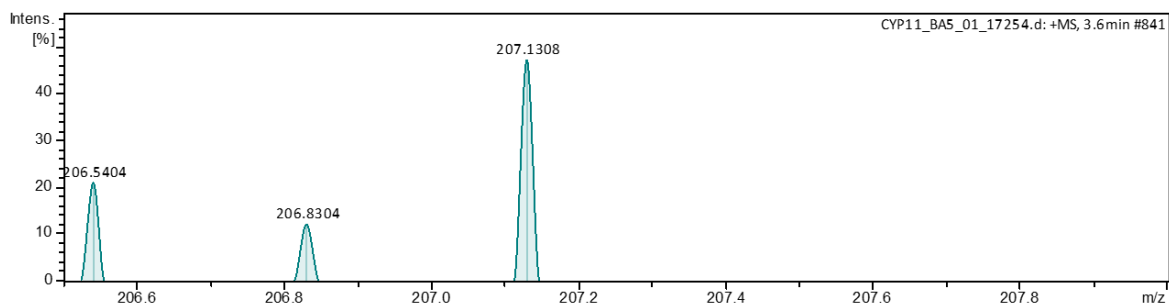
Figure 10-5 (+) HRMS spectrum of compound (**2**). The mass (m/z) is presented as Na adduct (Calculated: 207.1316 / Measured: 207.1308).
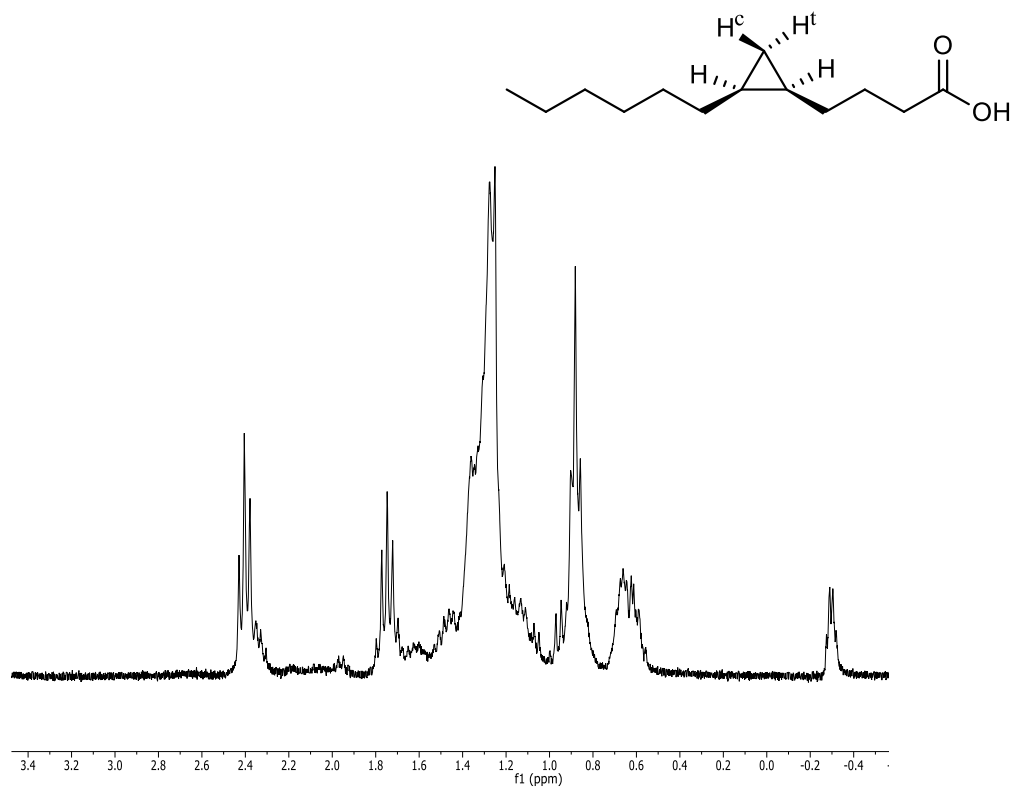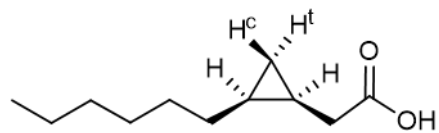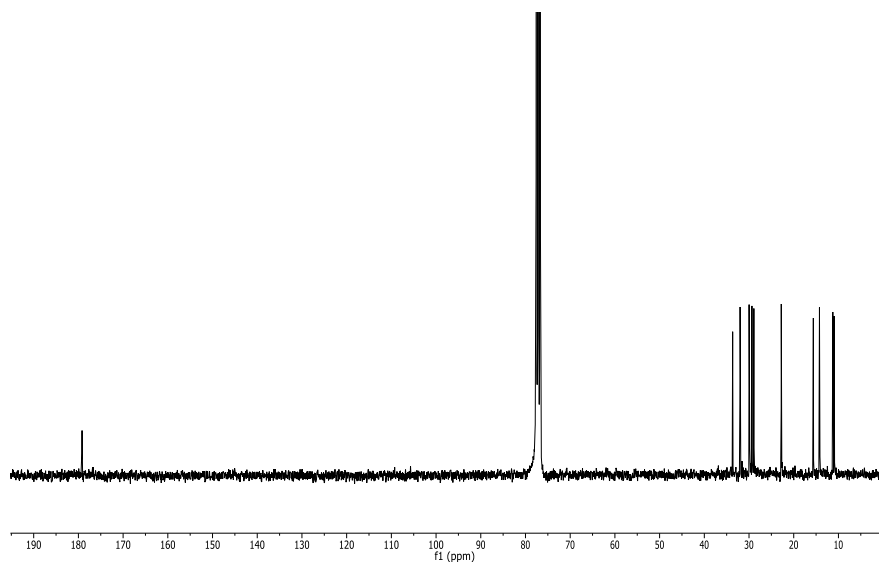
Figure 10-6 ^{1}H (300 MHz) Spectrum of compound **1** in CDCl$_3$
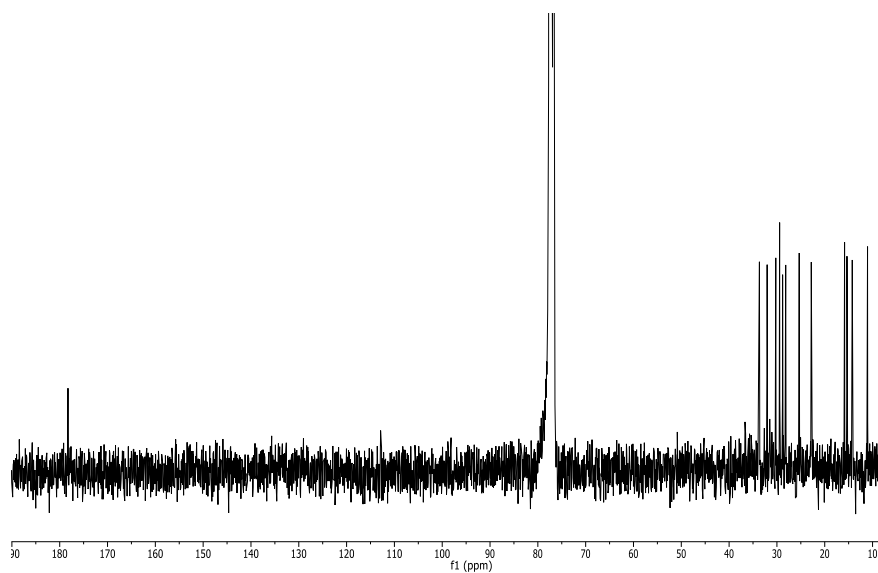
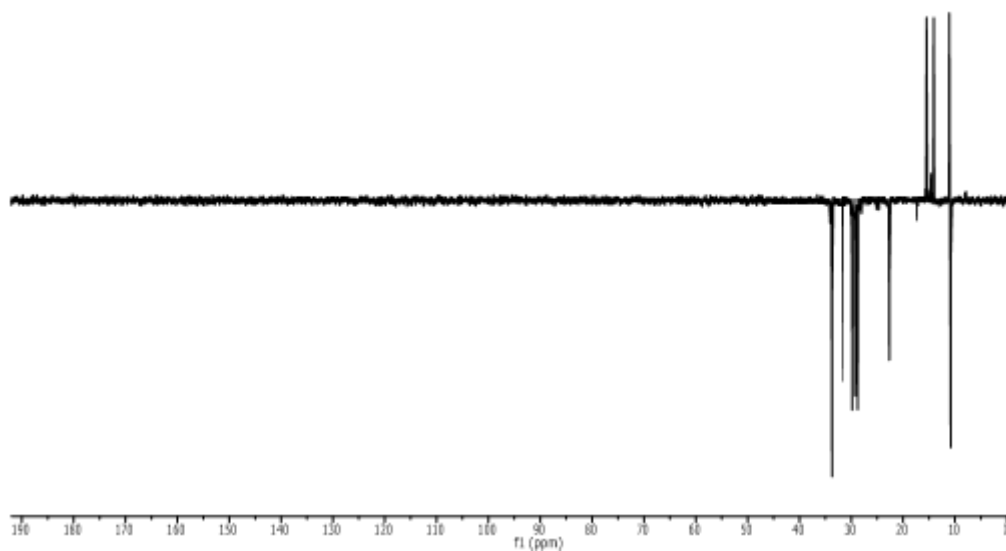**Figure 10-7** ^{13}C (300 MHz) Spectrum of compound **1** in CDCl$_3$
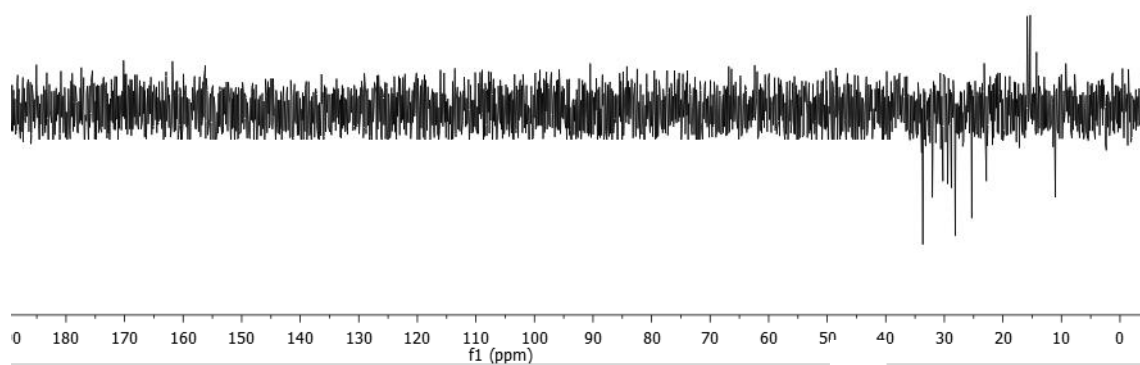
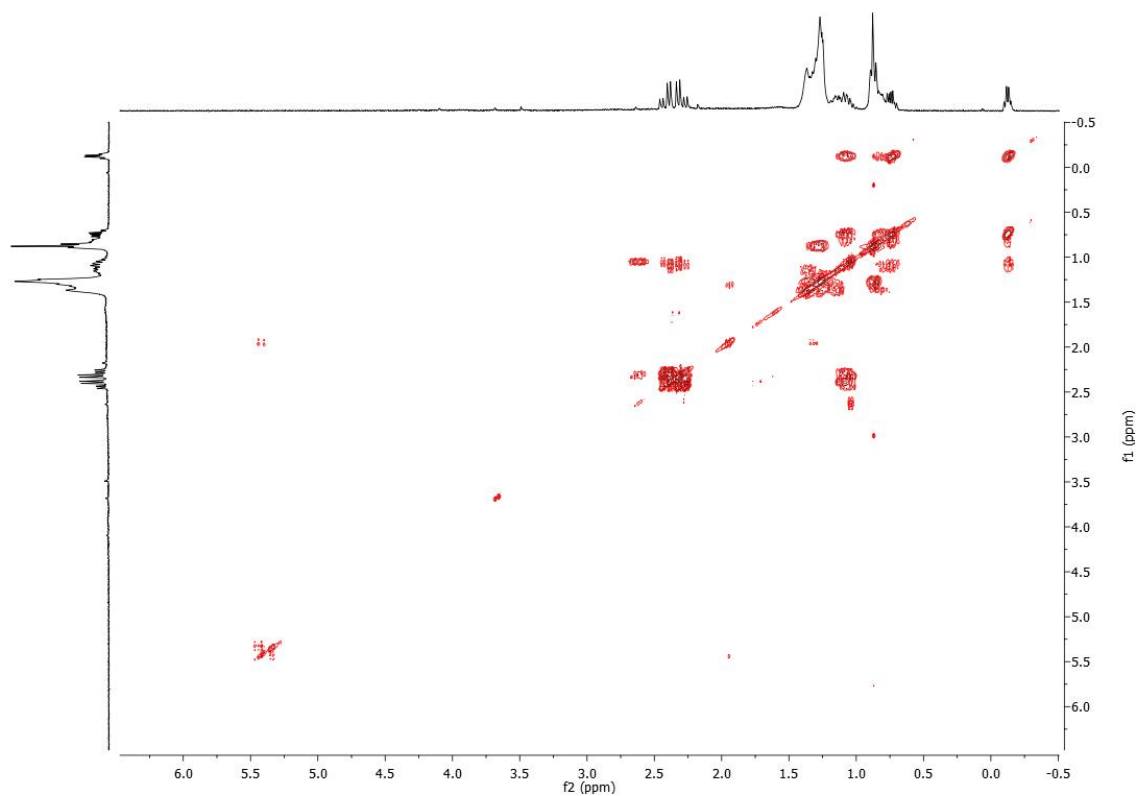**Figure 10-8** ^{13}C - DEPT135 (300 MHz) Spectrum of compound **1** in CDCl$_3$
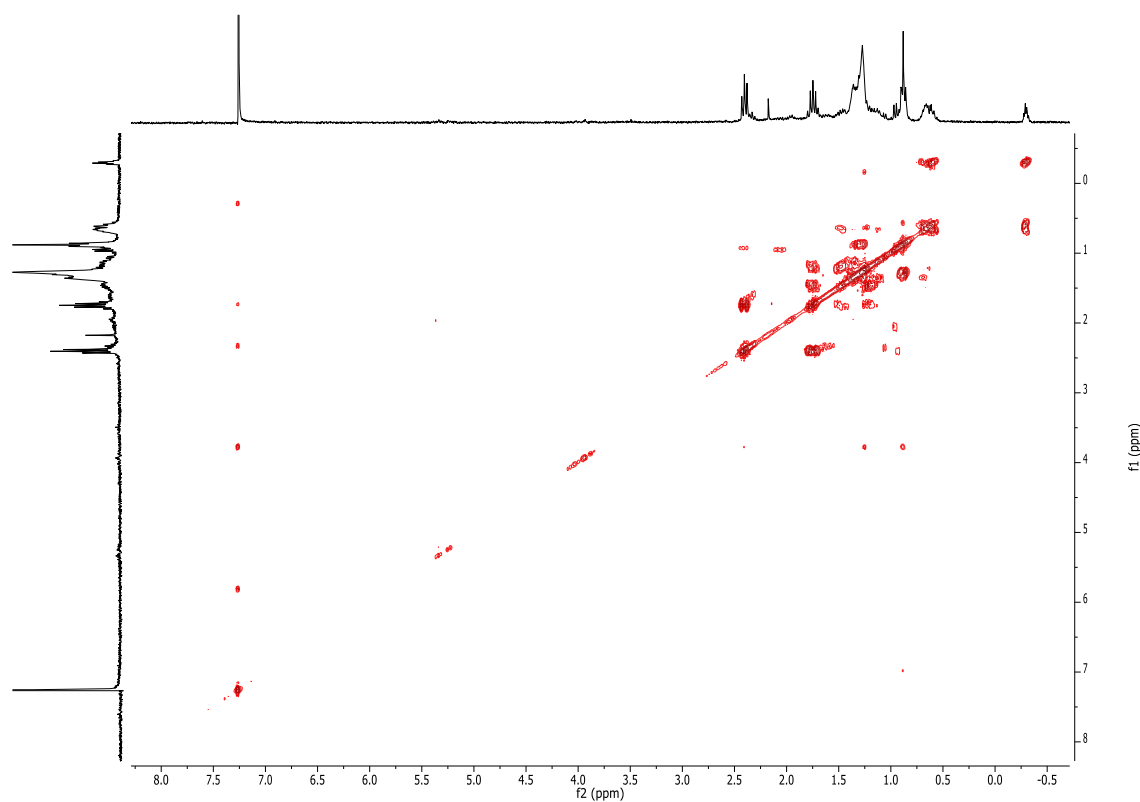
Figure 10-9 COSY (300 MHz) Spectrum of compound **1** in CDCl$_3$
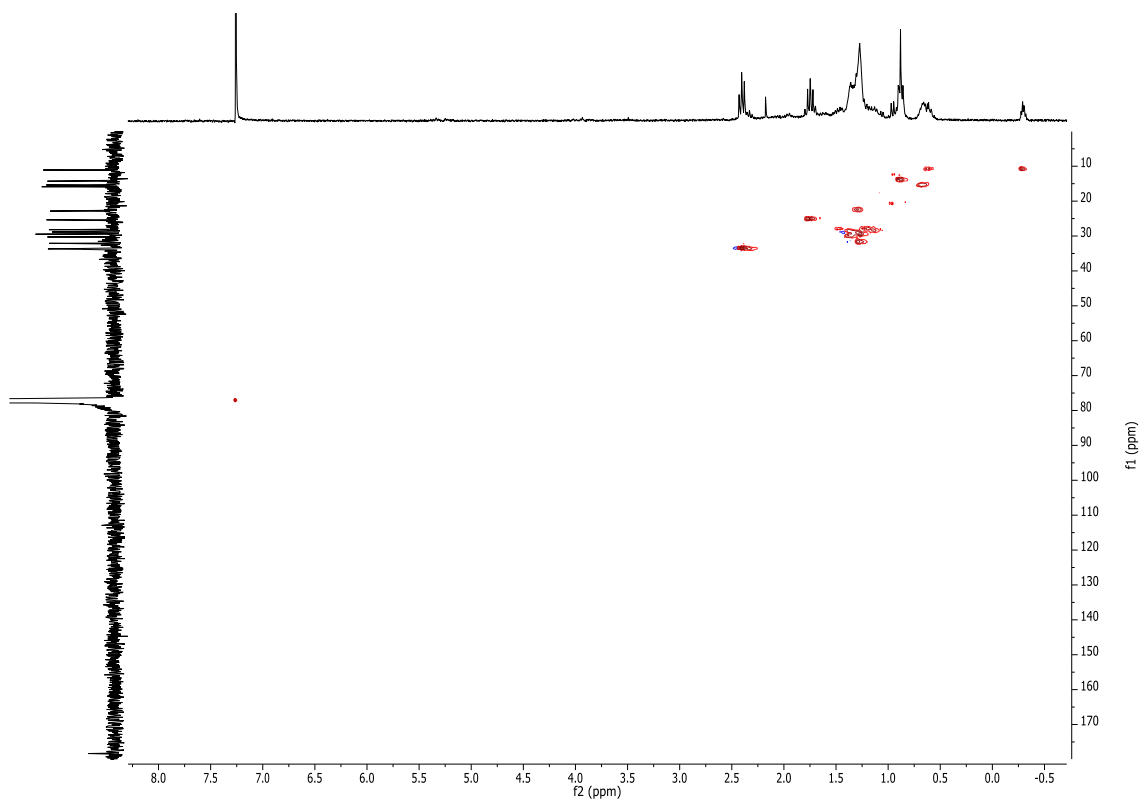
Figure 10-10 HSQC (300 MHz) Spectrum of compound **1** in CDCl$_3$
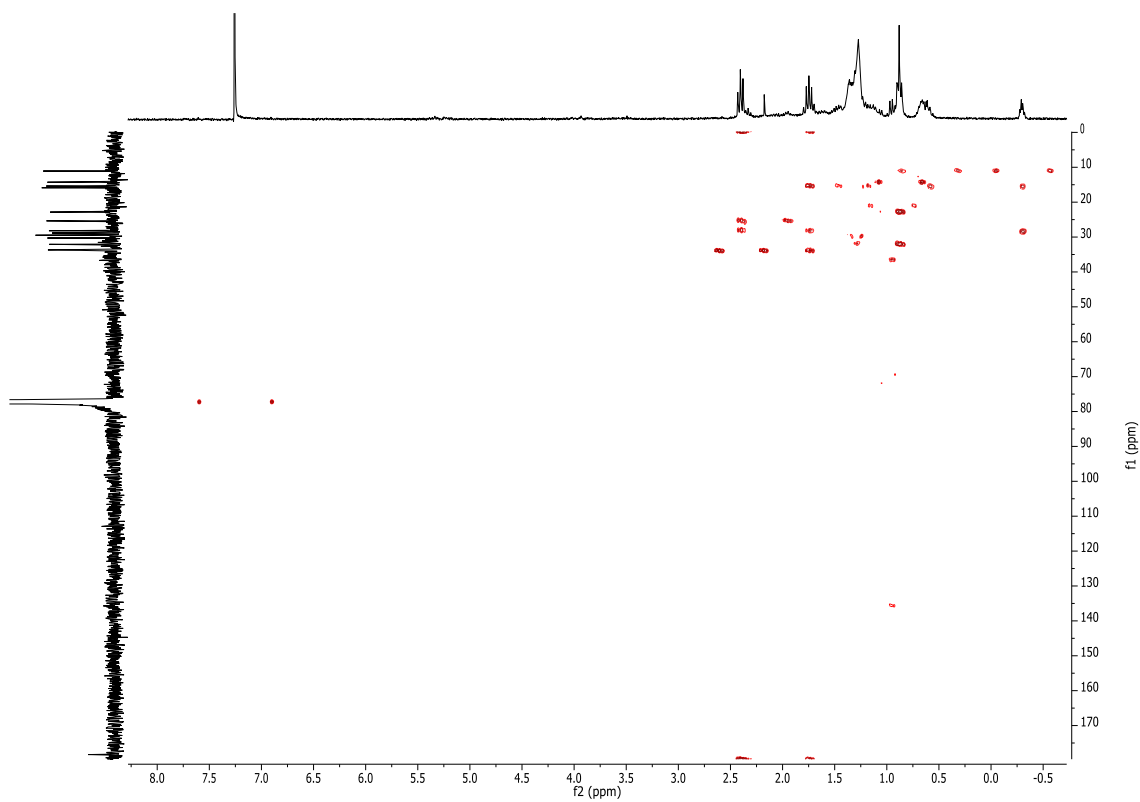
Figure 10-11 HMBC (300 MHz) Spectrum of compound **1** in CDCl3
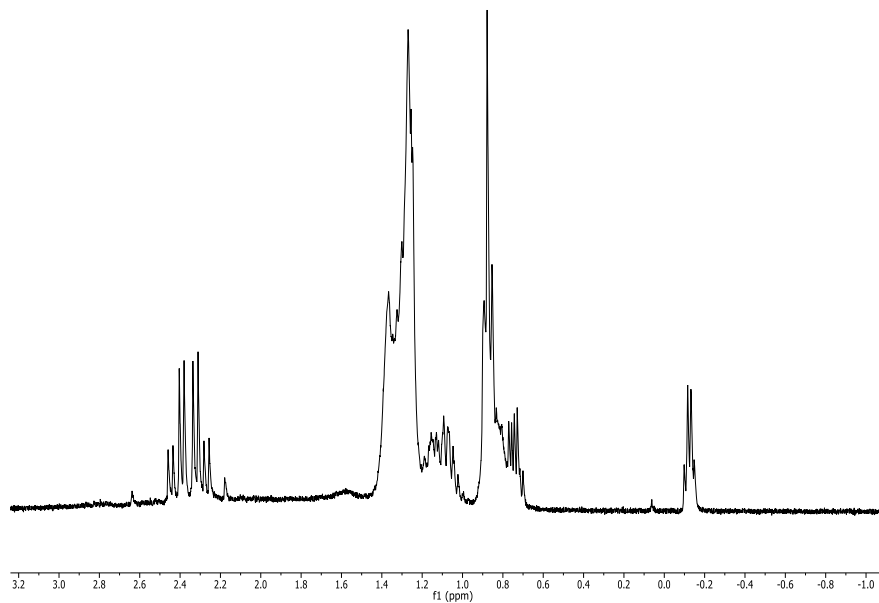
Figure 10-12 ^{1}H (300 MHz) Spectrum of compound **2** in CDCl$_3$

Figure 10-13 ^{13}C (300 MHz) Spectrum of compound **2** in CDCl$_3$

Figure 10-14 ^{13}C - DEPT135 (300 MHz) Spectrum of compound **2** in CDCl$_3$

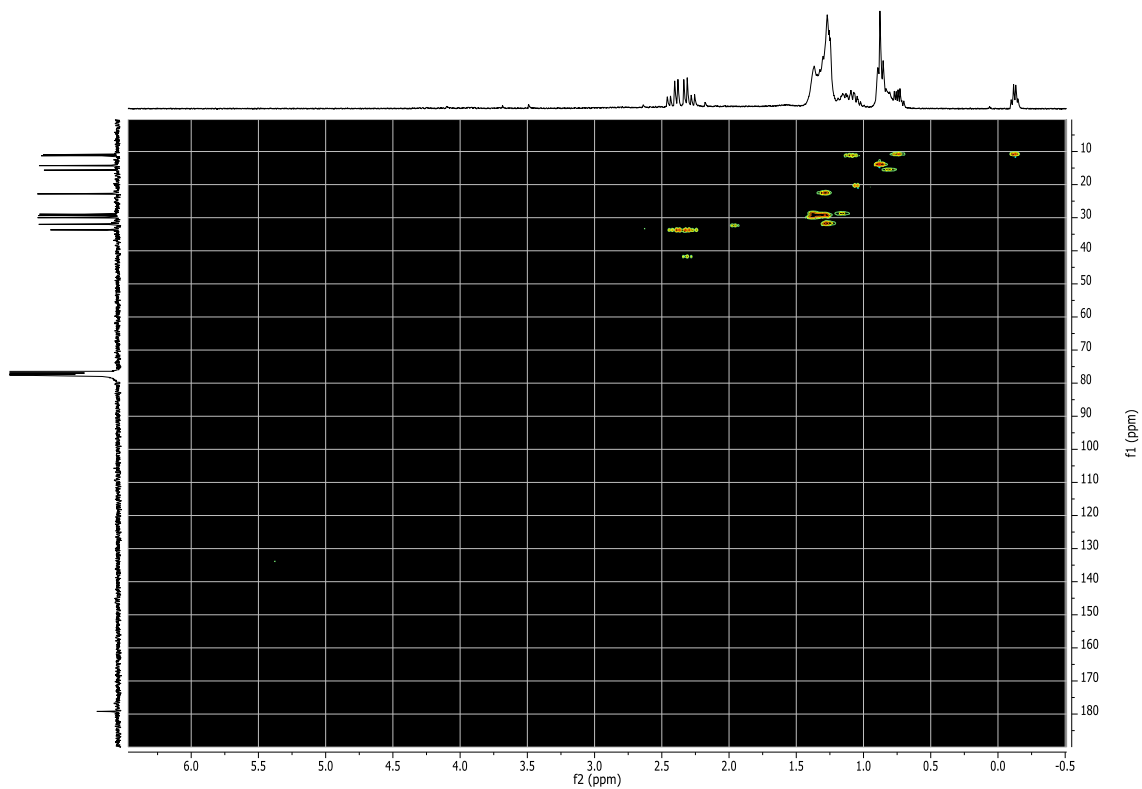**Figure 10-15** COSY (300 MHz) Spectrum of compound **2** in CDCl$_3$

Figure 10-16 HSQC (300 MHz) Spectrum of compound **2** in CDCl₃
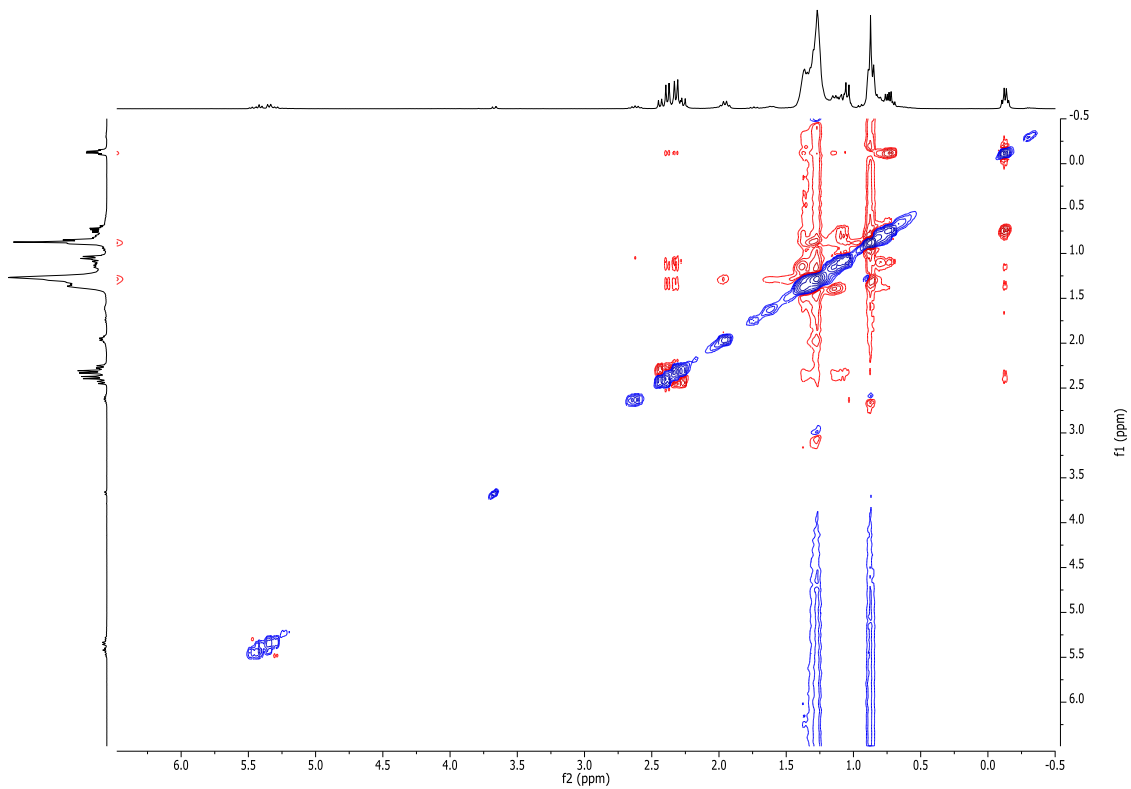

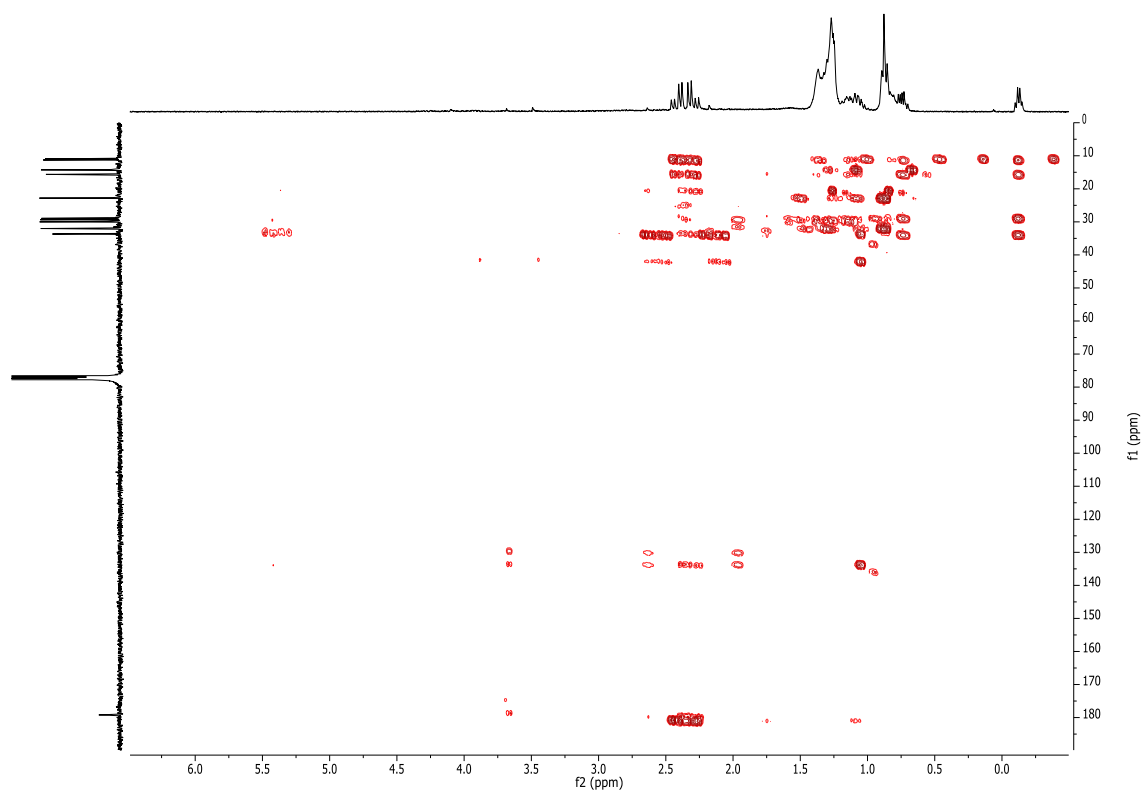**Figure 10-17** NOESY (300 MHz) Spectrum of compound **2** in CDCl₃

Figure 10-18 HMBC (300 MHz) Spectrum of compound **2** in CDCl₃

Table 10-1 Comparison between the calculated ^{1}H resonance values of **2** (300 MHz, CDCl$_3$) and the *cis*-isomer of cascarillic acid as published by (*126*) (220 MHz, CDCl$_3$). The measured and reference values are comparable, thus suggesting structural equivalence among **2** and *cis*-cascarillic acid.
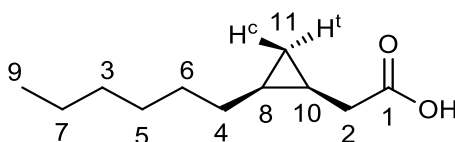
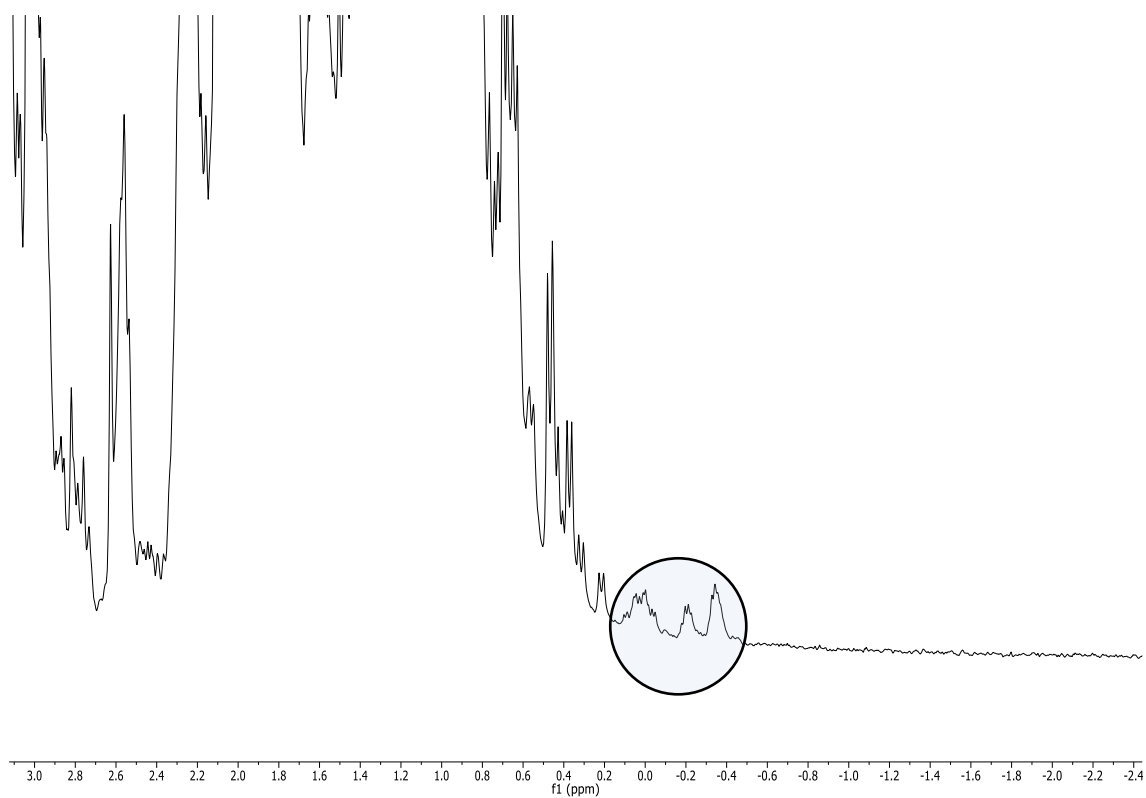| Position		δ_H (*J* in Hz) [ppm] calculated	δ_H [ppm] as published by (*126*)
1	C	-	-
2	CH$_2$	a: 2.42, dd (6.9, 16.0) b: 2.29, dd (7.8, 16.0)	2.30, 2H-m
3	CH$_2$	1.26, m	1.18 – 1.46, 10H-m
4	CH$_2$	1.37, m	1.18 – 1.46, 10H-m
5	CH$_2$	1.29, m	1.18 – 1.46, 10H-m
6	CH$_2$	1.35, m	1.18 – 1.46, 10H-m
7	CH$_2$	1.29, m	1.18 – 1.46, 10H-m
8	CH	0.81, m	0.66 – 0.88, 1H-m
9	CH$_3$	0.88, t (7.3)	0.89, 3H-t
10	CH	1.10, m	1.00 – 1.18, 1H-m
11	CH$_2$	a^t: 0.75, dq (8.4, 5.0) b^c: -0.13, q (5.0)	b^c: -0.11, q

Figure 10-19 ^{1}H (300 MHz) Spectrum of crude extract from Siel 3m in CD$_3$OD. The resonances from -0.4 ppm to 0.0 ppm are suggestive of protons conforming cycopropane groups (compare with Figures 9-6 and